Université d'Ottawa · University of Ottawa

Université d'Ottawa · University of Ottawa

FACULTÉ DES ÉTUDES SUPÉRIEURES ET POSTDOCTORALES

FACULTY OF GRADUATE AND POSTDOCTORAL STUDIES

ZHAO, Guangze

AUTEUR DE LA THÈSE - AUTHOR OF THESIS

M.A.Sc. (Electrical Engineering)

GRADE - DEGREE

School of Information Technology and Engineering

FACULTÉ, ÉCOLE, DÉPARTEMENT - FACULTY, SCHOOL, DEPARTMENT

TITRE DE LA THÈSE - TITLE OF THE THESIS

Impact of Multipath Clustering on Correlation and MIMO System Performance in Rayleigh Fading Channels

S. Loyka

DIRECTEUR DE LA THÈSE - THESIS SUPERVISOR

EXAMINATEURS DE LA THÈSE - THESIS EXAMINERS

D. McNamara

H. Yanikomeroglu

J.-M. De Koninck, Ph.D.

LE DOYEN DE LA FACULTÉ DES ÉTUDES SUPÉRIEURES ET POSTDOCTORALES

SIGNATURE

DEAN OF THE FACULTY OF GRADUATE AND POSTDOCTORAL STUDIES

Impact of Multipath Clustering on Correlation and MIMO System Performance in Rayleigh Fading Channels

GUANGZE ZHAO

Thesis submitted to the
Faculty of Graduate and Postdoctoral Studies
in partial fulfillment of the requirements
for the degree of Master of Applied Science in Electrical Engineering

School of Information Technology and Engineering
University of Ottawa

Your file Votre référence
ISBN: 0-612-90365-6
Our file Notre référence
ISBN: 0-612-90365-6

Abstract

This thesis extends single cluster of multipath channel model to multi-cluster one. This multi-cluster channel model, which is more accurate than single cluster, has a profound effect on MIMO channel correlation and system performances. Based on this multi-cluster channel model , closed-form expressions of channel correlation are derived. The results using multi-cluster channel model agree with those using single cluster one. The results of the derived equations are also in full agreement with the results obtained from Monte-Carlo simulations. Using two-cluster channel model, the MIMO channel correlation coefficient has an oscillatory behavior with respect to the antenna spacing. Besides the angular spread and mean angle of arrival of the 2^{nd} cluster , the power allocation has a significant effect on MIMO channel correlation. Similar to the behavior of channel correlation, both the MIMO channel capacity and diversity gain also oscillates with respect to the antenna spacing because of the 2^{nd} cluster. It is also demonstrated that it is possible to orient the antenna array in such a way that the correlation is minimized and the maximum capacity can be achieved provided that the minimum element spacing is respected.

Acknowledgement

I would like to express my gratitude to the following people:

- My supervisor, Dr. S. Loyka for his outstanding guidance.
- Prof. McNamara for his admittance for me to use his equipment
- To my family: thank you for giving me this opportunity and the moral support throughout my studies.

Acronyms and Abbreviations

AOA	Angle of Arrival
CCI	Co-Channel Interference
DOA	Direction of Arrival
DS	Delay Spread
EDOF	Effective Degrees of Freedom
EGC	Equal Gain Combining
GWSSUS	Gaussian Wide Sense Stationary Uncorrelated Scattering
GAA	Gaussian Angle of Arrival
ISI	Inter-Symbol Interference
i.i.d.	independent and identically distributed
LOS	Line of Sight
MC	Mutual Coupling
MIMO	Multiple Input Multiple Output
MRC	Maximum Ratio Combining
MS	Mobile Station
PDF	Probability Density Function
PDS	Power Delay Spectrum
PAS	Power Azimuth Spectrum
RMS	Root Mean Square
SAE	Squared Approximation Error
SC	Selection Combining
SISO	Single Input Single Output
SIMO	Single Input Multiple Output
SNR	Signal to Noise Ratio
TOA	Time of Arrival
UCA	Uniform Circular Array
ULA	Uniform Linear Array
WSSUS	Wide Sense Stationary Uncorrelated Scattering

Table of Symbols and Notations

Symbols		Section
A_r	Amplitude of Receiver Signal	2.1.2
a_i	Amplitude of i-th multipath	2.5
c	Normalizing Constant in Cosine Model	2.7.2
c_g	Normalizing Constant in Gaussian Model	2.7.4
c_l	Normalizing Constant in Laplacian Model	2.7.5
C	Channel Capacity	4.2.1
$\langle C \rangle$	Mean Channel Capacity	4.2.1
d	Antenna Spacing	2.6
d_0	Reference Distance	2.1.1
d_1	Transmitter and Receiver Separation Distance	2.1.1
d_f	Distance threshold	3.4.1
D	Distance between MS and antenna	2.7.1
E_t	Radiation Pattern of Transmit Antennas	2.8.1
E_r	Radiation Pattern of Receive Antennas	2.8.1
f	Frequency	2.3
f_c	Carrier Frequency	2.3
f_d	Doppler Frequency Shift	2.3
g	Channel Gain	4.2.1
G_d	Diversity Gain	5.2
h	Channel Impulse Response	2.8.2
$\mathbf{H}$	Channel Matrix	4.2.1
$I_0(\cdot)$	Zero-order Modified Bessel Function	2.7.6
$\mathbf{I}$	Identity Matrix	4.2.2
$J_m(\cdot)$	Bessel Functions of order m	3.2.1.1
k_v	Constant in Von Mises Model	2.7.6
L	Aperture of Uniform Linear Array	4.3.2.1
L_s	Number of Scatters	2.8.1
m	Number of Transmitter Antennas	4.2.1
n	Number of Receiver Antennas	3.2.2
n_c	Exponent Parameter in Cosine Model	2.7.2
n_p	Path Loss Exponent	2.1.1
N	Number of Multipath	2.5
N_c	Number of Clusters	2.8.3
N_s	Number of Scatters	2.7.1

p_{out}	Outage Probability	5.3
P_r	Signal Power at Receiver	2.1.1
P_t	Signal Power at Transmitter	2.1.1
$\overline{PL}$	Path Loss	2.1.1
r	Radius of Uniform Linear Array	3.2.2
R_s	Radius of Circle of Scatters	2.7.1
R	Correlation Coefficient	3.2.1
R_{real}, R_{xx}	Real part of R	3.3.1
R_{imag}, R_{xy}	Imaginary part of R	3.3.1
$\mathbf{R}$	Normalized Channel Correlation Matrix	4.3.1
Rio	Ratio of the Contributions by Clusters	3.4.2
S_φ , σ_φ	RMS Angular Spread	2.4
$\mathbf{v}$	Array Manifold Vector	2.6
x	Input Signal Amplitude	2.5
y	Amplitude of Receiver Signal	2.5
$\mathbf{Y}$	Amplitude matrix of Receiver Signal	4.2
z	Defined as $2\pi d / \lambda$	2.6
α	Rotation Angle	4.4.2
α_i	Weighting Factor	5.2.1
γ_i	SNR of i-th Branch	5.2.1
$\overline{\varphi}, \langle\varphi\rangle$	Mean AOA	2.4
$\overline{\tau}, \langle\tau\rangle$	Mean Excess Delay	2.2
σ	Standard Deviation	2.1
Δ	Cluster angular spread	2.7.3
λ	Signal Wavelength	2.6
λ_k	k-th Eigenvalue of $\mathbf{HH}^+$	4.2.3
ξ	Additive Noise	4.2.1
ρ	SNR at each Receive Antenna	4.2.1
$\rho(\cdot)$	Probability Density Function	2.7.2

CONTENTS

Chapter 1 Introduction

In the past two decades, wireless communications has grown with unprecedented speed from early radio paging, cordless telephone, and cellular telephony to today's personal communication and computing devices. These commercial wireless applications have had a profound impact on today's business world and people's daily lives. The growth and demand for wireless services will play a significant role in the evolution of Internet service from the current landline system to wireless systems. This evolution will almost certainly fuel further growth in wireless communications. This has motivated research investigating methods of increasing wireless system capacity. Space-time processing technology and multiple-input-multiple-output (MIMO) antenna architectures hold great promise to vastly improve spectrum efficiency (capacity) by providing considerably lower cost than cell-splitting approach. Furthermore, MIMO architecture utilizing multiple antennas provides small-scale temporal and spatial diversity at both transmitter and receiver, which will be required for future-generation high capacity wireless communication systems. MIMO is one of the important enabling techniques for meeting the expected demand for high-speed wireless data service [1].

1.1 Motivation of this Research

The system performances of MIMO systems mainly depend on the channel correlation. In classical channel model, MIMO channel correlation and system performances are evaluated assuming that uncorrelated multipath arrive the receiver in single cluster. Various power azimuth spectrum (PAS) in the single cluster channel model has been investigated. However, measurements in practical environments show that the multipath is distributed in multi clusters (See section 2.8.4). It is required to develop a more accurate channel model to evaluate MIMO channel correlation and system performances.

1.2 Objectives

The main focus of this research is to develop a more accurate channel model, which can be deployed to evaluate MIMO system performances. The proposed channel

model is multi-cluster of multipath channel model. The efforts in this area of research are to study the impact of multi clusters on channel correlation of the MIMO channel. The second focus of this research is to evaluate system performance such as information-theoretic MIMO channel capacity and diversity for multi antenna systems.

1.3 Methodology and Approaches

The approaches used in this research are the following:

(1). Using correlation approach to evaluate MIMO system performances including channel capacity and diversity gain.

(2). Comparing published results on envelope correlation based on single cluster channel model with simulating results to validate simulating programs.

(3). Comparing published results on envelope correlation based on two-cluster channel model with simulating results to validate simulating programs.

(4). Deploying Monte-Carlo simulation to validate analytical results on the multi-cluster channel correlation.

(5). Using analytical derivation to validate the channel correlation of multi-cluster channel in agreement with that of single cluster channel.

(6). Comparing published results on channel capacity of single cluster channel model with simulating results to validate simulating programs.

(7). Deploying Monte-Carlo simulation to validate the channel capacity of multi-cluster channel in agreement with that of single cluster channel.

(8). Using analytical results to validate the simulating results on diversity gain of multi-cluster channel.

(9). Deploying MATLAB to make all the simulations.

1.4 Outline of Thesis

In chapter1, the motivation, objectives and methods in this work is discussed, and then outline our channel modeling efforts and contributions in this research field.

In chapter 2, we review the characteristics of wireless propagation channel, such as signal attenuation, time dispersion, and frequency dispersion for conventional single-

input single-output (SISO) system, and the angle of arrival (AOA) signal dispersion for MIMO systems. Vector channel model using both uniform linear array (ULA) and uniform circular array (UCA) for SIMO channel are derived. The review of various power azimuth spectrum (PAS) and multi-cluster models are given. We extended single cluster model to multi-cluster one.

In chapter 3, the channel correlation of two-cluster channel is studied in details, including both symmetrical and asymmetrical location of the clusters, and equal/unequal angular spreads and power distributions. It is shown that the correlation coefficient has an oscillatory behavior with respect to the antenna spacing. As a cluster moves away from the array broadside direction, its contribution to the total correlation decreases (inverse cosine law). In the case of identical symmetrically-located clusters, the envelope of correlation is determined by a single cluster angular spread while the oscillations within the envelope are determined by the inter-cluster angular spread (for both clusters). If the clusters are identical and located asymmetrically (i.e., broadside-endfire), the impact of the endfire cluster is, in many cases, much smaller and can be neglected for proportional power allocation. Hence, one-cluster model can be used, which simplifies the analysis substantially.

In chapter 4, we examine channel capacity using the two-cluster multipath channel model. We evaluate the channel capacity of a MIMO channel with both ULA and UCA. It is shown that the channel capacity with UCA is lower than ULA with the same aperture because some elements in UCA are "lost" due to correlation. The behavior of channel capacity is in full agreement with the correlation behavior studied in chapter 3. To have an insight on the effects of the 2nd cluster on the channel capacity, we study the capacity of a two-cluster channel for various cluster locations and array geometries. We demonstrate that the maximum capacity is achieved provided that the minimum element spacing is respected. When two cluster are widely separated (i.e., the angular separation is larger than the cluster widths), it is possible to orient the antenna array in such a way that the correlation is minimized and, hence, the capacity are maximized. Monte-Carlo simulations which validate our calculations are also described.

In chapter 5 we examine diversity combining gain for two-cluster multipath channel model. We find that, similar to the channel capacity behavior, the 2nd cluster

also caused oscillation in diversity gain and the oscillation is much stronger than that of the channel capacity.

In chapter 6, we summarize our research work on the propagation channel modeling and its effects on system performance, and discuss the problems that need to be further studied.

1.5 Contributions of this Work

The work presented here makes a number of novel contributions to this research field. Some of the significant contributions of this report include:

- A multi-cluster channel model developed for MIMO system
- A derivation of the analytical result on the spatial correlation using multi-cluster MIMO channel model
- The impact of the 2nd cluster on MIMO channel correlation is evaluated
- An information-theoretic channel capacity of the MIMO channels is evaluated for UCA and ULA based on multi-cluster MIMO channel model
- The channel capacities of the MIMO channels with UCA and ULA are compared
- The impact of the 2nd cluster on the channel capacity of the MIMO channel are evaluated
- The impact of the 2nd cluster on diversity gain is evaluated

Chapter 2 Review of MIMO Channel Modeling

In a wireless communication system, a signal transmitted into the channel interacts with the environment structures such as buildings, hills, tree, mountains, and moving vehicles in a very complex process. This process can result in a single line-of-sight (LOS) propagation path, many non-LOS reflected propagation paths, or a combination of LOS and non-LOS propagation paths (multipath environment). The multipath propagation results from reflection from large objects, diffraction of the electromagnetic waves around objects and scattering from rough object surfaces. An illustration of wireless propagation environment is shown in Figure 2-1. In classical channel model, there are three important effects of multipath channels: signal strength fluctuation, time dispersion and frequency dispersion. When adaptive arrays are investigated, besides the time of arrival (TOA), the angle –of- arrival (AOA) or direction- of- arrival (DOA) must also be considered.

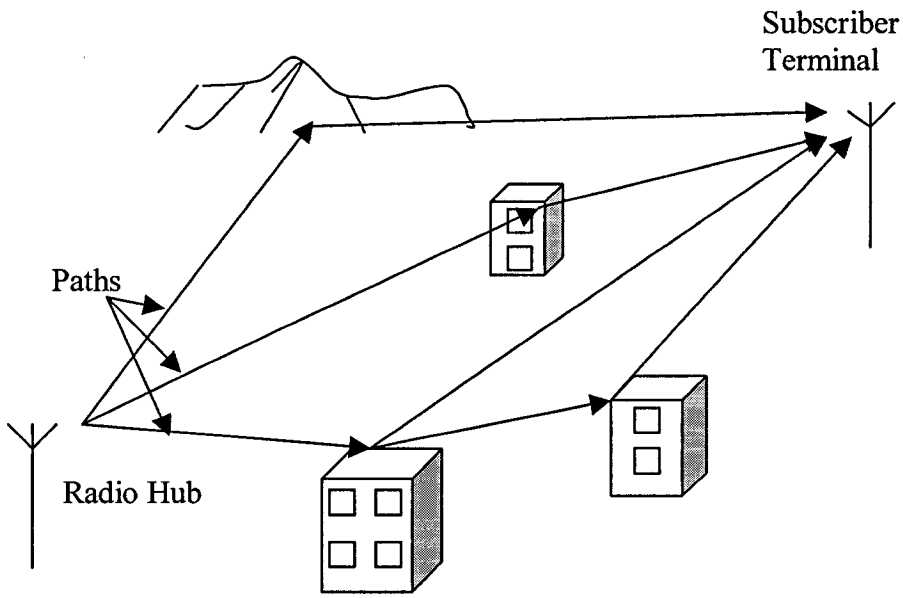

Figure 2-1. Multipath in wireless communication channel

2.1 Signal Strength Fluctuation

In detail, reflection occurs when propagation waves impinging upon a physical object which has a large surface relative to the wavelength of the propagation wave. In general, reflection results from the surface of the earth, mountains, or the wall of a building. Diffraction results from the resultant bending of waves that occurs when the propagation wave is obstructed by an irregularly sharp surface or edges, scattering occurs when the size of the physical objects in the propagation medium are smaller than the propagation wavelength. Scattered waves generally result from foliage, street signs, or lampposts.

2.1.1 Large Scale Fading

The large-scale signal attenuation in mobile radio propagation includes path loss and shadowing (known as slow fading) [2]. Path loss (PL) is due to the physical separation between the transmitter and the receiver. Shadowing is the received power variation resulting from signal attenuation due to physical obstructions between the transmitter and the receiver, as seen in Figure 2-2.

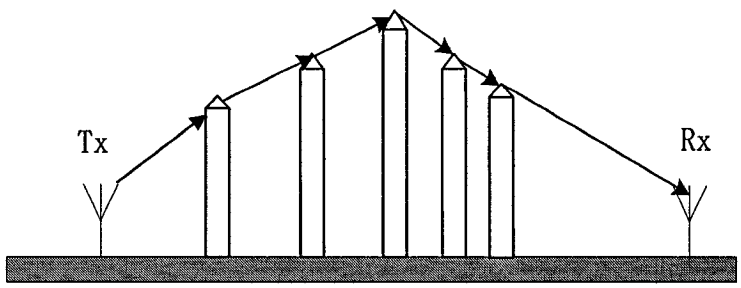

Figure 2-2. Large scale fading (shadowing) propagation

Path loss $\overline{PL}$ is related to the ratio of the received power to the transmitted power

$$\overline{PL} \propto \frac{P_r}{P_t} \tag{2.1}$$

where P_r is the received power and P_t is the transmitted power. In practice, $\overline{PL}$ can be evaluated as a function the distance between the transmitter and the receiver

$$\overline{PL}(d_1) \propto \left(\frac{d_1}{d_0}\right)^{n_p} \tag{2.2}$$

or $$\overline{PL}(d_1)[dB] = \overline{PL}(d_0) + 10n_p \log\left(\frac{d_1}{d_0}\right) \tag{2.3}$$

where n_p is the path loss exponent , and d_0 is the close-in reference distance which is determined from measurements close to the transmitter, and d_1 is the transmitter and the receiver separation distance. The value of n_p is depending on the propagation environment. In free space $n_p = 2$, in typical urban areas n is about 3.8 to 4.5 and in rural areas n is about 2.5 to 3 **[1]**.

The physical obstacles between the transmitter and the receiver result in a variation around the mean received power p_r, known as shadowing. Shadowing is considered to be slow fading and is statistically characterized by a lognormal distribution (normal distribution in dB scale). That is

$$PL(d_1)[dB] = \overline{PL}(d_1) + X_\sigma = \overline{PL}(d_0) + 10n\log\left(\frac{d_1}{d_0}\right) + X_\sigma \tag{2.4}$$

where X_σ is a zero-mean Gaussian distributed random variable (in dB) with standard deviation σ (also in dB).

2.1.2 Small Scale Fading

Multipath propagation, which results from reflection, diffraction, and scattering, gives rise to many non-LOS propagation paths. These non-LOS propagation paths arrive with displacement at the receiving antenna with respect to one another in the time and spatial domains; the random phase and amplitudes of the different multipath components cause fluctuations in signal strength, thereby inducing small-scale fading, signal distortion or both. Multipath time delay spread results in either flat fading or selective fading. If the bandwidth of the radio channel is greater than the bandwidth of the transmitted signal, then the channel is called flat fading channel, otherwise is called frequency selective fading channel. And the former is the most common type of fading channel. In this literature, we assume radio channel undergo flat fading.

The well known flat fading channel model is the Rayleigh fading channel model, which assumes that the probability of amplitude of receiver signal varies in time according Rayleigh distribution as shown in (2.5).

$$p(A_r)=\begin{cases}\frac{A_r}{\sigma^2}e^{-\frac{A_r^2}{2\sigma^2}} & (0\le A_r\le\infty)\\ 0 & (A_r<0)\end{cases} \tag{2.5}$$

where σ^2 is the time-average power of the received signal before envelope detection.

2.2 Time Dispersion

The time dispersive properties of different multipath channel are always quantified by their delay spread. Delay spread is the measure of the relative propagation delays among the non-LOS propagation paths caused by the reflectors such as mountains or a cluster of buildings. It can be derived from an average small-scale power delay profile, which comes from measurement and is found by averaging instantaneous power delay profile over a local area. The mean excess delay is defined as

$$\bar{\tau}=\langle\tau\rangle=\frac{\sum_k P(\tau_k)\tau_k}{\sum_k P(\tau_k)} \tag{2.6}$$

The root mean square (RMS) delay spread is defined as

$$\sigma_\tau=\sqrt{\langle\tau^2\rangle-\bar{\tau}^2} \tag{2.7}$$

where $\langle\tau^2\rangle=\frac{\sum_k P(\tau_k)\tau_k^2}{\sum_k P(\tau_k)}$

2.3 Frequency Dispersion

Doppler shift is another property of a wireless channel. It results from the motion of the receiver, the transmitter, and/or any other objects in the channel relative to local scatters in the multipath propagation environment. In addition, with the composite sum of many non-LOS propagation paths, the multipath propagation results in signal fluctuation in received signal amplitude, thereby inducing signal fading and signal distortion. For the case of the dense-scatterer model , a vertical receive of antenna with constant azimuthal

gain(omni directional), a uniform distribution of signals arriving at all arrival angles throughout the range $[0,2\pi]$, and an unmodulated CW signal, the signal power spectrum of Doppler effect can be presented as [3][4]

$$S_f(f)=\begin{cases}\dfrac{1}{\pi f_d\sqrt{1-\left(\dfrac{f-f_c}{f_d}\right)^2}} & |f|\le f_d \\ 0 & otherwise\end{cases} \tag{2.8}$$

where f_c is the carrier frequency, the frequency shifts of f are in the range $\pm f_d$ about the carrier frequency and are zero out side that range .The Doppler power spectrum is a classical U-shaped as seen in Fig 2-3.

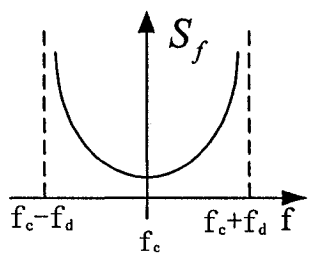

Figure 2-3. Doppler frequency spread

For our channel modeling efforts, our focus in this study is the multipath propagation effects for transmitter and/or receivers employing antenna arrays. In our later research, we will not take account the motion of the transmitter and/or receiver.

2.4 AOA Dispersion

Angular spread is the measure of the angle displacement due to non-LOS propagation with respect to the angle of LOS propagation. Figure 2.4 shows the angle displacement caused by the non-LOS propagation paths.

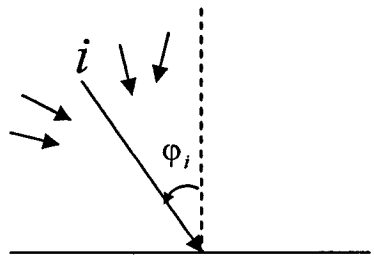

Figure 2-4. Multipath AOA dispersion

Similarly to delay spread, introduce mean AOA and angular spread of multipath[5] [6]. The mean AOA of N discrete multipath is defined as

$$\overline{\varphi} = \langle \varphi \rangle = \frac{1}{N} \sum_{i=1}^{N} \varphi_i \tag{2.9}$$

The root mean square (RMS) angular spread is

$$\sigma_\varphi = \sqrt{\langle \varphi^2 \rangle - \overline{\varphi}^2} \tag{2.10}$$

where $\langle \varphi^2 \rangle = \frac{1}{N} \sum_{i=1}^{N} \varphi_i^2$

If the number of multipath is large and the AOA of multipath is distributed according to a specific distribution $\rho(\varphi)$, then the angular spread is defined as[7][8]

$$S_\varphi = \sqrt{\oint_\theta (\varphi - \overline{\varphi})^2 \rho(\varphi) d\varphi} \tag{2.11}$$

where $\overline{\varphi} = \oint_\varphi \varphi \rho(\varphi) d\varphi$

2.5 Impulse Response Channel Model

In traditional single input single output (SISO), assuming the multipath channel is quasi-static, its channel impulse response has been represented as

$$h(t) = \sum_{i=1}^{N} a_i e^{j\theta_i} \delta(t - \tau_i) \tag{2.12}$$

where N is the number of multipath components, as mentioned before, the amplitude a_i is usually modeled as a Rayleigh distributed random variable, while the phase shift θ_i is uniformly distributed. The output of the traditional channel is

$$y(t) = h(t) * x(t) = \sum_{i=1}^{N} a_i e^{j\theta_i} x(t - \tau_i) \tag{2.13}$$

This equation is very useful model because it models the channel parameters including fading distribution, delay and Doppler spread. However, for multi-antenna system, one must consider the AOA of each multipath component, then the channel response need to be modified as

$$h(t, \varphi) = \sum_{i=1}^{N} a_i e^{j\theta_i} \delta(t - \tau_i, \varphi - \varphi_i) \tag{2.14}$$

2.6 Vector Channel Model

For multiple-in multiple-out (MIMO) system, we deploy a statistical multi-path vector channel model. For simplicity, only azimuth angles of incoming plane waves are considered in the propagation geometry (assume its elevation angle is 90°). Note the results can also be generalized to three dimensions. Here, we first define the array response vectors for uniform linear arrays (ULA) and uniform circular arrays (UCA), then give vector channel impulse response of MIMO channel with ULA/UCA.

Figure 2-5 shows a wireless communications system employing a uniform linear antenna array with evenly spaced receive elements. The antenna elements, assumed to be identical and omni directional, are uniformly distributed in a line.

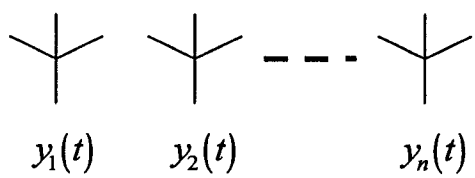

Figure 2-5. Uniform linear array

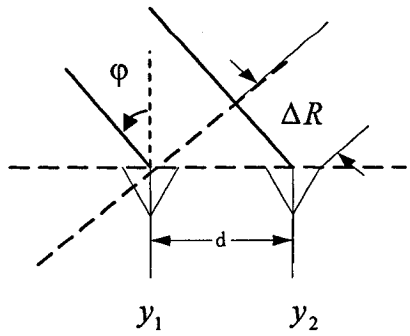

Figure 2-6. ULA geometry

Furthermore, we can use the phase of element 1 as reference point, hence $\Psi_1(\varphi)=0$, see Figure 2-6, the phase shift at i-th element is $\Psi_i(\varphi)=\frac{2\pi}{\lambda}\Delta R_i=\frac{2\pi}{\lambda}(i-1)d\sin\varphi$, where $\lambda=c/f$, λ is the wavelength, c is the speed of light , f is the carrier frequency and d is the adjacent antenna spacing. Define $z\triangleq 2\pi d/\lambda$, then $\Psi_i(\varphi)=(i-1)z\sin\varphi$. So the array manifold vector $\mathbf{v}(\varphi)$ for a single received plane wave in a uniform linear array with n receiver elements can be written as

$$\mathbf{v}(\varphi)=\begin{bmatrix} v_1(\varphi) \\ v_2(\varphi) \\ \vdots \\ v_n(\varphi) \end{bmatrix}=\begin{bmatrix} 1 \\ e^{-jz\sin\varphi} \\ \vdots \\ e^{-j(n-1)z\sin\varphi} \end{bmatrix} \tag{2.15}$$

Similarly, the geometry of UCA is shown in Fig 2-7, φ is the mean angle of arrival (AOA) of the incoming multi-path plane waves. Element i of the array is displaced by an angle $\theta_i=2\pi i/n$ from y-axis. The position vector at this location is $\mathbf{p}_i=(r\sin\theta_i, r\cos\theta_i)$. Consider a narrowband plane wave with wave number $k_0=2\pi/\lambda$ propagating in the direction $-\hat{\mathbf{r}}$, with azimuth φ . The unit vector is $\hat{\mathbf{r}}=(\sin\varphi,\cos\varphi)$. The phase difference between the complex envelopes of the signals received at the origin and at element i at given time is [9]

$$\Psi_i=e^{-jk_0\hat{\mathbf{r}}\cdot\mathbf{p}_i}=e^{-jk_0 r\cos(\varphi-\theta_i)} \tag{2.16}$$

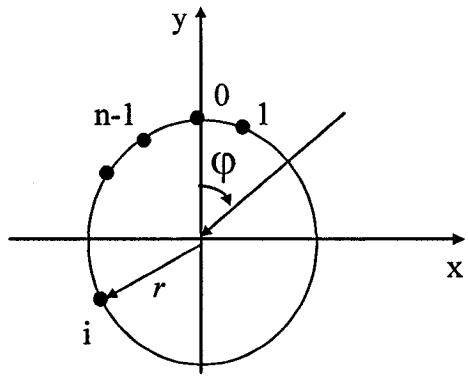

Figure 2-7. UCA geometry

Then the array manifold vector $\mathbf{v}(\varphi)$ for a single received plane wave in a uniform circular array can be written as

$$\mathbf{v}(\varphi)=\begin{bmatrix} v_1(\varphi) \\ v_2(\varphi) \\ \vdots \\ v_n(\varphi) \end{bmatrix}=\begin{bmatrix} e^{-j2\pi r\cos\varphi/\lambda} \\ e^{-j2\pi r\cos\left(\varphi-\frac{2\pi}{n}\right)/\lambda} \\ \vdots \\ e^{-j2\pi r\cos\left(\varphi-\frac{2\pi(n-1)}{n}\right)/\lambda} \end{bmatrix} \tag{2.17}$$

For N arriving plane multipath waves, the multipath vector channel impulse response for received antenna arrays can be presented as

$$\mathbf{h}(t,\tau)=\sum_{i=1}^{N}\mathbf{v}(\varphi_i)a_i e^{j\theta_i}\delta(t-\tau_i) \tag{2.18}$$

where $\mathbf{v}(\varphi_i)=\left[v_1(\varphi_i) \quad v_2(\varphi_i) \quad \cdots \quad v_n(\varphi_i)\right]^T$ is the array response vector for the i-th non-LOS propagation path, n is the number of array elements, $[\cdot]^T$ denotes transposition.

The output of the single-in multiple-out (SIMO) channel can be expressed as

$$\mathbf{Y}(t)=\mathbf{h}(t)*x(t)=\sum_{i=1}^{N}\mathbf{v}(\varphi_i)a_i e^{j\theta_i}x(t-\tau_i) \tag{2.19}$$

For flat fading channel, we can rewrite (2.19) as

$$\mathbf{Y}(t)=x(t)\cdot\sum_{i=1}^{N}\mathbf{v}(\varphi_i)a_i e^{j\theta_i} \tag{2.20}$$

If we assume that the $a_i\,(i=1,2,\ldots,N)$ are independent and identically distributed (i.i.d.) and independent of the φ_i, then $\sum_{i=1}^{N} v_m(\varphi_i)a_i e^{j\theta_i}$ for $m=1,2,\cdots,N$ will be a complex Gaussian random variable as the number of scatterers N becomes large according to the central limit theorem [10]. In such a case, the same as the conventional SISO, the envelope of the received signal $a_i\,(i=1,2,\ldots,N)$ has a Rayleigh distribution.

In [15] , the power azimuth-delay spectrum is defined as

$$P(\tau,\varphi)=E\{P_I(\tau,\varphi)\} \tag{2.21}$$

where $P_I(\tau,\varphi)=\sum_{i=1}^{N}|a_i|^2\,\delta(t-\tau_i,\varphi-\varphi_i)$ is defined as the instantaneous power azimuth-delay spectrum. Then the power azimuth spectrum is derived as

$$P_A(\varphi)=\int P(\tau,\varphi)d\tau \tag{2.22}$$

And power delay spectrum is respectively

$$P_D(\tau)=\int P(\tau,\varphi)d\varphi \tag{2.23}$$

The mean square value of a_i is always described as the channel power delay spectrum (PDS) , which has been investigated experimentally in numerous studies. It is found that the PDS is accurately modeled by a one-sided exponential decaying function as [11]

$$P_D(\tau)=\begin{cases} ce^{-\tau/\sigma_D} & \text{for } \tau>0 \\ 0 & \text{otherwise} \end{cases} \tag{2.24}$$

where the delay spread (DS) σ_D is the root second central moment of $P_D(\tau)$.

The power azimuth spectrum is not well researched as power delay spectrum, however, because the power azimuth spectrum depends on the spatial distribution of the scatters, there are several different PDFs for the azimuth distribution of the incident waves as seen from the receiver in the literature. In next two sections, we review the published power azimuth spectrum models.

2.7 Single Cluster PAS Models

2.7.1 Lee's Model

All the scatters are located on the circle (of radius R), mobile is located at the circle centre. The discrete scatters are equivalent scatters (represent composite effect of actual scatters).

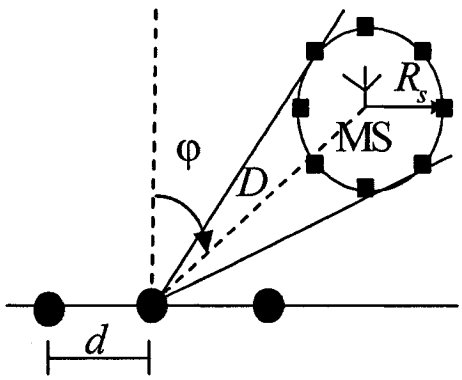

Figure 2-8. Lee's model

At the receiver array, the AOA of i-th multipath, which come from the i-th scatter can be approximately presented as

$$\varphi_i \approx \varphi + \frac{R_s}{D}\sin\left(\frac{2\pi i}{N_s}\right), i = 0,1,\ldots,N_s - 1 \tag{2.25}$$

where N_s scatterers and $R_s \ll D$ are assumed. Clearly, the multipath is confined in the single cluster ($\left[\varphi - \sin^{-1}(R_s/D), \varphi + \sin^{-1}(R_s/D)\right]$).

This model is one of the typical discrete scatters model, There are many other modified discrete scatter models based on Lee's model. These discrete scatter models are very useful in predicting the correlation between any two elements of the array, but they fail to include all the phenomena of radio propagation channel, such as delay spread and Doppler spread [12].

2.7.2 Cosine Model

[13] proposed a cosine function of the azimuth distribution as

$$\rho(\theta)=\begin{cases} c\bullet[\cos(\theta-\varphi)]^{n_c}, & \theta\in\left[-\frac{\pi}{2}+\varphi,\frac{\pi}{2}+\varphi\right] \\ 0 & otherwise \end{cases} \tag{2.26}$$

where c is a normalizing constant, which made $\rho(\theta)$ as a probability density function, hence

$$\int_0^{2\pi}\rho(\theta)d\theta=1 \tag{2.27}$$

The parameter n_c controls the angular spread

$$S_\theta=\int_{-\frac{\pi}{2}-\varphi}^{\frac{\pi}{2}+\varphi}(\theta-\varphi)^2\cdot c\left[\cos(\theta-\varphi)\right]^{n_c}d\theta \tag{2.28}$$

The larger n_c, the smaller the angular spread. Note although (2.28) can be computed analytically, the result is a sum of n_c terms of $\cos^{n_c}x$ and $\sin^{n_c}x$, it is not practical when n_c is large. This model has to be evaluated numerically.

2.7.3 Uniform Model

In [14], Salz and Winter proposed a model of multi-path arriving at the base station within ± Δ at mean arrive of angle φ. As shown in Fig 2-4, they assume the probability densities function of θ is to be uniformly distributed as

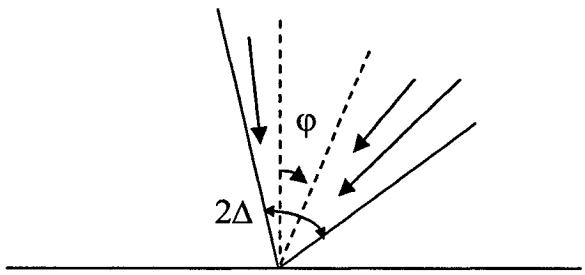

Figure 2-9. Uniform model

$$\rho(\theta)=\begin{cases} \frac{1}{2\Delta} & \theta\in[\varphi-\Delta,\ \varphi+\Delta] \\ 0 & \text{elsewhere} \end{cases} \tag{2.29}$$

All the components (waves) are concentrated within 2Δ of average AOA θ_0. Following equation (2.11), the angular spread is

$$S_\theta = \int_{\varphi-\Delta}^{\varphi+\Delta} (\theta-\varphi)^2 \cdot \frac{1}{2\Delta} d\theta = \frac{\Delta}{\sqrt{3}} \tag{2.30}$$

In [7], it is mentioned that a uniform spatial distribution of the scatterers does not lead to a uniform distribution of the AOAs and distributions of scatters that lead to a uniform distribution of AOAs are difficult to justify physically. However, because it is a good approximation of propagation channel, the uniform AOA model is widely used.

2.7.4 Truncated Gaussian Model

It is proposed in [3][15], that the azimuth distribution as

$$\rho(\theta) = \begin{cases} c_g \cdot e^{-\frac{(\theta-\varphi)^2}{2\sigma^2}}, & \theta \in \left[-\frac{\pi}{2}+\varphi, \frac{\pi}{2}+\varphi\right] \\ 0 & otherwise \end{cases} \tag{2.31}$$

c_g is a normalizing constant which made $\rho(\theta)$ as a probability density function, σ is standard deviation of power azimuth spectrum (PAS) which controls the angular spread. Following (2.27), it can be shown that

$$c_g = \frac{1}{\sqrt{2\pi}\sigma erf\left(\frac{\pi}{2\sqrt{2}\sigma}\right)} \tag{2.32}$$

Inserting (2.32) into (2.31) and then (2.11), after integration the angular spread is

$$S_\theta = c_g \int_{\frac{\pi}{2}+\varphi}^{\frac{\pi}{2}+\varphi} (\theta-\varphi)^2 e^{-\frac{(\theta-\varphi)^2}{2\sigma^2}} d\theta = \sigma \sqrt{1 - \frac{\sqrt{\frac{\pi}{2}} e^{-\frac{\pi^2}{8\sigma^2}}}{\sigma \cdot erf\left(\frac{\pi}{2\sqrt{2}\sigma}\right)}} \tag{2.33}$$

2.7.5 Truncated Laplacian Model

[16] proposed that the azimuth distribution as

$$\rho(\theta) = \begin{cases} c_l \cdot e^{-\frac{\sqrt{2}|\theta-\varphi|}{\sigma}}, & \theta \in \left[-\frac{\pi}{2}+\varphi, \frac{\pi}{2}+\varphi\right] \\ 0 & otherwise \end{cases} \tag{2.34}$$

where c_l is a normalizing constant, σ is standard deviation of power azimuth spectrum (PAS) which controls the angular spread. Similar to section 2.7.4 , we can derived the normalizing constant

$$c_l = \frac{1}{\sqrt{2}\sigma\left(1-e^{-\pi/\sqrt{2}\sigma}\right)} \tag{2.35}$$

And the angular spread is

$$S_\theta = \sqrt{c_l\left[\sqrt{2}\sigma^3 - \frac{\sigma}{2\sqrt{2}}e^{-\frac{\pi}{\sqrt{2}\sigma}}\left(\pi^2+4\sigma^2+2\sqrt{2}\pi\sigma\right)\right]} \tag{2.36}$$

Based on the measure of squared approximation error (SAE), [17] made a comparison of the goodness of fit of the Laplacian and Gaussian function for the measured power azimuth spectrum (PAS) for three different antenna heights. It shows that the Laplacian distribution gives the better match in both urban and rural area even in a non-LOS situation.

2.7.6 Von Mises Model

It was proposed in [18] that the azimuth distribution as

$$\rho(\theta) = \frac{e^{k_v\cos(\theta-\varphi)}}{2\pi I_0(k_v)}, \quad \varphi\in[-\pi,\pi] \tag{2.37}$$

where $I_0(.)$ is the zero-order modified Bessel function. The constant $k_v \geq 0$ controls the width of AOA. For $k_v = 0$, $\rho(\theta) = 1/2\pi$ is the isotropic scattering case (Clark model). For $k_v = \infty$, $\rho(\theta) = \delta(\theta-\varphi)$ (Dirac delta function) is the extremely non-isotropic scattering respectively. Note that the parameter k_v can be justified by empirical data .

2.8 Multi-cluster Models

2.8.1 Elliptical Sub-region Model

Lu et al. [19] proposed a model of multipath propagation based on the distribution of the scatters in elliptical sub-regions. The channel impulse is given by

$$h(t,t_0)=\sum_{i=1}^{N_s} E_t\left(\theta_i^{(t)}\right)\times\sum_{k=0}^{K_i}\alpha_{ik}e^{-(2\pi f_{ik}t_0+\gamma_{ik})}\delta\left(t-\tau_{ik}\right)E_r\left(\theta_{ik}\right) \tag{2.38}$$

where N_s is the number of scatters, and each scatter has K_i reflecting points, α_{ik}, τ_{ik} and γ_{ik} correspond to the amplitude, time delay, and phase of the signal component from the ik-th reflecting point, respectively. f_{ik} is the Doppler frequency shift of each individual path, θ_{ik} is the angle between the ik-th path and the receiver to transmitter direction, and $\theta_i^{(t)}$ is the angle of the i-th scatterer as seen from the transmitter. $E_t(\theta)$ and $E_r(\theta)$ are the radiation patterns of the transmitter and receiver antennas, respectively. The variable θ_{ik} are assumed to be Gaussian distributed as

$$\rho(\theta)=\frac{1}{\sqrt{2\pi\sigma}}e^{-\frac{1}{2\sigma}\left(\theta-\theta_i^{(r)}\right)^2} \tag{2.39}$$

where $\theta_i^{(r)}$ is the mean angle of path components around the i-th scatterer as seen from the receiver. Note that the truncated Gausssian distribution is used in single cluster multipath channel model (refer to section 2.7.4).

2.8.2 Modified Saleh-Valenzuela's Model

Saleh and Valenzula developed a multipath channel model for indoor environment based on the clustering phenomena observed in experimental data [20] . Spencer et al. proposed an extension to the Saleh-Valenzuela's model [21] , assuming the time and the angle are statistically independent. The impulse response is given by

$$h(t,\theta)=h(t)h(\theta) \tag{2.40}$$

$$h(t)=\sum_{i=0}^{\infty}\sum_{j=0}^{\infty}\alpha_{ij}\delta\left(t-T_i-\tau_{ij}\right),\quad h(\theta)=\sum_{i=0}^{\infty}\sum_{j=0}^{\infty}\alpha_{ij}\delta\left(\theta-\Theta_i-\omega_{ij}\right) \tag{2.41}$$

where α_{ij} is the amplitude of the j-th ray in the i-th cluster, the variable α_{ij} are Rayleigh distributed with the mean square valued described by a double-exponential decay given by $\overline{\alpha_{ij}^2}=\overline{\alpha_{00}^2}e^{-T_i/\Gamma}e^{\tau_{ij}/\gamma}$, Γ and γ are the cluster and ray time decay constant, respectively. The variable Θ_i is the mean angle of the i-th cluster and is assumed to be uniformly

distributed in $[0,\ 2\pi]$. The variable ω_{ij} corresponds to the ray angle within a cluster and is model as a Laplacian distributed random variable with zero mean and standard deviation σ. The probability function can be written as

$$p(\omega)=\frac{1}{\sqrt{2}\sigma}e^{-\left|\frac{\sqrt{2}\omega}{\sigma}\right|} \tag{2.42}$$

Note that the truncated Laplacian distribution is used in single cluster multipath channel model (refer to section 2.7.5).

2.8.3 WSSUS Model

Assume that different scatters are not correlated with each other, hence the multipath delay time is uncorrelated, and then the channel correlation can be represented as [22]

$$R(\tau_1,\tau_2)=\left\langle h(t_1,\tau_1)h^*(t_2,\tau_2)\right\rangle=R_t(t_1,t_2)\delta(\tau_1-\tau_2) \tag{2.43}$$

Furthermore, $R_t(t_1,t_2)=R_t(t_1-t_2)$ depends on Δt but not on t_1 or t_2 individually. The signal at receiver can be represented as [23]

$$\mathbf{x}_b(t)=\sum_{k=1}^{N_c}\mathbf{v}_{k,b}s(t-\tau_k) \tag{2.44}$$

where $s(t-\tau_k)$ is the source signal $s(t)$ delayed by the k-th cluster delay τ_k, $\mathbf{v}_{k,b}=\sum_{i=1}^{N_c}\alpha_{k,i}e^{j\varphi_{k,i}}a(\theta_{0k}-\theta_{k,i})$ is the superposition of the steering vectors during the b-th data burst within k-th cluster. N_c denotes the number of scatters in the k-th cluster, if it is large, the elements of $v_{k,b}$ are Gaussian distributed. In this model, second-order statistics of the channel does not change in time (in practice, true for not too many periods of time). If we further assume that $\alpha_{k,i}$ are complex Gaussian, then it becomes Gaussian Wide Sense Stationary Uncorrelated Scattering (GWSSUS) model [24]. For special case, if $N_c=1$ (Single cluster), the model is a narrowband channel model that is valid when the time spread of the channel is small compared to the inverse of the signal bandwidth, if further assume AOA statistics as Gaussian distributed about nominal angle, then this model reduces to Gaussian Angle of Arrival (GAA) model [25].

2.8.4 Proposed PAS Model

Outdoor measurement in typical urban environments shows that the azimuth is distributed in multi clusters [21][26]. Pedersen et. al [26] found two clusters in their measurements . The 1st cluster corresponds to the power coming directly from the MS. The 2nd cluster is contributed by waves which propagate over a river and are then reflected on building fronts located on the north side of the river back to the base station. (see Figure 2-10).

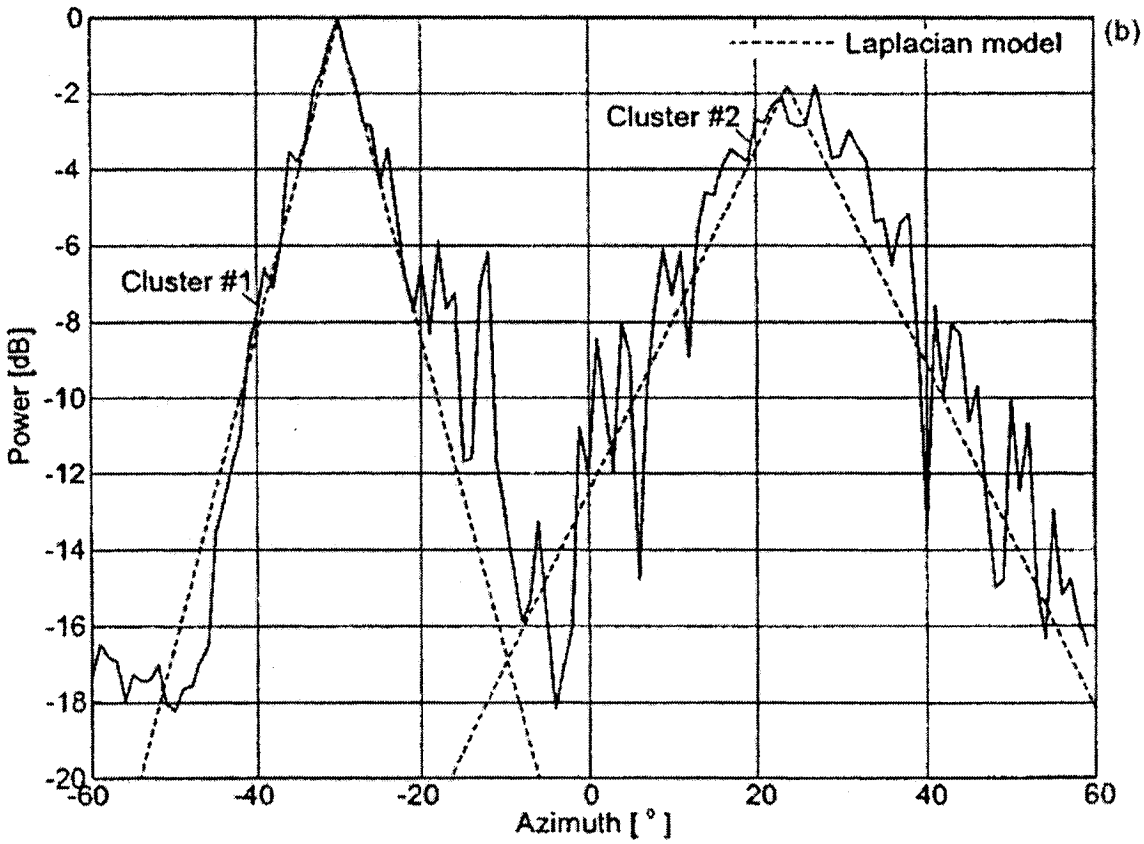

Figure 2-10. PAS with two clusters in measurement [26]

Hence, the one cluster model cannot be applied in this case. Because situations with more that two clusters may also appear, we extend one cluster channel model to multi-cluster one assuming that multipath components arriving in N_c clusters are uncorrelated (note that this assumption is justified by the physical mechanism of clustering) and uniformly angular-distributed within the corresponding clusters. The scenario is shown in

Figure 2-11. Note that other angular distribution within each cluster such as truncated Gaussian, Laplacian distribution can also be deployed in this multi-cluster channel model.

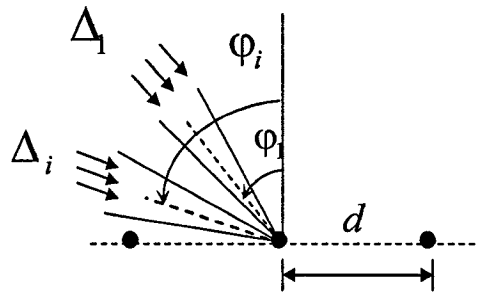

Figure 2-11. Multi-clusters of multipath model

The probability densities function of θ is to be uniformly distributed as

$$\rho(\theta)=\begin{cases}\dfrac{1}{\sum_{i=1}^{N_c}\Delta_i} & \theta\in\left[\varphi_i-\dfrac{\Delta_i}{2},\varphi_i+\dfrac{\Delta_i}{2}\right] \\ 0 & \text{otherwise}\end{cases} \tag{2.45}$$

2.9 Summary

In this chapter , We extended single cluster model to multi-cluster one. This multi-cluster model enables us to study the MIMO element crosscorrelation more accurately. It also permits for the analysis of MIMO capacity and performance more practically. There are in principle no limitations on the number of AOA clusters. In later chapters, we will study MIMO spatial correlation and performance in detail. The contributions in this chapter include:

- Reviewed the characteristics of wireless propagation channel, such as signal attenuation, time dispersion, and frequency dispersion for conventional single-input single-output (SISO) system, and the angle of arrival (AOA) signal dispersion for MIMO systems.
- Derived vector channel model using both uniform linear array (ULA) and uniform circular array (UCA) for SIMO channel

- Reviewed various power azimuth spectrum (PAS) in single cluster channle model
- Reviewed multi-cluster channel models
- Extented sigle cluster channel model to multi-cluster channel model

Chapter 3 Spatial Fading Correlation of MIMO Channel

3.1 Introduction

In this chapter, based on the uniform AOA propagation model, we first derive analytical expressions for spatial fading correlation of the MIMO channel as function of antenna spacing and angle spread. Then we extend the result from single cluster uniform AOA model to two-cluster model, which is the fundamental case of the multi-cluster model. Both the UCA and ULA are considered for MIMO systems. The analytical correlation expressions derived here can be used for estimating the information-theoretic channel capacity and diversity gain of MIMO systems. The information-theoretic channel capacity and diversity gain of MIMO systems will be discussed in detail in Chapter 4 and Chapter 5.

3.2 Single Cluster Uniform PAS MIMO Channel Model

For simplicity, we consider the case of a flat fading channel. We assume a multi-element receive array in a mobile cellular environment, also assume all transmitters are statistically independent and have the same statistics. Both a ULA and a UCA are considered in this section. For AOA dispersion, we use uniform model, the distribution of AOA of multipath is given in section 2.4.2

3.2.1 Single Cluster Model with ULA

For uniform spatial correlation model (see Figure 3-1), multi-path is arriving at the base station within $\pm\Delta$ of the mean angle φ.

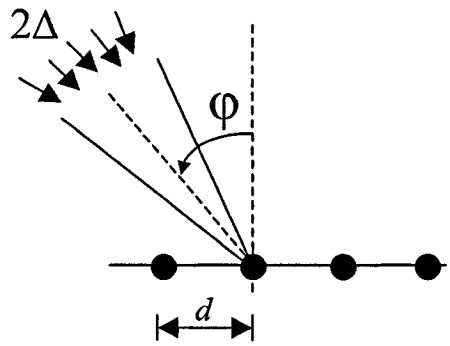

Figure 3-1. ULA geometry with one-cluster model

3.2.1.1 Analytical Results

As depicted in Fig 3.1, the distribution of multipath $\rho(\theta)$ is given by equation (2.29), and array manifold vector is given by equation (2.14). Then the spatial correlation between the *i*-th and *k*-th antenna receiver element is

$$R_{ik} = \int_0^{2\pi} v_i v_k^* \rho(\theta) d\theta = \frac{1}{2\Delta} \int_{\varphi-\Delta}^{\varphi+\Delta} e^{jz(i-k)\sin\theta} d\theta \tag{3.1}$$

where $z = 2\pi d / \lambda$, d is the inter-element distance, λ is the wavelength, 2Δ is the angular spread of the incoming multipath. φ is the average angle of arrival of the cluster, and j is the imaginary unit.

Salz and Winters [14] derived a closed-form expression for (3.1) as

$$R_{ik} = R_{xx} + jR_{xy} \tag{3.2}$$

$$R_{xx} = J_0[(i-k)z] + 2\sum_{m=1}^{\infty} J_{2m}[(i-k)z]\cos(2m\varphi)\mathrm{sinc}(2m\Delta) \tag{3.3}$$

$$R_{xy} = \sum_{m=0}^{\infty} J_{2m+1}[(i-k)z]\sin[(2m+1)\varphi]\mathrm{sinc}[(2m+1)\Delta] \tag{3.4}$$

where the Jm's are Bessel Functions of integer order, $\mathrm{sinc}(x) \triangleq \frac{\sin x}{x}$.

For general distribution of scatters, Teal, Abhayapala and Kennedy give a theoretical expression for spatial correlation [27]

$$\rho(\mathbf{x}_2-\mathbf{x}_1)=\sum_{m=-\infty}^{\infty} j^m\gamma_m J_m\left(\frac{2\pi}{\lambda}\|\mathbf{x}_2-\mathbf{x}_1\|\right) \tag{3.5}$$

where $\mathbf{x}_2$ and $\mathbf{x}_1$ are antenna elements location vector, J_m's are Bessel Functions of integer order, and $\gamma_m=\int_0^{2\pi}\rho(\theta)e^{-jm\theta}d\theta$, $\rho(\theta)$ is the probability density function of multipath AOA. For single cluster uniform AOA multipath channel model, $\rho(\theta)$ is defined as in equation (2.29), following (3.5), we have

$$\gamma_m=\frac{1}{2\Delta}\int_{\varphi-\Delta}^{\varphi+\Delta} e^{jm\theta}d\theta=e^{-jm\varphi}\mathrm{sinc}(m\Delta) \tag{3.6}$$

Then we derive another expression for R_{ik} as

$$R_{ik}=\sum_{m=-\infty}^{\infty} j^m e^{-jm\varphi}\mathrm{sinc}(m\Delta)J_m[(i-k)z] \tag{3.7}$$

Now we show that these two different closed-form expressions, (3.2) and (3.7), are equivalent. Actually in (3.7), if $m=2l$ (l is integer)

$$R_{ik}=\sum_{m=-\infty}^{\infty} j^m e^{-jm\varphi}\mathrm{sinc}(m\Delta)J_m[(i-k)z]$$

$$=J_0[(i-k)z]+\sum_{l=1}^{\infty}e^{-j2l\varphi}\mathrm{sinc}(2l\Delta)J_{2l}[(i-k)z]+\sum_{l=-\infty}^{-1}e^{-j2l\varphi}\mathrm{sinc}(2l\Delta)J_{2l}[(i-k)z]$$

Substituting $l=-l$, $\mathrm{sinc}(-x)=\mathrm{sinc}(x)$, and $J_{-n}(x)=(-1)^n J_n(x)$ in the third term, we have

$$R_{ik}=J_0[(i-k)z]+\sum_{l=1}^{\infty}e^{-j2l\varphi}\mathrm{sinc}(2l\Delta)J_{2l}[(i-k)z]+\sum_{l=1}^{\infty}e^{j2l\varphi}\mathrm{sinc}(2l\Delta)J_{2l}[(i-k)z]$$

$$=J_0[(i-k)z]+\sum_{l=1}^{\infty}(e^{-j2l\varphi}+e^{j2l\varphi})\mathrm{sinc}(2l\Delta)J_{2l}[(i-k)z]$$

$$=J_0[(i-k)z]+2\sum_{l=1}^{\infty}\cos(2l\varphi)\mathrm{sinc}(2l\Delta)J_{2l}[(i-k)z]$$

If $m=2l-1$ (l is integer), one obtains

$$R_{ik} = \sum_{m=-\infty}^{\infty} j^m e^{-jm\varphi} \mathrm{sinc}(m\Delta) J_m[(i-k)z]$$

$$= \sum_{l=1}^{\infty} j e^{-j(2l-1)\varphi} \mathrm{sinc}[(2l-1)\Delta] J_{2l-1}[(i-k)z] + \sum_{l=-\infty}^{0} j e^{-j(2l-1)\varphi} \mathrm{sinc}[(2l-1)\Delta] J_{2l-1}[(i-k)z]$$

$$= \sum_{l=1}^{\infty} j e^{-j(2l-1)\varphi} \mathrm{sinc}[(2l-1)\Delta] J_{2l-1}[(i-k)z] - \sum_{l=1}^{\infty} j e^{j(2l-1)\varphi} \mathrm{sinc}[(2l-1)\Delta] J_{2l-1}[(i-k)z]$$

$$= 2\sum_{l=0}^{\infty} j \sin[(2l+1)\varphi] \mathrm{sinc}[(2l+1)\Delta] J_{2l}[(i-k)z]$$

The computation convergence in both (3.2)and (3.7) are slow [27][28]. For the sake of computation efficiency, a very good approximation for small angular spread Δ ($\varphi = 0$ case) was given as [28]

$$R_{ik} = \mathrm{sinc}[(i-k)z\Delta] \tag{3.8}$$

For small angular spread Δ ($\varphi \neq 0$ case), we have

$$R_{ik} = \frac{1}{2\Delta} \int_{\varphi-\Delta}^{\varphi+\Delta} e^{jz(i-k)\sin\theta} d\theta \approx \mathrm{sinc}[(i-k)z\Delta\cos\varphi] e^{jz\sin\varphi} \tag{3.9}$$

3.2.1.2 Simulation Results

(1). For validation purpose, we set incident angle $\varphi = 0°, 60°, 90°$ and angular spread $s_\varphi = 1°, 3°, 5°, 10°, 20°, 40°, 52°, 104°$ which was used in [8]. We deploy Monte-Carlo simulation to get the envelope correlations , see Figure 3-2,Figure 3-3 and Figure 3-4, our results are very similar to the published results in [8]. Note that the envelope correlation is defined as [8]

$$\rho_{env} = \frac{E^2[x_1 x_2] + E^2[x_1 y_2]}{E^2[x_1^2]} = \rho_{real}^2 + \rho_{imag}^2 \tag{3.10}$$

where $E[.]$ denotes expectation over location (space), $x_i(y_i)$ is the real (imaginary) part of the signal at antenna element i. The magnitude of correlation coefficient in (3.1) is

$$R_{12} = \sqrt{\rho_{env}} = \sqrt{\rho_{real}^2 + \rho_{imag}^2} = \sqrt{R_{xx}^2 + R_{yy}^2} \tag{3.11}$$

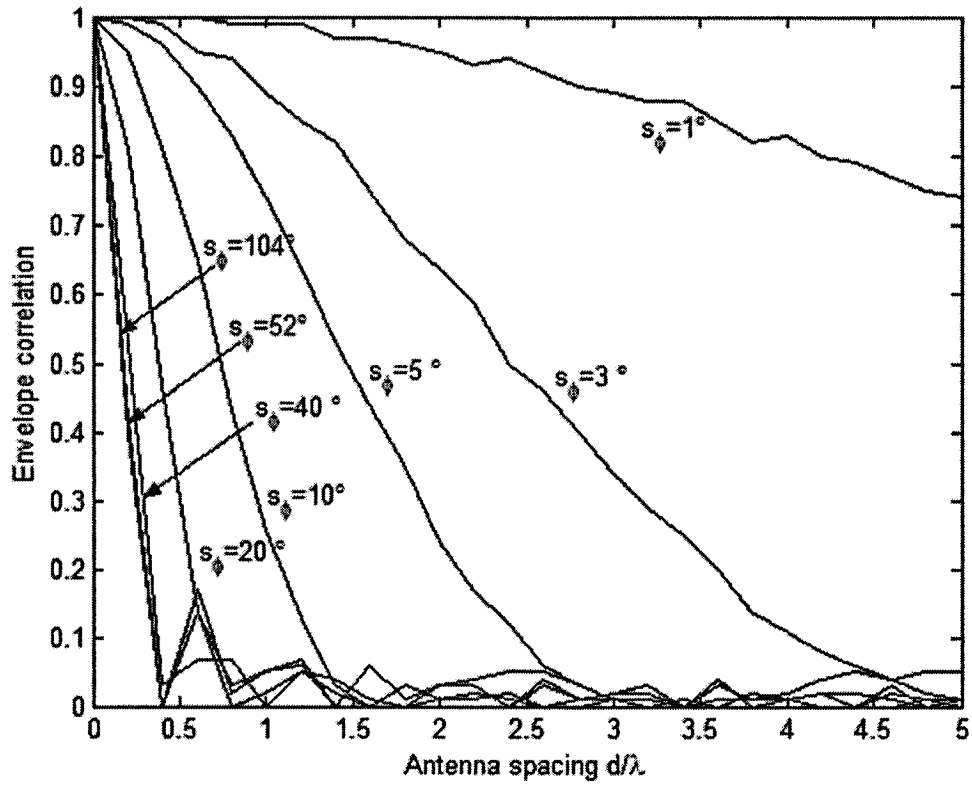

Figure 3-2. Envelope correlation coefficient for $\varphi = 0°$ versus antenna spacing with angular spread s_φ as parameter, uniform APS

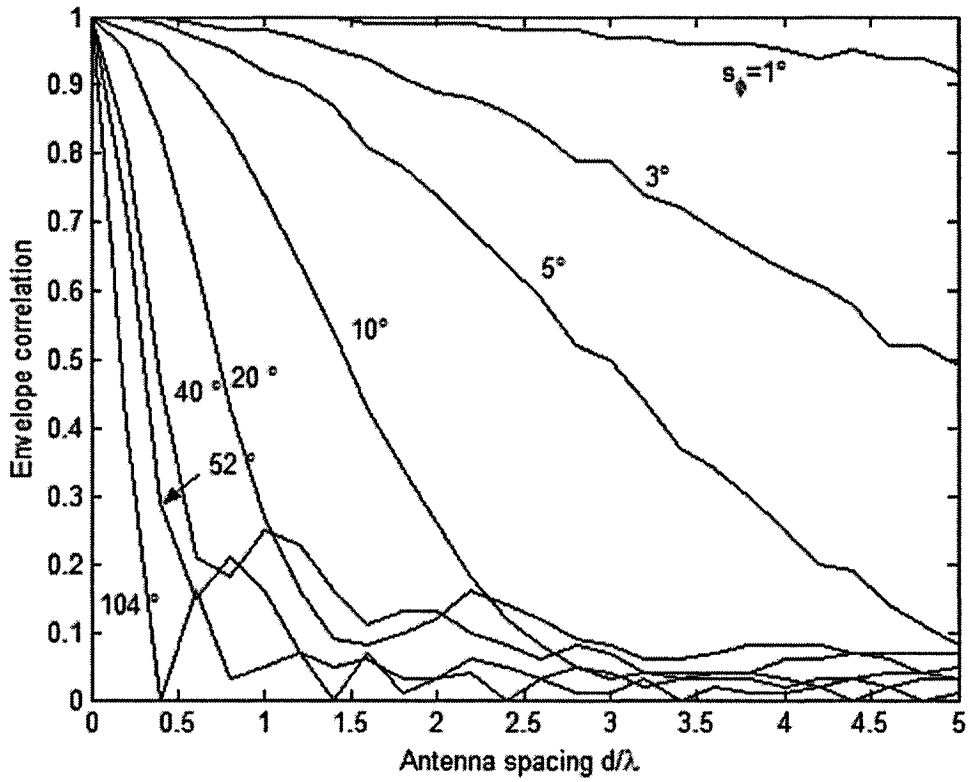

Figure 3-3. Envelope correlation coefficient for $\varphi = 60°$ versus antenna spacing with angular spread s_φ as parameter, uniform APS

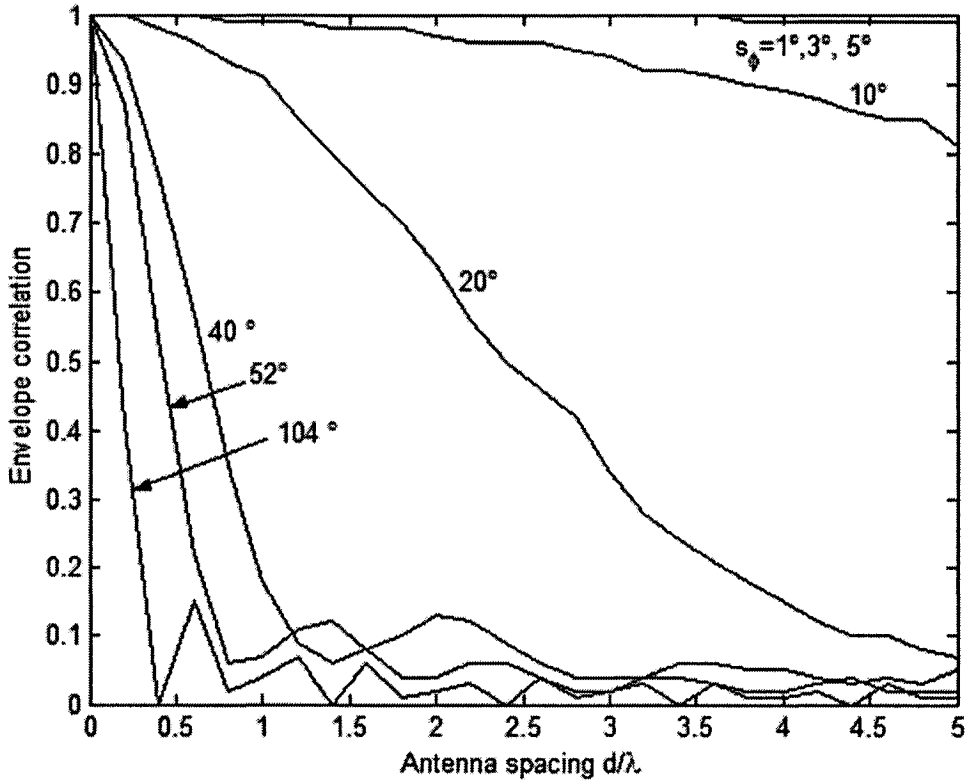

Figure 3-4. Envelope correlation coefficient for $\varphi = 90°$ versus antenna spacing with angular spread s_φ as parameter, uniform APS

(2). We use the Monte Carlo simulation results to compare with equation (3.9) (see Figure 3-5). The simulation results agree well with the analytical results.

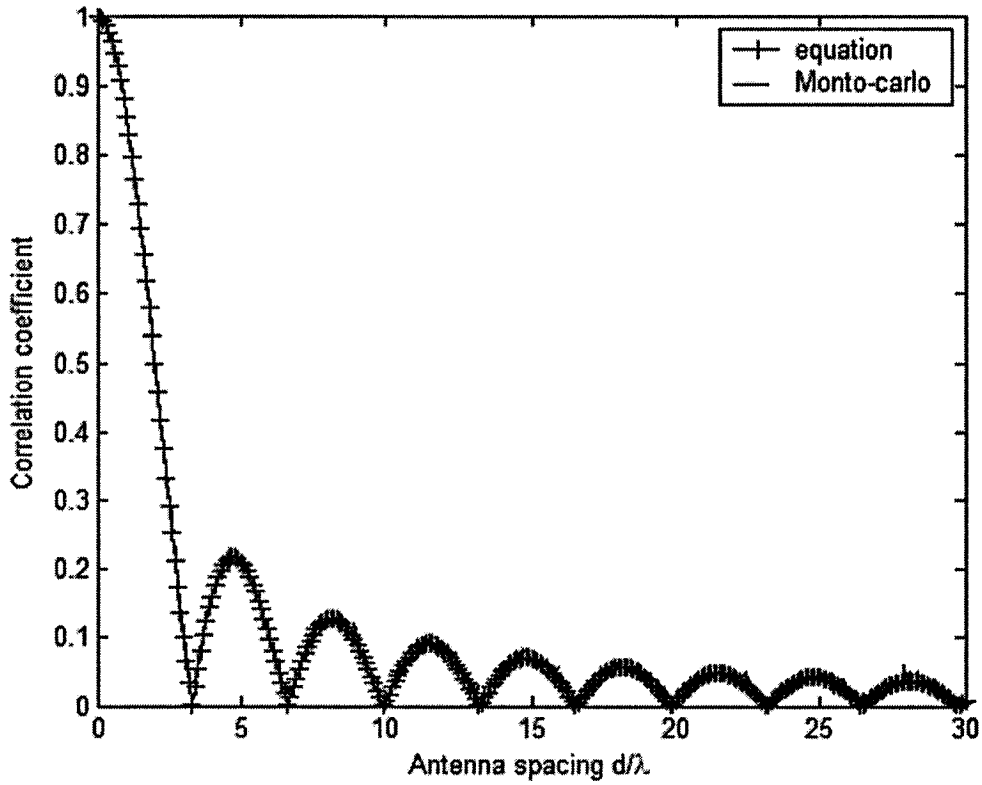

Figure 3-5. Correlation coefficient for angle of incident $\varphi = 30°$ versus antenna spacing with analytical expressions, uniform APS

3.2.2 Single Cluster Model with UCA

For uniform circular array (see Figure 3-6), we use the same geometry for the vector channel derived in section 2.6.

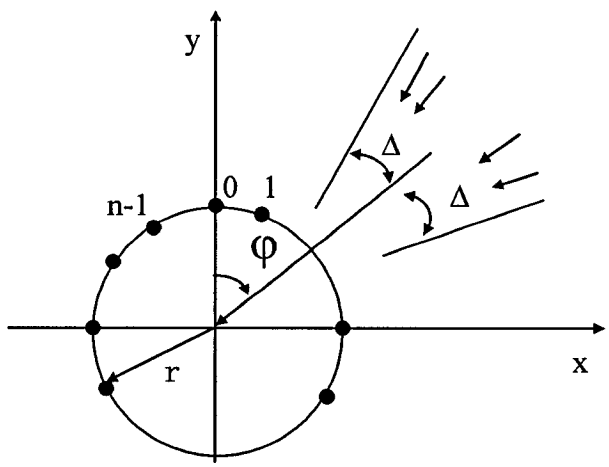

Figure 3-6. UCA geometry with one-cluster model

3.2.2.1 Analytical Results

The channel model is shown in Figure 3-6, and the array manifold vector is given by equation (2.17). The spatial correlation between the *i*-th and *k*-th antenna receiver element is

$$R_{ik} = \int_0^{2\pi} v_i v_k^* \rho(\theta) d\theta = \frac{1}{2\Delta} \int_{\varphi-\Delta}^{\varphi+\Delta} e^{-jz_{ik}\sin(\alpha_{ik}+\beta)} d\beta = \frac{1}{2\Delta} \int_{\varphi+\alpha_{ik}-\Delta}^{\varphi+\alpha_{ik}+\Delta} e^{-jz_{ik}\sin\beta} d\beta \tag{3.12}$$

where $z_{ik} = \frac{2\pi}{\lambda} 2r \sin\left[\frac{\varphi_i - \varphi_k}{2}\right], \alpha_{ik} = -\frac{\varphi_i + \varphi_k}{2}$, and φ_i is the azimuth of i-th element , $i = 0,1,\ldots,n-1$. Now we define the adjacent element spatial correlations on the circular array. From equation (3.12) we have

$$R_i = R_{i(i+1)} = \frac{1}{2\Delta} \int_{\varphi-\alpha_i-\Delta}^{\varphi-\alpha_i+\Delta} e^{jz_i\sin\beta} d\beta = \frac{1}{2\Delta} \int_{\varphi-\alpha_i-\Delta}^{\varphi-\alpha_i+\Delta} e^{jkd\sin\beta} d\beta \tag{3.13}$$

where $z_i = z_{i(i+1)} = \frac{2\pi}{\lambda} 2r \sin\frac{\pi}{n} = kd$, $\alpha_i = \alpha_{i(i+1)} = \frac{\pi}{n}(2i+1), i = 0,1,\ldots,n-1$, d is the spacing between the adjacent elements, α_i is central angle between the i-th and (i+1)-th elements. When we vary the index i from 0 to $n-1$ to move around the circle, in fact we actually keep the adjacent antenna spacing and change the mean AOA $\varphi - \alpha_i$ from φ to $\varphi + 2\pi$. The effect is the same as that of rotation of two elements with spacing d around the circle (see Figure 3-7). Note that R_i is a periodical function with period $[0, 2\pi]$. We can predict that R_i should change periodically when we move the index i around the circle. The minimum adjacent correlation occurs at the element pair number $i = 0, [n/2]$, whose AOA is orthogonal to the income signal ($\varphi - \alpha_i = \frac{\pi}{n}, \pi + \frac{\pi}{n}$), and the maximum lies at the element pair number $i = [n/4], [3n/4]$, whose AOA is "inline" direction to the income signal respectively ($\varphi - \alpha_i = \frac{\pi}{2} + \frac{\pi}{n}, \frac{3\pi}{2} + \frac{\pi}{n}$).

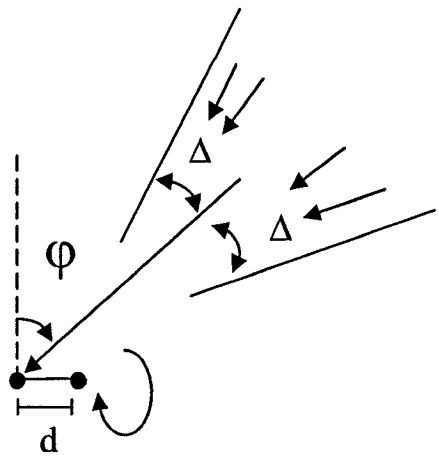

Figure 3-7. UCA adjacent element rotating model

3.2.2.2 Simulation Results

We use Monte-Carlo simulation to find the adjacent elements spatial correlation (equation (3.13)), the maximum adjacent elements spatial correlation (equation 3.11). We assume the incoming signal cluster angular spread (Δ) is $10°$, number of multipath is 20, number of elements is $n = 10$, and the radius of UCA is $r = 22.5\lambda$.

As expected the adjacent correlation changes periodically when we move around the circle (See Figure 3-8). There are 10 elements, the adjacent elements spacing is about $13.9\,\lambda$, which results almost zero correlation in ULA case. There are two peaks of $R \approx 0.9$ at $n = 3$ and 8, and hence these 2 pairs of elements (3, 4) and (7, 8) are highly correlated, which results in the channel capacity loss of UCA. It seems like there are some elements that are "lost" in UCA compared with ULA.

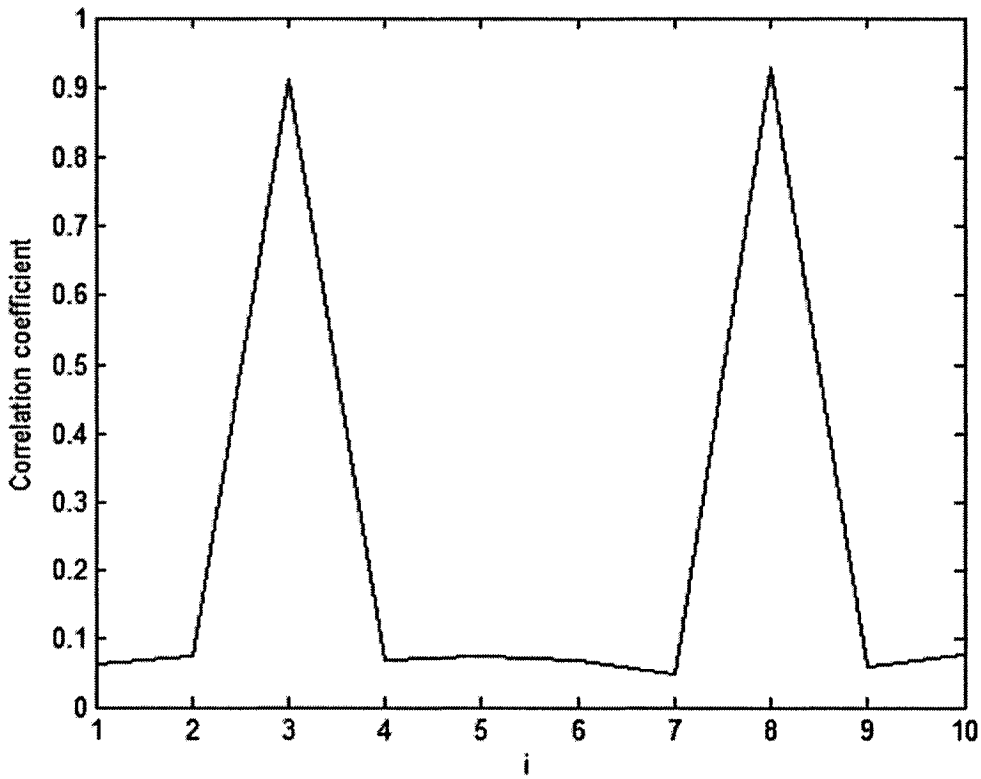

Figure 3-8. UCA adjacent elements correlation for n=10, single cluster angular spread $\Delta = 10°$, the radius of UCA $r = 22.5\lambda$, $\varphi = 0°$

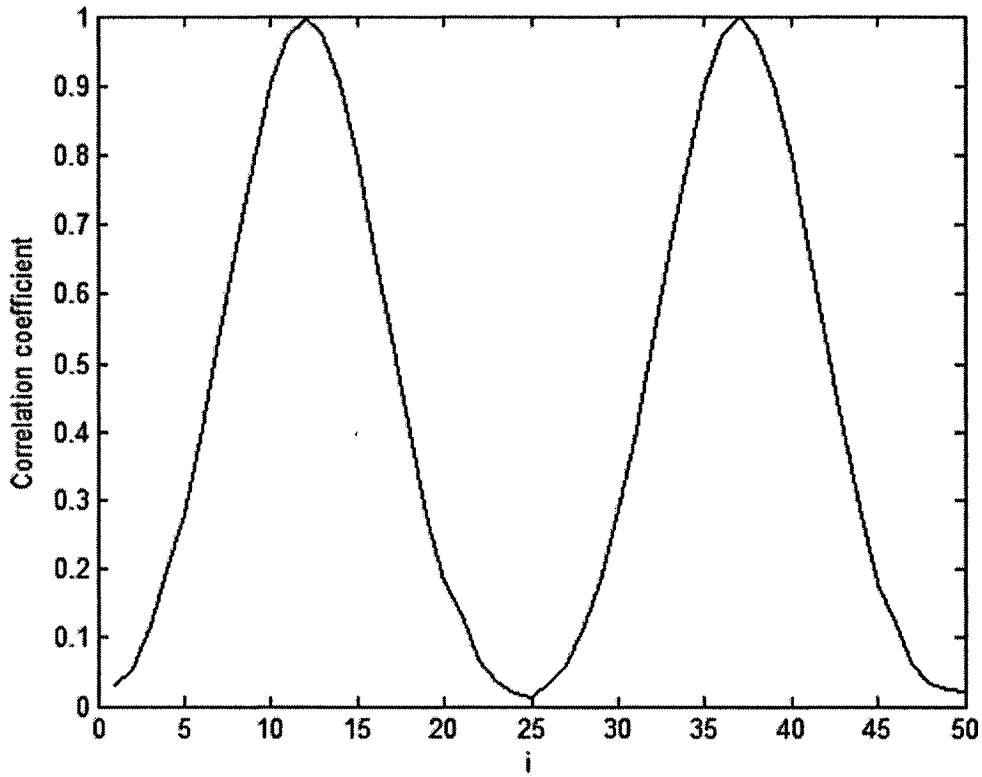

Figure 3-9. UCA adjacent elements correlation for n=50, single cluster angular spread $\Delta = 10°$, the radius of UCA $r = 22.5\lambda$, $\varphi = 0°$

If we keep the same radius of UCA and increase the receiver number of elements, the adjacent spacing becomes much smaller (about 2.8λ), the adjacent correlation also changes periodically (see Figure 3-9), and the only difference is that the maximum correlation for $n = 50$ is 1. The maximum adjacent correlation is supposed to become larger and larger with the number of elements increasing. However, it actually comes out oscillating (see Figure 3-10). These results in the capacity oscillation with the number of elements increasing.

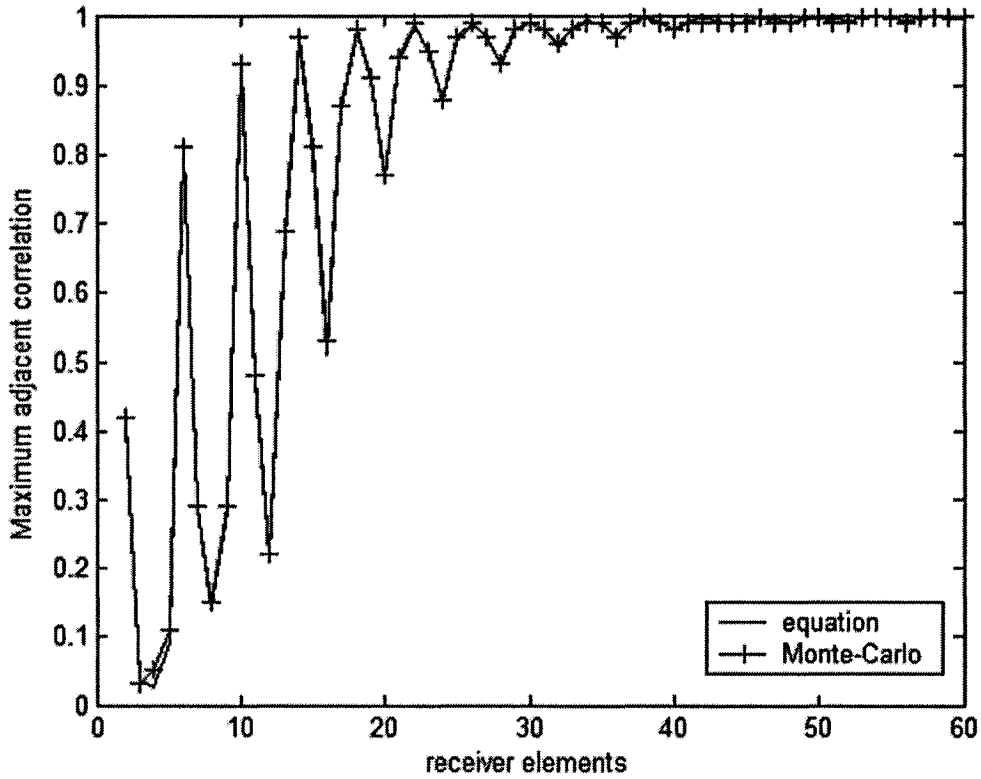

Figure 3-10. UCA maximum adjacent elements correlation versus number of elements, single cluster angular spread $\Delta = 10°$, the radius of UCA $r = 22.5\lambda$, $\varphi = 0°$

3.3 Two-cluster Uniform PAS MIMO Channel Model

Based on the multi-cluster channel model developed in Section 2.4.6, we deploy two-cluster model for ULA, as shown in Figure 3-11.

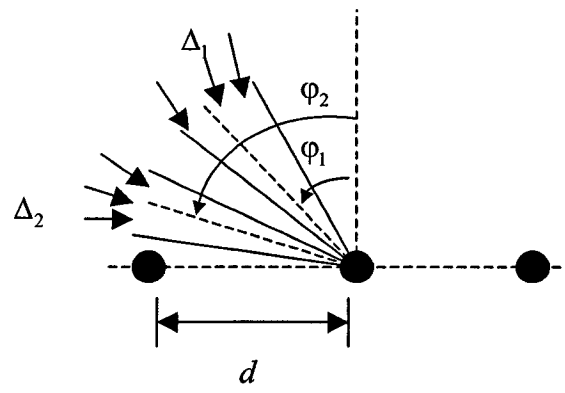

Figure 3-11. Two-cluster multipath channel model in MIMO channel

We assume the multipath components arriving in different clusters are statistically independent, the probability densities function of φ_i is to be uniformly distributed. The power of incoming multipath is allocated uniformly in two clusters. The probability density function (PDF) of the angle of arrival (AOA θ) can be written as

$$\rho(\theta)=\begin{cases}\dfrac{1}{\Delta_1+\Delta_2} & -\dfrac{\Delta_1}{2}+\varphi_1\le\theta\le\dfrac{\Delta_1}{2}+\varphi_1,-\dfrac{\Delta_2}{2}+\varphi_2\le\theta\le\dfrac{\Delta_2}{2}+\varphi_2\\ 0 & \text{elsewhere}\end{cases} \tag{3.14}$$

3.3.1 Analytical Results

The spatial correlation coefficient between adjacent antenna array elements can be written as

$$R=\frac{1}{\Delta_1+\Delta_2}\left\{\int_{\varphi_1-\frac{\Delta_1}{2}}^{\varphi_1+\frac{\Delta_1}{2}}\exp(\,jz\sin\,\beta)d\beta+\int_{\varphi_2-\frac{\Delta_2}{2}}^{\varphi_2+\frac{\Delta_2}{2}}\exp(\,jz\sin\,\beta)d\beta\right\} \tag{3.15}$$

where $\Delta_i(i=1,2)$ is the angle spread of the $1^{st}(2^{nd})$ cluster of the incoming multipath, $\varphi_{1(2)}$ is the average angle of arrival of the $1^{st}(2^{nd})$ cluster. Note that for i-th and k-th elements correlation coefficient, just replace z with $(i-j)z$ in equation (3.14). Making use of well-known series representations,

$$\begin{aligned}\cos(\,z\cos\,\theta)&=J_0(z)+2\sum_{m=1}^{\infty}J_{2m}(z)\cos(\,2m\theta)\\ \sin(\,z\sin\,\theta)&=2\sum_{m=0}^{\infty}J_{2m+1}(z)\sin[(\,2m+1)\theta]\end{aligned} \tag{3.16}$$

we can rewrite equation (3.15) as

$$R=R_{real}+jR_{imag} \tag{3.17}$$

$$R_{real}=J_0(z)+2\sum_{m=1}^{\infty}J_{2m}(z)\frac{\cos(2m\varphi_1)\sin(m\Delta_1)+\cos(2m\varphi_2)\sin(m\Delta_2)}{m(\Delta_1+\Delta_2)} \tag{3.18}$$

$$R_{imag}=2\sum_{m=0}^{\infty}J_{2m+1}(z)\frac{\sin[(2m+1)\varphi_1]\sin\dfrac{(2m+1)\Delta_1}{2}+\sin[(2m+1)\varphi_2]\sin\dfrac{(2m+1)\Delta_2}{2}}{(2m+1)\dfrac{\Delta_1+\Delta_2}{2}} \tag{3.19}$$

For validation purpose, let two clusters $((\Delta_1,\varphi_1),(\Delta_2,\varphi_2))$ merger to one bigger cluster with the mean AOA $\varphi=\varphi_1+\frac{\Delta_2}{2}=\varphi_2-\frac{\Delta_1}{2}$ and the angle spread $\Delta=\Delta_1+\Delta_2$. The correlation using two-cluster channel model must be "physically" consistent with that using single cluster channel model. Actually for one cluster channel model with mean AOA $\varphi=\varphi_1+\frac{\Delta_2}{2}=\varphi_2-\frac{\Delta_1}{2}$ and angle spread $\Delta=\Delta_1+\Delta_2$, from (3.2)-(3.4), the correlation can be expressed as

$$R = R_{xx} + jR_{xy} \tag{3.20}$$

$$R_{xx} = J_0(z)+2\sum_{m=1}^{\infty} J_{2m}(z)\cos[2m(\varphi_1+\frac{\Delta_2}{2})]\sin c(2m\frac{\Delta_1+\Delta_2}{2}) \tag{3.21}$$

$$R_{xy} = \sum_{m=0}^{\infty} J_{2m+1}(z)\sin[(2m+1)(\varphi_1+\frac{\Delta_2}{2})]\sin c[(2m+1)\frac{(\Delta_1+\Delta_2)}{2} \tag{3.22}$$

It can be readily checked that $R_{real}=R_{xx}, R_{imag}=R_{xy}$

We have shown that the more compact closed-form expression in (3.7) is equivalent with equations (3.2)-(3.4) using one cluster channel model. Here we derive a more compact expression using two-cluster channel model. The AOA distribution $\rho(\theta)$ is given in (3.14), the correlation coefficient between i-th and k-th elements can be presented as

$$R_{ik} = \sum_{m=-\infty}^{\infty} j^m \gamma_m J_m[(i-k)z] \tag{3.23}$$

where

$$\begin{aligned}\gamma_m &= \int_0^{2\pi} p(\theta)e^{-jm\varphi}d\theta = \frac{1}{\Delta_1+\Delta_2}\left(\int_{\varphi_1-\frac{\Delta_1}{2}}^{\varphi_1+\frac{\Delta_1}{2}} e^{jm\theta}d\theta + \int_{\varphi_2-\frac{\Delta_2}{2}}^{\varphi_2+\frac{\Delta_2}{2}} e^{jm\theta}d\theta\right) \\ &= \frac{e^{-jm\varphi_1}\sin(m\Delta_1/2)+e^{-jm\varphi_2}\sin(m\Delta_2/2)}{m(\Delta_1+\Delta_2)/2}\end{aligned} \tag{3.24}$$

Using the same validation method as before, let two clusters $((\Delta_1,\varphi_1),(\Delta_2,\varphi_2))$ merge into one bigger cluster with mean AOA $\varphi=\varphi_1+\frac{\Delta_2}{2}=\varphi_2-\frac{\Delta_1}{2}$ and angle spread

$\Delta = \Delta_1 + \Delta_2$. The correlation using one cluster channel model must agree with that using two-cluster channel model. Actually equation (3.24) can be rewritten as

$$\begin{aligned}\gamma_m &= \frac{e^{-jm(\varphi_1+\Delta_2/2)}e^{jm\Delta_2/2}\sin(m\Delta_1/2)+e^{-jm(\varphi_2-\Delta_1/2)}e^{-jm\Delta_1/2}\sin(m\Delta_2/2)}{m(\Delta_1+\Delta_2)/2} \\ &= \frac{e^{-jm\varphi}\left[e^{jm\Delta_2/2}\sin(m\Delta_1/2)+e^{-jm\Delta_1/2}\sin(m\Delta_2/2)\right]}{m(\Delta_1+\Delta_2)/2} \\ &= \frac{e^{-jm\varphi}\sin\left[m(\Delta_1+\Delta_2)/2\right]}{m(\Delta_1+\Delta_2)/2} \\ &= e^{-jm\varphi}\sin c\left[m(\Delta_1+\Delta_2)/2\right]\end{aligned} \tag{3.25}$$

Comparing equation (3.25) with (3.6), we see that (3.25) is exactly the result which deploys single cluster channel model with mean AOA $\varphi = \varphi_1 + \frac{\Delta_2}{2} = \varphi_2 - \frac{\Delta_1}{2}$ and angle spread $\Delta = \Delta_1 + \Delta_2$.

To have a good insight on the spatial correlation, we consider three special cases.

3.3.1.1 Symmetric Clusters

Two clusters have equal angular spread ($\Delta_1 = \Delta_2 = \Delta$) and symmetric AOA ($\varphi_1 = -\varphi_2$), see Figure 3-12.

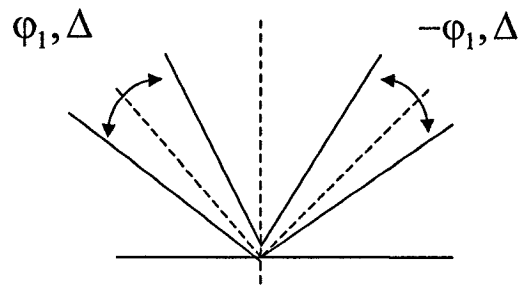

Figure 3-12. Two symmetric clusters

The correlation coefficient in (3.12) can be simplified as

$$R = \frac{1}{2\Delta}\left[\int_{\varphi_1-\frac{\Delta}{2}}^{\varphi_1+\frac{\Delta}{2}} e^{jz\sin\beta}\, d\beta + \int_{-\varphi_1-\frac{\Delta}{2}}^{-\varphi_1+\frac{\Delta}{2}} e^{jz\sin\beta}\, d\beta\right]$$
$$= \frac{1}{\Delta}\int_{\varphi_1-\frac{\Delta}{2}}^{\varphi_1+\frac{\Delta}{2}} \cos\left(z\sin\beta\right) d\beta \tag{3.26}$$

Using (3.13), we have

$$R = J_0(z) + 2\sum_{m=1}^{\infty} J_{2m}(z)\cos(2m\varphi_1)\mathrm{sinc}(m\Delta) \tag{3.27}$$

We can also get the same result from (3.17)-(3.19) by using $\Delta_1 = \Delta_2 = \Delta$ and $\varphi_1 = -\varphi_2$,

$$R_{real} = J_0(z) + 2\sum_{m=1}^{\infty} J_{2m}(z)\cos(2m\varphi_1)\mathrm{sinc}(m\Delta) \tag{3.28}$$

$$R_{imag} = 0 \tag{3.29}$$

$$R = R_{real} = J_0(z) + 2\sum_{m=1}^{\infty} J_{2m}(z)\cos(2m\varphi_1)\mathrm{sinc}(m\Delta) \tag{3.30}$$

Clearly, these results agree though we derived them in different way.

One can further present equation (3.26) as

$$R = \frac{1}{2\Delta}\left[\int_{\varphi_1-\frac{\Delta}{2}}^{\varphi_1+\frac{\Delta}{2}} e^{jz\sin\beta}\, d\beta + \int_{-\varphi_1-\frac{\Delta}{2}}^{-\varphi_1+\frac{\Delta}{2}} e^{jz\sin\beta}\, d\beta\right]$$
$$= \frac{1}{2\Delta}\int_{-\frac{\Delta}{2}}^{\frac{\Delta}{2}} \left[e^{jz(\sin\varphi_1\cos t+\cos\varphi_1\sin t)} + e^{jz(-\sin\varphi_1\cos t+\cos\varphi_1\sin t)}\right] dt \tag{3.31}$$
$$= \frac{1}{2\Delta}\int_{-\frac{\Delta}{2}}^{\frac{\Delta}{2}} \left[2\cos\left(z\sin\varphi_1\cos t\right)e^{jz\cos\varphi_1\sin t}\right] dt$$

For small Δ, $\cos t \approx 1, \sin t \approx t$

$$R = \frac{1}{2\Delta}\int_{-\frac{\Delta}{2}}^{\frac{\Delta}{2}}\left[2\cos(z\sin\varphi_1)e^{jz\cos\varphi_1 t}\right]dt$$

$$\approx \cos(z\sin\varphi_1)\,\mathrm{sinc}\left(\frac{\Delta}{2}z\cos\varphi_1\right) \tag{3.32}$$

$$\approx \cos(2\pi d\sin\varphi_1/\lambda)\,\mathrm{sinc}\left(\frac{\Delta}{2}\cdot 2\pi d\cos\varphi_1/\lambda\right)$$

Zero correlation coefficient occurs at the following points

$$\frac{d}{\lambda} = \begin{cases} \dfrac{m_1}{4\sin\varphi_1} & m_1 = 1,3,\cdots,(2k-1),\cdots,\cdots \\ \dfrac{m_2}{\Delta\cos\varphi_1} & \mathrm{m}_2 = 1,2,\cdots,k,\cdots \end{cases} \tag{3.33}$$

As stated in [46], first-type zeros are due to the cosine and second-type zeros are due to the sinc. The spacing between first-type zeros is $\Delta d_{01} = 1/(2\sin\varphi_1)$ and it does not depend on the angular spread Δ; the spacing of the second- type zeros is $\Delta d_{02} = 1/(\Delta\cos\varphi_1)$ and its does depend on the angular spread – the larger the spread the smaller the spacing. The second- type zeros are the same as for the single cluster model. The minimum spacing for the first-type zeros is $d_{01,\min} = 1/(4\sin\varphi_1)$ and the minimum spacing for the second- type zeros is $d_{02,\min} = 1/(\Delta\cos\varphi_1)$.

Good system performance (capacity, diversity gain etc.) requires for low (ideally – zero) correlation. Normally, this is accomplished by setting d large enough. However, as (3.33) demonstrates, in a two-cluster scenario the spacing d can also be set, when possible, at zero locations. For small Δ and when φ is not too close to 0, $d_{01,\min} < d_{02,\min}$, and, hence, the two-cluster effect of oscillation can be beneficially used to achieve low correlation at smaller spacing $d = d_{01,\min} = 1/(4\sin\varphi_1)$ (as compared to the single-cluster case). Note however that, in this case, zero correlation will be achieved for all the pairs spaced apart by $m_1 d$; all the pair spaced by even number of d may be correlated. Hence, the performance is guaranteed to be the best only in the case of 2-element Rx antenna. This does not happen when $d = d_{02,\min}$: all the pair wise correlations are zero in this case and the performance is the best for any n.

3.3.1.2 Asymmetric Clusters

Two clusters have unequal angular spread ($\Delta_1 \neq \Delta_2$), multipath are distributed uniformly in all the clusters, hence we can use (3.14) as the PDF of incident angles, one cluster is orthogonal with receiver elements (mean AOA $\varphi_1 = 0°$), as shown in Figure 3-13.

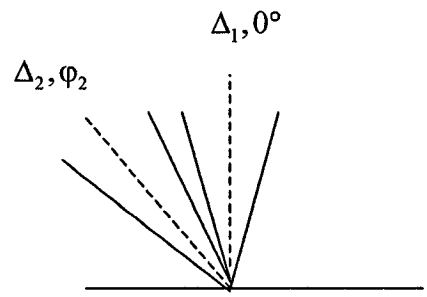

Figure 3-13. Two asymmetric clusters

The correlation is

$$R = \frac{1}{\Delta_1 + \Delta_2}\left(\int_{\varphi_1 - \frac{\Delta_1}{2}}^{\varphi_1 + \frac{\Delta_1}{2}} e^{jz\sin\theta} d\theta + \int_{\varphi_2 - \frac{\Delta_2}{2}}^{\varphi_2 + \frac{\Delta_2}{2}} e^{jz\sin\theta} d\theta \right) \tag{3.34}$$

Hence

$$R = w_1 R_1 + w_2 R_2 \tag{3.35}$$

where $R_i = \frac{1}{\Delta_i} \int_{\varphi_i - \frac{\Delta_i}{2}}^{\varphi_i + \frac{\Delta_i}{2}} e^{jz\sin\theta} d\theta \ (i = 1,2)$ is the correlation coefficient of one cluster located at the mean AOA direction (φ_i). $w_i = \frac{\Delta_i}{\sum \Delta_i} (i = 1,2)$ is the weight of cluster size. It is clear that the contribution of a cluster depends on its correlation R_i weighted by the size of its angular spread. For small angle spread Δ_1 , Δ_2 , using (3.9) R_i can be approximated as

$$R_i = \mathrm{sinc}(\frac{\Delta_i}{2} z\cos\varphi_i) e^{jz\sin\varphi_i} \tag{3.36}$$

Then

$$R = w_1 \text{sinc}(\frac{\Delta_1}{2} z\cos\varphi_1)e^{jz\sin\varphi_1} + w_2 \text{sinc}(\frac{\Delta_2}{2} z\cos\varphi_2)e^{jz\sin\varphi_2} \tag{3.37}$$

For $\varphi_1 = 0$, we have

$$R = w_1 \text{sinc}(\frac{\Delta_1}{2} z) + w_2 \text{sinc}(\frac{\Delta_2}{2} z\cos\varphi_2)e^{jz\sin\varphi_2} \tag{3.38}$$

The maxima and minima of the correlation magnitude occur at approximately $\cos(z\sin\varphi_2) = \pm 1$, which leads to the following

$$\begin{aligned} |R|_{\max} &= R(d_{\max}),\ d_{\max} = k/\sin\varphi_2 \\ |R|_{\min} &= R(d_{\min}),\ d_{\min} = (k+1/2)/\sin\varphi_2 \end{aligned} \tag{3.39}$$

where $k = 0,1,2,\cdots,n,\cdots$

3.3.1.3 Fixed Power Allocation

If the power of incoming multipath allocation is fixed in both clusters, the respective PDF of θ can be presented as

$$\rho(\theta) = \begin{cases} \dfrac{k}{\Delta_1} & -\dfrac{\Delta_1}{2} + \varphi_1 \le \theta \le \dfrac{\Delta_1}{2} + \varphi_1 \\ \dfrac{1-k}{\Delta_2} & -\dfrac{\Delta_2}{2} + \varphi_2 \le \theta \le \dfrac{\Delta_2}{2} + \varphi_2 \\ 0 & \text{elsewhere} \end{cases} \tag{3.40}$$

where the parameter $0 \le k \le 1$ can be decided by measurements. $\dfrac{k}{1-k}$ is the power ratio of the two clusters. We call this as "fixed power allocation", which differs with "proportional power allocation" in which PDF of θ was expressed as in (3.14). The correlation is

$$R = \frac{1}{2\Delta_1}\int_{\varphi_1-\frac{\Delta_1}{2}}^{\varphi_1+\frac{\Delta_1}{2}} \exp(jz\sin\theta)d\theta + \frac{1}{2\Delta_2}\int_{\varphi_2-\frac{\Delta_2}{2}}^{\varphi_2+\frac{\Delta_2}{2}} \exp(jz\sin\theta)d\theta \tag{3.41}$$

For small angle spread Δ_1 and Δ_2, R can be approximated as

$$R \approx kR_1 + (1-k)R_2 \tag{3.42}$$

Where R_i is the same expression in (3.36). Note that (3.42) is identical to (3.37) with $w_1 = k$ and $w_2 = 1-k$, as it intuitively should be.

The different weights, which do not depend anymore on the angular spreads, have however a profound effect on the correlation behaviors with the angular spread. For example, when one angular spread equals to zero, this cluster gives the dominant contribution to the total correlation, as opposed to the proportional power allocation in Section 3.3.3, where this cluster did not contribute anything. Note: (1) The smaller the cluster angular spread Δ_i, the higher the correlation R_i. (2) The larger the incident angle φ_i, the bigger the correlation R_i. (3) Asymptotically, when $\Delta_i \to 0$, $R_i \to 1$ and when $\varphi_i \to 90°, R_i \to 1$. In the other word, the cluster with smaller angular spread makes even bigger contribution to the correlation if they have the same power as the cluster with larger angular spread.

Consider, for example, the case of $k = 1/2$.

$$R = \left[\operatorname{sinc}\left(\pi\Delta_1 d\cos\varphi_1/\lambda\right) e^{j2\pi d\sin\varphi_1} + \operatorname{sinc}\left(\pi\Delta_2 d\cos\varphi_2/\lambda\right) e^{j2\pi d\sin\varphi_2} \right] \Big/ 2 \qquad (3.43)$$

Note that the 2nd cluster provides the same contribution to the correlation as the 1st one when $\Delta_1\cos\varphi_1 = \Delta_2\cos\varphi_2$. Clearly, the larger φ_2, the larger Δ_2 is required for equal contribution. When $\Delta_1\cos\varphi_1 < \Delta_2\cos\varphi_2$, the 1st cluster gives dominant contribution. Hence, as a general tendency, the clusters located closely to the endfire direction provide small contribution only when they have larger angular spread as compared to the clusters located closely to the broadside directions.

In the limiting case, $\Delta_1 \ll \Delta_2$, the 2nd cluster can be totally ignored. For example, when $\Delta_1 = 0$ and $\Delta_2 \geq \lambda/(d\cos\varphi_2)$, following (3.43), we have

$$R = \left[e^{jz\sin\varphi_1} + \operatorname{sinc}\left(\frac{\Delta_2}{2} z\cos\varphi_2\right) e^{jz\sin\varphi_2} \right] \Big/ 2 \approx e^{jz\sin\varphi_1}/2 \qquad (3.44)$$

Hence $|R| \approx 1/2$ regardless of Δ_2. This is in sharp contrast to proportional power allocation (recall that in Section 3.3.1.2 the 1st cluster can be totally ignored and one would obtain $|R| = \left|\operatorname{sinc}\left(\pi\Delta_2 d/\lambda\cos\varphi_2\right)\right| << 1$). Hence, power allocation among clusters has a dominant effect on the correlation. In general, the larger the power, the larger the contribution of that cluster to the correlation.

3.3.2 Simulation Results

We employ Monte-Carlo simulation to get 1,000 channel matrices with Rayleigh fading and then calculate the correlation coefficient average <R> over these matrices.

3.3.2.1 Case 1: Symmetric Clusters

We set $\Delta_1 = \Delta_2 = \Delta = 10°$, $\varphi_1 = -\varphi_2 = 30°$. From (3.28)-(3.29), we know the envelope of R is a cosine function multiplied by a sinc function. The first uncorrelated spacing point ($R = 0$) is $d = \lambda/(4\sin 30°) = 0.5\lambda$, the difference between adjacent uncorrelated element spacing point is $d = 2\lambda/(4\sin 30°) = \lambda$, the first uncorrelated spacing of the sinc() envelope comes at $d = \lambda/(\cos 30° \cdot \pi/18) = 6.6\lambda$. As Figure 3-14 shows, Monte-Carlo simulation result shows a good agreement with the Bessel equation (3.27) and our approximation (3.32)

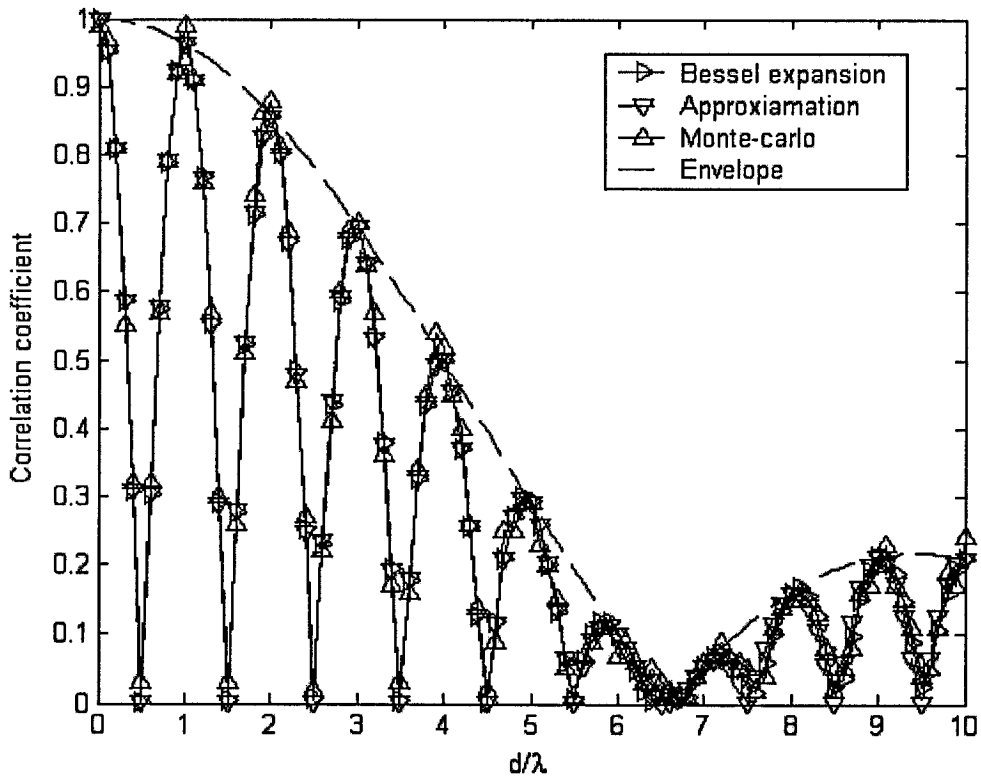

Figure 3-14. Two-symmetric-cluster channel correlation

3.3.2.2 Case 2: Asymmetric Clusters

Set Δ_1=10°, at incident angel $\varphi_1 = 0°$, and change Δ_2 from 0° to 10°. $\varphi_2 = 30°$

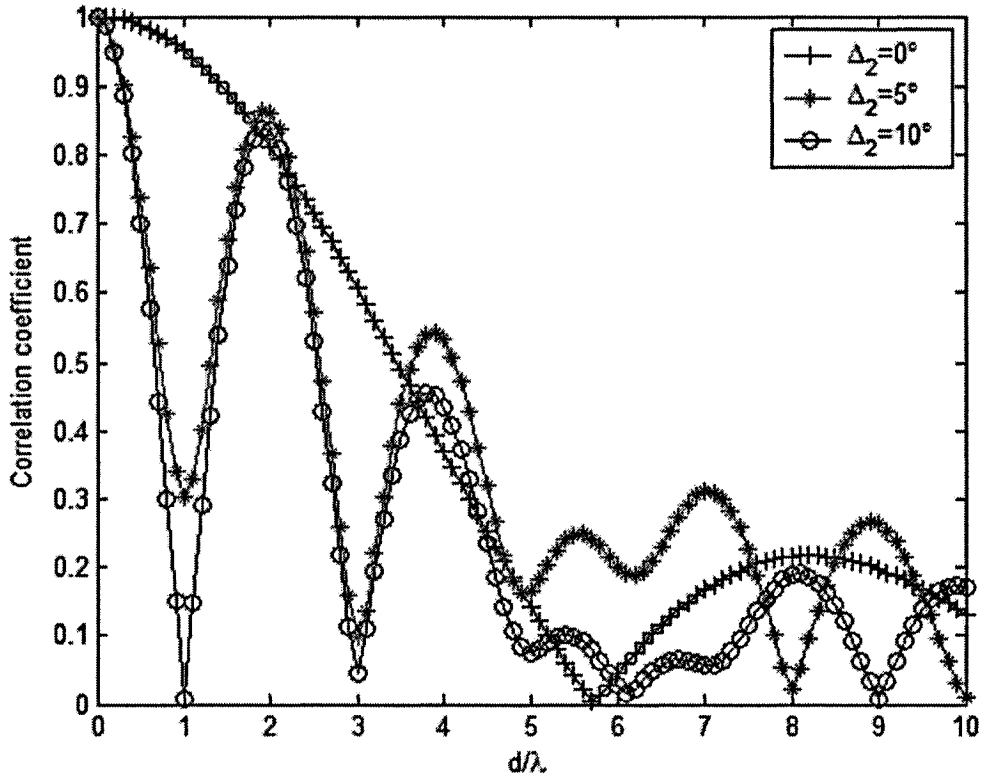

Figure 3-15. Two- asymmetric-cluster channel correlation with small angular spread

When the angle spread of the 2nd cluster Δ_2=0°, only 1st cluster exist. From Figure 3-15, one can see that the contribution of the 2nd cluster becomes more pronounced as Δ_2 increases (in full agreement with (3.35)). The effect of the 2nd cluster on the correlation is weighed by its angle spread Δ_2.

3.3.2.3 Case 3: Fixed Power Allocation

Set Δ_1=10° and $\varphi_1 = 0°$, and change Δ_2 from 0° to 10°, $\varphi_2 = 30°$. Comparing it with Figure 3-15, one can clearly see the difference. The 2nd cluster in the former case can be totally ignored when $\Delta_1 \geq 1/d$. However, in the latter case the 1st cluster can be totally ignored when $\Delta_1 >> \Delta_2$ regardless of Δ_1. It is instructive to consider the case of $\Delta_2 = 0$. In this case, the correlation periodically oscillates and its peak value never decreases below ½, regardless of d. This is in sharp contrast with case 2, where the

correlation peaks can be decreased to any small value by sufficiently increasing spacing d.

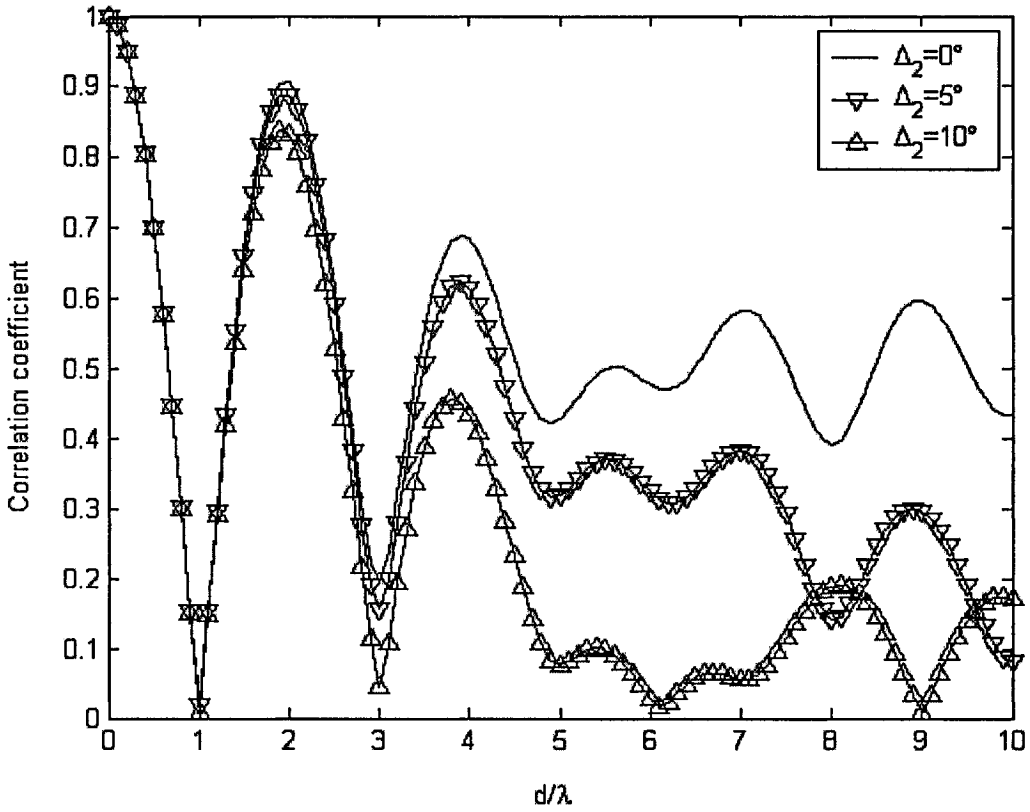

Figure 3-16. Channel correlation for two asymmetric clusters with the same power.

3.3.3 Validation

For validation purpose, we set two clusters with different power, which is the fixed power allocation case. The two clusters are located at mean AOA $\varphi_1 = 90°, \varphi_2 = -90°$. Both clusters have the same PAS $S_\varphi \approx 60°$ (correspondingly we have $\Delta = 104°$ using equation (2.30)). The 90° cluster has half power of the –90° one. The envelope correlation using this channel model is shown in Figure 3-17, which was published in [29]. Note that the solid line is with uniform PAS model.

Actually the PDF of AOA can be expressed as in (3.40), where $\Delta_1 = \Delta_2 = 104°$, $\varphi_1 = 90°, \varphi_2 = -90°$ and $k = \frac{1}{3}$. Note that in this case our approximations are not valid

any more because the angular spreads of both clusters are larger than 45°. We use Monte Carlo simulation to compute the envelope correlation. As Figure 3-18 shows, the simulation result agrees very well with the published paper.

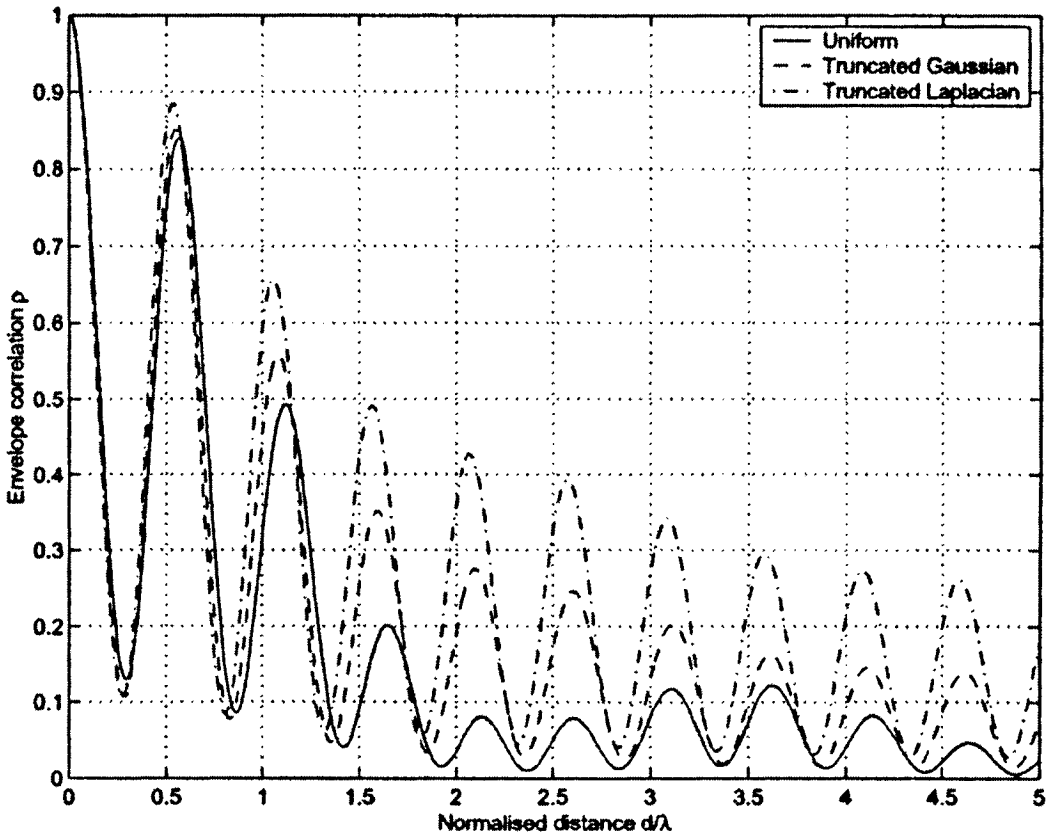

Figure 3-17. Two-unbalanced-power cluster channel correlation [29]

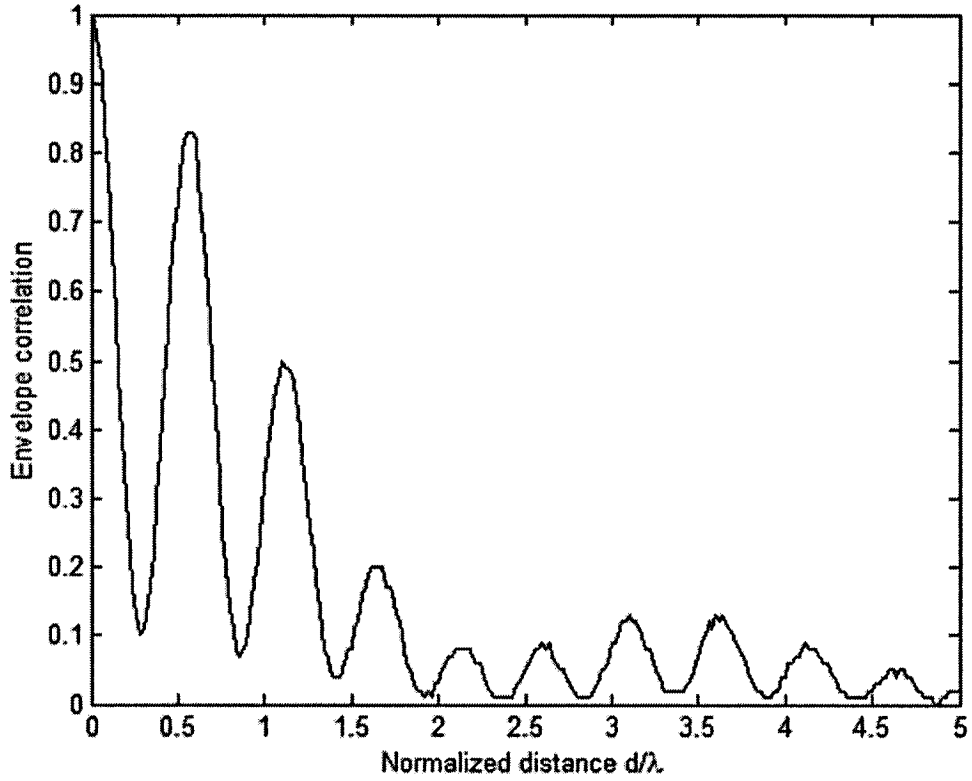

Figure 3-18. Monte-Carlo simulation for two unbalanced power clusters correlation

3.4 Influence of the 2nd Cluster

In our two-cluster channel model, both clusters will contribute to the channel correlation. Here we will find the condition to ignore the contribution of the 2nd cluster.

3.4.1 Case 1: Proportional Power Allocation

The probability density function is expressed as in (3.14), the effect of clusters on the correlation is expressed in section 3.3.3.

As stated in [46] considering R, $R_1(z)$ and $R_2(z)$ in equation (3.38),one may observe the following. The first zero of $R_1(z)$ is $z_{01} = 2\pi/\Delta_1$ (respectively $d_{01} = 1/\Delta_1$) and R_1 is small for $d \geq d_{01}$. Hence, we say then that the rate of decay of $R_1(z)$ is Δ_1. Similarly, $d_{02} = 1/(\Delta_2 \cos\varphi)$ and the rate of decay of $R_2(z)$ is $\Delta_2 \cos\varphi$. When $\Delta_1 > \Delta_2 \cos\varphi$, the first term in (3.38) is dominant for $d \in [0, d_f]$ and the 2nd term is dominant for $d \in [d_f, \infty]$,

where $|R_1(z_f)| = |R_2(z_f)|$ and $z_f = 2\pi d_f / \lambda$. Approximately, $d_f \approx 1/(\Delta_2 \cos\varphi_2)$. $R(z)$ decays quickly on the 1st interval and more slowly on the 2nd. In a sense, $R_2(z)$ provides a floor for $R(z)$ when $d > d_f$. Hence, when the spacing is small, neglecting the 2nd cluster does do change the correlation significantly. Figure 3-19 illustrates these effects. Note that $d_f \approx 2\lambda$ for $\Delta_2 = 60^0, \varphi_2 = 60^0$.

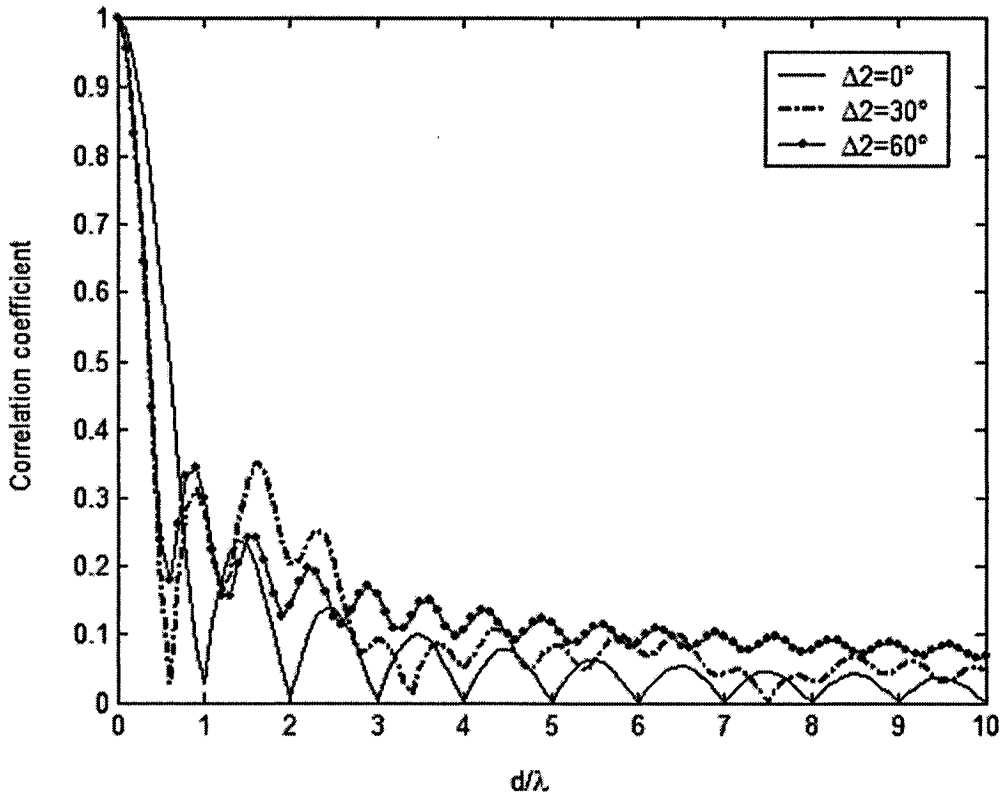

Figure 3-19. Two-asymmetric-cluster channel correlation with large angular spread

3.4.2 Case 2 : Fix Power Allocation

Measurements show that the powers of two clusters can be unequal in some cases [25]. Define a parameter $Rio \triangleq \frac{(1-k)|R_2|}{k|R_1|}$, which is the ratio of the contribution to the channel correlation by these two clusters. If the ratio *Rio* is small (for an example ≤ 0.5), the 2nd cluster can be neglected.

Consider the same example as in Section 3.3.4. Assume the first cluster with angular spread $\Delta_1 = 10°$ is located at $\varphi_1 = 90°$, and $k = \frac{1}{2}$. Then $R_1 = \frac{1}{\Delta_1}\int_{\varphi_1-\frac{\Delta_1}{2}}^{\varphi_1+\frac{\Delta_1}{2}} e^{jz\sin\beta}d\beta \approx 1$. We try to find the required condition to ignore the 2nd cluster, then the contribution from the 1st cluster is dominant, hence $|R| = |kR_1 + (1-k)R_2| \approx \frac{1}{2}$. Following equation (3.44), we have

$$Rio = \sin c(\frac{\Delta_2}{2} z\cos\varphi_2) \tag{3.45}$$

then $\Delta_2 = const/\cos\varphi_2$ (3.46)

where $const = \frac{2\text{sinc}^{-1}(Rio)}{z} = \frac{\lambda\text{sinc}^{-1}(Rio)}{\pi d}$ is a constant for a specific Rio and antenna spacing d. Hence, if the angular spread of the 2nd cluster with mean AOA at $\varphi(\le 45°)$ is larger than a value ($\Delta \ge \frac{const}{\cos\varphi}$), then the 2nd cluster can be neglected. Note that from (3.45) to keep the same small Rio for large $\varphi_2 (> 45°)$, the respective angular spread Δ_2 need to be large ($> 45°$). Asymptotically, for $\varphi_2 = 90°$, $Rio = 1$. It is evident that in this case one cannot get (3.46) because the approximation in (3.37) is not valid anymore.

In fact, for $k = 1/2, R_1 \approx 1$ and $\varphi_2 = 90°$

$$R_2 = \frac{1}{\Delta_2}\int_{\varphi_2-\frac{\Delta_2}{2}}^{\varphi_2+\frac{\Delta_2}{2}} e^{jz\sin\beta}d\beta = \frac{1}{\Delta_2}\int_{-\frac{\Delta_2}{2}}^{\frac{\Delta_2}{2}} e^{jz\cos\beta}d\beta \tag{3.47}$$

and $Rio = \frac{(1-k)R_2}{kR_1} = R_2$ (3.48)

Unfortunately, the analytical result or approximation of (3.48) is not available. We have to find Δ_2 numerically for a specific Rio. Calculation shows that one can get small Rio (such as 0.1) when the angular spread of the 2nd cluster is large ($\Delta_2 > \frac{\pi}{2}$). In this case, we can ignore the effect of the 2nd cluster if $\Delta_2 >> \Delta_1$.

The 1st cluster is located at mean AOA $\varphi_1 = 90°$, angular spread $\Delta_1 = 10°$, antenna spacing at typical value $d = 2.38\lambda$. Figure 3-20 shows the required Δ_2 versus mean AOA φ_2 for equal power ($k = 1/2$) with $Rio = 0.5$. It is clear that Monte-Carlo simulation matches the analytical approximation equation (3.46).

Figure 3-21 shows the required Δ_2 versus mean AOA φ_2 for different Rio. We see that the smaller the angular spread of 2nd cluster, the larger Rio, and the 2nd cluster will make big contribution to the channel correlation. Hence we cannot ignore the smaller cluster.

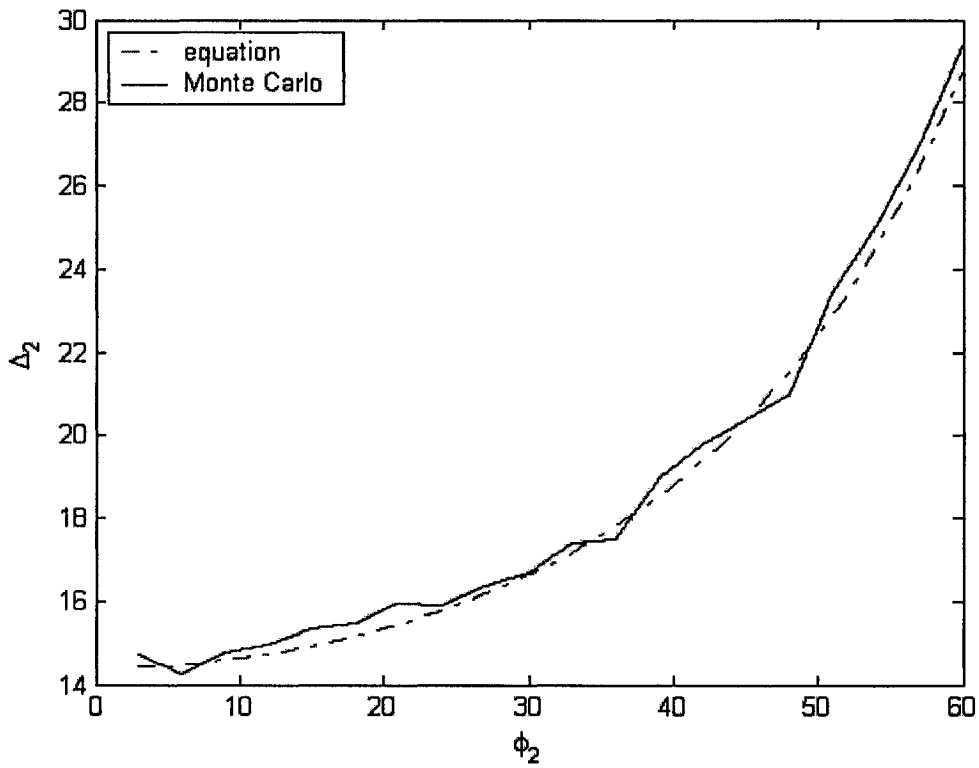

Figure 3-20. The 2nd cluster angular spread versus its mean AOA for equal power, $Rio = 0.5$ analytical result compare with Monte-Carlo simulation

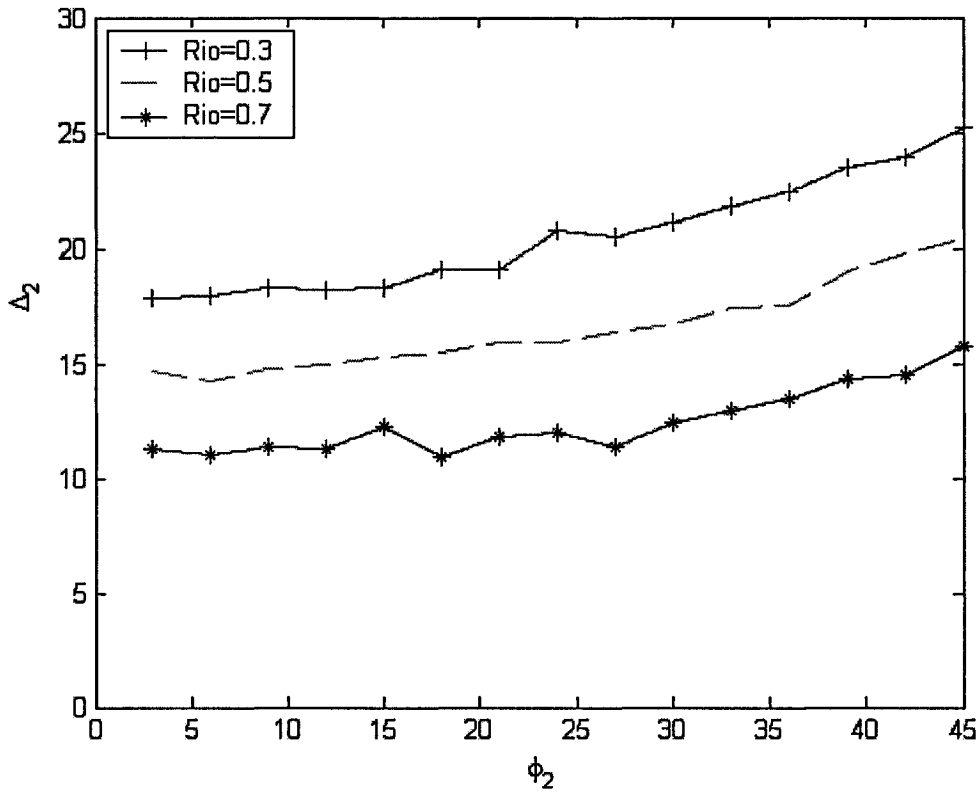

Figure 3-21. The 2nd cluster angular spread versus its mean AOA for different Rio

3.5 Multi-cluster Channel Model

The extension from two-cluster channel model to multi-cluster is straightforward. For N_c clusters channel, the spatial channel correlation can be presented as

$$R = \frac{1}{\sum_{i=1}^{N_c} \Delta_i} \sum_{i=1}^{N_c} \int_{\varphi_i - \frac{\Delta_i}{2}}^{\varphi_i + \frac{\Delta_i}{2}} \exp(jz \sin\beta) d\beta \tag{3.49}$$

This can be rewritten as

$$R = \sum_{i=1}^{N_c} \frac{\Delta_i}{\sum_{i=1}^{N_c} \Delta_i} R_i \tag{3.50}$$

where $R_i = \frac{1}{\Delta_i}\int_{\varphi_i-\frac{\Delta_i}{2}}^{\varphi_i+\frac{\Delta_i}{2}} \exp(jz\sin\theta)d\theta$ is the correlation of i-th cluster. Again the contribution made by a cluster is weighed by its angular spreads. Following the same steps as in (3.2),

$$R_i = \frac{1}{\Delta_i}\int_{\varphi_i-\frac{\Delta_i}{2}}^{\varphi_i+\frac{\Delta_i}{2}} \exp(jz\sin\beta)d\beta = R_{ixx} + jR_{iyy} \tag{3.51}$$

$$R_{ixx} = J_0(z) + 2\sum_{m=1}^{\infty} J_{2m}(z)\cos(2m\varphi_i)\sin c(m\Delta_i) \tag{3.52}$$

$$R_{ixy} = \sum_{m=0}^{\infty} J_{2m+1}(z)\sin[(2m+1)\varphi_i]\sin c[(2m+1)\Delta_i/2] \tag{3.53}$$

Inserting (3.51)-(3.53) into (3.50), we have

$$R = R_{xx} + jR_{xy} = \sum_{i=1}^{N_c}\frac{\Delta_i}{\sum_{i=1}^{N_c}\Delta_i}R_{ixx} + j\sum_{i=1}^{N_c}\frac{\Delta_i}{\sum_{i=1}^{N_c}\Delta_i}R_{ixy} \tag{3.54}$$

Then we have

$$R_{xx} = \sum_{i=1}^{N_c}\frac{\Delta_i}{\sum_{i=1}^{N_c}\Delta_i}R_{ixx} = J_0(z) + 2\sum_{m=1}^{\infty} J_{2m}(z)\frac{\sum_{i=1}^{N_c}\cos(2m\varphi_i)\sin(m\Delta_i)}{m\sum_{i=1}^{N_c}\Delta_i} \tag{3.55}$$

$$R_{xy} = \sum_{i=1}^{N_c}\frac{\Delta_i}{\sum_{i=1}^{N_c}\Delta_i}R_{ixy} = 2\sum_{m=0}^{\infty} J_{2m+1}(z)\frac{\sum_{i=1}^{N_c}\sin[(2m+1)\varphi_i]\sin[(2m+1)\Delta_i/2]}{m\sum_{i=1}^{N_c}\Delta_i} \tag{3.56}$$

Using the same validation method in section 3.3, let N_c clusters merge to one bigger cluster. Equation (3.54)-(3.56) must agree with the correlation using one cluster channel model, this means "self convergence ". In the other word, we can divide one big cluster

to N_c independent smaller clusters, then sum the correlations of those smaller clusters to get the correlation of the big cluster.

When N clusters merge to one bigger cluster, we have

$$\varphi_i = \varphi_{i-1} + \frac{\Delta_i - \Delta_{i-1}}{2}, \quad i = 1,2,\ldots,N_c \tag{3.57}$$

The mean AOA and angular spread of the big cluster are

$$\varphi_0 = \frac{1}{2}\left[\varphi_{N_c} + \varphi_1 + \frac{\Delta_{N_c} - \Delta_1}{2}\right] \tag{3.58}$$

$$\Delta = \sum_{i=1}^{N_c} \Delta_i = \varphi_{N_c} - \varphi_1 + \frac{\Delta_{N_c} + \Delta_1}{2} \tag{3.59}$$

Inserting (3.57) into

$$2\cos(2m\varphi_i)\sin(m\Delta_i) = \sin\left[m\left(2\varphi_i + \Delta_i\right)\right] - \sin\left[m\left(2\varphi_i - \Delta_i\right)\right] \tag{3.60}$$

We have

$$2\cos(2m\varphi_i)\sin(m\Delta_i) = \sin\left[m\left(2\varphi_i + \Delta_i\right)\right] - \sin\left[m\left(2\varphi_{i-1} + \Delta_{i-1}\right)\right] \tag{3.61}$$

Then

$$\begin{aligned}\frac{\sum_{i=1}^{N_c}\cos(2m\varphi_i)\sin(m\Delta_i)}{m\sum_{i=1}^{N_c}\Delta_i} &= \frac{\sin\left[m\left(2\varphi_{N_c} + \Delta_{N_c}\right)\right] - \sin\left[m\left(2\varphi_1 - \Delta_1\right)\right]}{2m\sum_{i=1}^{N_c}\Delta_i} \\ &= \cos\left[m\left(\varphi_{N_c} + \varphi_1 + \frac{\Delta_{N_c} - \Delta_1}{2}\right)\right]\frac{\sin\left[m\left(\varphi_{N_c} - \varphi_1 + \frac{\Delta_{N_c} + \Delta_1}{2}\right)\right]}{m\sum_{i=1}^{N_c}\Delta_i}\end{aligned} \tag{3.62}$$

Finally (3.55) can be simplified as

$$R_{xx} = J_0(z) + 2\sum_{m=1}^{\infty} J_{2m}(z)\cos\left[m(\varphi_{N_c} + \varphi_1 + \frac{\Delta_{N_c} - \Delta_1}{2})\right]\text{sinc}\left(m\sum_{i=1}^{N_c}\Delta_i\right) \quad (3.63)$$

which is exactly the real part of correlation using the single cluster channel with mean AOA as in (3.58) and angular spread as in (3.59). Similar to these steps, one can show that R_{xy} using multi-cluster channel model also agrees with that using single cluster model. Hence, the correlation derived from N independent small clusters is in full agreement with that from the single cluster as it should be. One can also show "self convergence" using the more compact form as in (3.5).

3.6 Summary

In chapter 3, we studied the effect of receiver array geometry and the second cluster on the spatial correlation of MIMO channel. The contributions in this chapter include the following:

- We derived two closed-form expressions ((3.17)-(3.19), (3.23)-(3.24)) of spatial channel correlation and its approximations using the multi-cluster channel model.
- We found that some elements of UCA are highly correlated which may result in the performance loss.
- We found that the spatial channel correlation oscillates with antenna spacing which never happened in one cluster channel model.
- As a cluster moves away from the array broadside direction, its contribution to the total correlation decreases (inverse cosine law).
- In the case of identical symmetrically-located clusters, the envelope of correlation is determined by a single cluster angular spread while the oscillations within the envelope are determined by the inter-cluster angular spread (for both clusters).
- If the clusters are identical and located asymmetrically (i.e., broadside-endfire), the impact of the endfire cluster is, in many cases, much smaller and can be neglected for proportional power allocation. Hence, one-cluster model can be used, which simplifies the analysis substantially.

- It was validated that the correlation using multi-cluster model is consistent with that using single cluster model , and also agrees with the results in published papers.

Chapter 4 MIMO Channel Capacity

4.1 Introduction

Since 1948, when Shannon published his now famous paper, "Communications in the presence of noise", MIMO is one of the most significant discovery in the field of communications. This domain is a totally different approach to wireless communications, which has been discovered by Foschini [30] and Telatar [31] in 1995-1996. The remarkable Shannon capacity can be improved significantly by deploying multiple antennas at both the transmitter and receiver of a wireless system. When the channel exhibits rich scattering and its variations can be accurately tracked, the performance improvement in terms of capacity (spectral efficiency) [bit/s/Hz] is 10-fold and even more as compared to conventional systems. The key idea behind MIMO is not to combat multipath, but to create multipath parallel channels (virtual) and to use them to send n times more data. Thus, multipath becomes an ally rather than enemy.

The performance of MIMO system depends heavily on the statistical properties and transmitter and receiver antenna correlations of the channel. We begin with the MIMO channel information capacity in this chapter, and will discuss combining gain in next chapter. Some recent literature has calculated the spatial MIMO channel capacity using both analytical and measurement-based MIMO channel models for typical indoor and outdoor environments[32][33].

As shown in chapter 3, the evolution of antenna correlation coefficient as a function of the distance between transmitter and receiver drastically depends on the scattering environment which included the number of multipath, the angle of arrival (AOA) of these multipaths or power azimuth spectrum (PAS), the radiation pattern of antenna elements, and the Doppler spread [34]. The effect of channel correlation on capacity depends on what is known about the channel at the transmitter and receiver, channels with very low correlation between antennas can exhibit a "keyhole" effect where the rank of the channel gain matrix is very small, leading to limited capacity gains [35][36].

In this chapter, we evaluate the information-theoretic channel capacity using the multi-cluster channel model. Both ULA and UCA are considered. This chapter is organized as follows: in Section 4.2, we will present an overview of the information-theoretic channel capacity for the MIMO wireless communications. In Section 4.3, we will study MIMO channel capacity using the single cluster channel model. We will compare the channel capacity of UCA with that of ULA. Monte-Carlo simulation that validates our results will be also described in this section. The MIMO channel capacity using the two-cluster channel model will be presented in Section 4.4. Finally, concluding remarks will be given in Section 4.5.

4.2 Theoretic MIMO Channel Capacity

4.2.1 MIMO System Model

MIMO-based signal-processing techniques such as BLAST, V-BLAST, D-BLAST architecture, space-time trellis codes, and space-time block codes have been proposed and examined for future wireless applications [1][37][38] . Comparing with the traditional multi-antenna system, the key idea of the BLAST is to split the incoming bit stream into N independent sub-streams and launch them independently (see Figure 4-1), and results in significant increase of channel capacity.

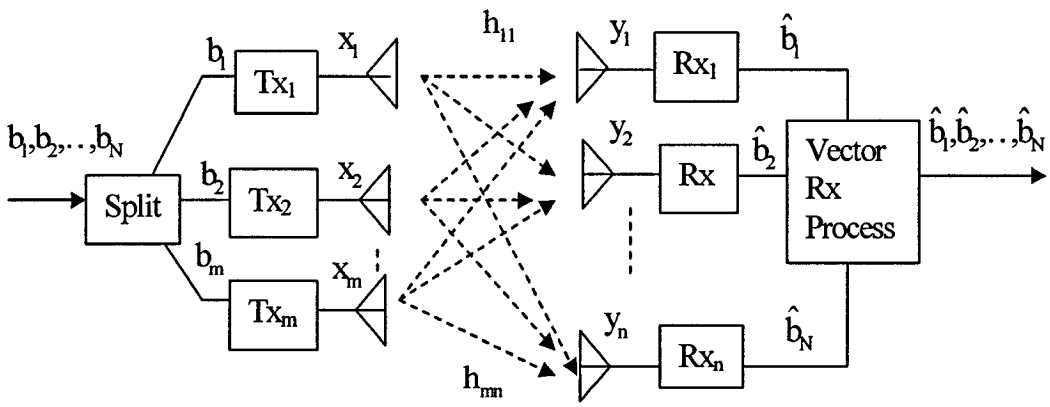

Figure 4-1. System model of a MIMO antenna arrays system

Consider BLAST system, the discrete received signal model can be expressed as

$$\mathbf{Y} = \mathbf{HX} + \mathbf{N} \tag{4.1}$$

where **H** is the channel matrix , **Y** is the received signal vector. $\mathbf{X}=\begin{bmatrix} b_1 & b_2 & \cdots & b_m \end{bmatrix}^T$ is the transmit signal vector. **N** is an additive white Gaussian noise vector and each component can be modeled as Gaussian random variable with zeros mean and unit variance.

The component-wise representation of equation (4.1) is

$$y_i = \sum_{j=1}^{n} g_{ij} x_j + \xi_i \tag{4.2}$$

under the transmit power constraint $\left\langle |\mathbf{x}|^2 \right\rangle = P_t$, then the channel matrix **H** whose components come from the normalized channel gain g_{ij} as $h_{ij} = \sqrt{P_t / P_r}\, g_{ij}$ can be modeled as a complex Gaussian random variable with zero mean and unit variance . The channel capacity has been shown as the famous Foschini-Telatar formula [28]:

$$C = \log_2 \det\left(\mathbf{I}_m + \frac{\rho}{n} \mathbf{H}\mathbf{H}^+ \right) \tag{4.3}$$

where det is the determinant of a matrix, $\mathbf{I}_m$ is the $m \times m$ identity matrix, and $\mathbf{H}^+$ is the Hermitian transpose of the Rayleigh fading channel matrix **H**. $\rho = P_r / \sigma_0^2$ is the SNR at each receiver antenna.

Because the channel matrix h_{ij} is a random variable, the channel capacity C is also a random variable. For ergotic channel, the mean channel capacity can be written as

$$\langle C \rangle = \left\langle \log_2 \det\left(\mathbf{I}_m + \frac{\rho}{n} \mathbf{H}\mathbf{H}^+ \right) \right\rangle \tag{4.4}$$

4.2.2 Compare with Conventional SISO and Multi Antenna System

We compare the capacity of MIMO system with the conventional SISO and multi antenna system. More intuitively, assuming the n transmitter and receiver elements and channels are i.i.d , then the channel correlation matrix $\mathbf{R} = \left\langle \mathbf{H}\mathbf{H}^+ \right\rangle = \mathbf{I}$, equation (4.4) can be reduced to

$$C = n \log\left(1 + \frac{\rho}{n} \right) \tag{4.5}$$

Hence, the incoming bit stream is splitted into n independent sub-streams and transmitted independently over n channels. Since the total Tx power is fixed to P_t , per-channel SNR is ρ/n . That is, the channel capacity increases almost linearly with increasing the number of antenna elements.

In the traditional channel multi-antenna system, see Figure 4-2, all the bits are not splitted and transmitted over all the sub-channel. Because of the diversity gain, channel fading can be reduced and system performance can be improved.

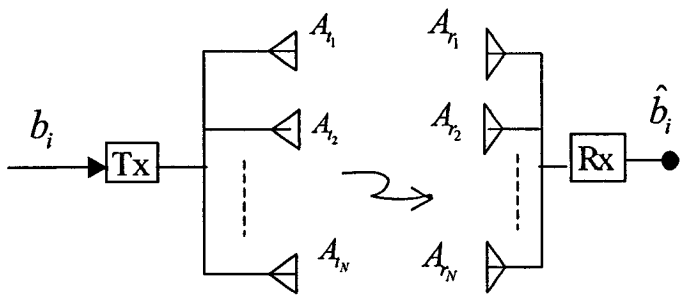

Figure 4-2. Traditional multi antenna system model

The capacity of conventional multi antennae system is

$$C = \log_2\left(1+n^2 \cdot SNR\right) \tag{4.6}$$

The channel capacity increases with logarithmic in number of elements n , comparing (4.5) with (4.6) , clearly MIMO system has a significant improvement .

In the traditional single input and single output (SISO) channel, as shown in Figure 4-3, all the bits are transmitted over one sub-channel only.

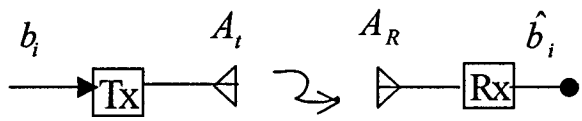

Figure 4-3. Traditional SISO model

The capacity of SISO is

$$C_1 = \log\left(1+\rho\right) \tag{4.7}$$

Asymptotically, when we have infinite number of elements $(n \to \infty)$, from (4.5) the MIMO channel capacity can be written as

$$C \approx \frac{\rho}{\ln 2} \tag{4.8}$$

Comparing equation (4.8) and (4.5), clearly the MIMO asymptotical capacity increases proportionally with the signal to noise ratio (SNR) with is much faster than the traditional channel (SISO).

4.2.3 Remarks on MIMO Channel Capacity

It has been shown that the MIMO channel capacity C is limited by the minimum of the number of transmit elements m, receiver elements n and the number of multipath M under the condition of deterministic channels, hence the channel capacity can be written as [39]

$$C = \sum_{i=1}^{M_0} \log\left(1 + \frac{\rho}{n}\lambda_i\right) \quad , \quad M_0 = \min(m, n, M) \tag{4.9}$$

where λ_i are eignevalues of $\mathbf{HH}^+$. Hence, the channel can be decomposed into an equivalent system of M_0 SISO sub-channels whose power gains are λ_i. If the $\frac{\rho}{n}\lambda_k$ is much smaller than 1, the capacity provided by k-th sub-channel is nearly zero. Then the k-th sub-channel is inactive, otherwise is called "active" sub-channel. The parameter M_0 that represents the number of sub-channels actively participating in conveying information under a given set of operating condition is defined as effective degrees of freedom (EDOF), which is introduced in [39].

Note that power allocation may also affect the channel capacity. Previous work shows water-filling power allocation scheme (assuming the transmitter and receiver know the channel) can improve the channel capacity [29]. However, in many applications, without any knowledge of the channel characteristics, it is more practical to distribute power equally on all the transmit antenna elements. In this thesis, we assume a uniform power allocation to the sub-channels.

4.3 Single Cluster Channel Capacity

2.8

We assume a narrow band case, flat Rayleigh fading channel. Using the channel model derived in chapter 2, we study the relationship between the MIMO channel capacity and the receiver antenna spacing, the 2nd cluster multipath, and the receiver geometry.

4.3.1 Capacity of ULA

In [31], for fixed linear $n \times n$ matrix channel with additive white Gaussian noise and when the transmitted signal vector is composed of statistically independent equal power components each with a Gaussian distribution , the mean channel capacity can be written as

$$\langle C \rangle = \left\langle \log_2 \det\left(\mathbf{I} + \frac{\rho}{n} \mathbf{H}\mathbf{H}^{+} \right) \right\rangle \tag{4.10}$$

It is further shown in [28] that after proper normalization, the mean channel capacity is upper bounded by

$$\langle C \rangle \le \overline{C} = \log_2 \det\left[\mathbf{I} + \frac{\rho}{n} \mathbf{R} \right] \tag{4.11}$$

where $\mathbf{R}$ is the normalized correlation matrix. With ULA / UCA receiver, the component of $\mathbf{R}$ can be expressed as equation (3.2) and (3.11) respectively.

Loyka [28] has also studied the mean channel capacity and its upper bound of ULA, he found that the channel mean capacity is a function of antenna spacing d. For small d, the mean channel capacity $\langle C \rangle$ increases almost linearly as d increase. For large d, $\langle C \rangle$ saturates and does not change significantly with d. MIMO mean capacity saturate at $d_{\min} = 1/2\Delta$ which corresponds approximately to the first zero of the normalized correlation coefficient $R_{ik}(d)$ for $i = k \pm 1$. And the capacity upper bound can be written as

$$\overline{c}(d) \approx \min\left\{ \frac{d}{d_{\min}} C_{\max} + C_0, C_{\max} \right\} , \tag{4.12}$$

where $C_0 = \bar{C}(d=0) = \log_2(1+\rho)$ is the single-input single-output channel capacity (with the same radiated power) and $C_{\max} = n\log_2\left(1+\frac{\rho}{n}\right)$ is the channel capacity of an uncorrelated matrix channel. As Figure 4-4 shows, our result agrees with that in [28].

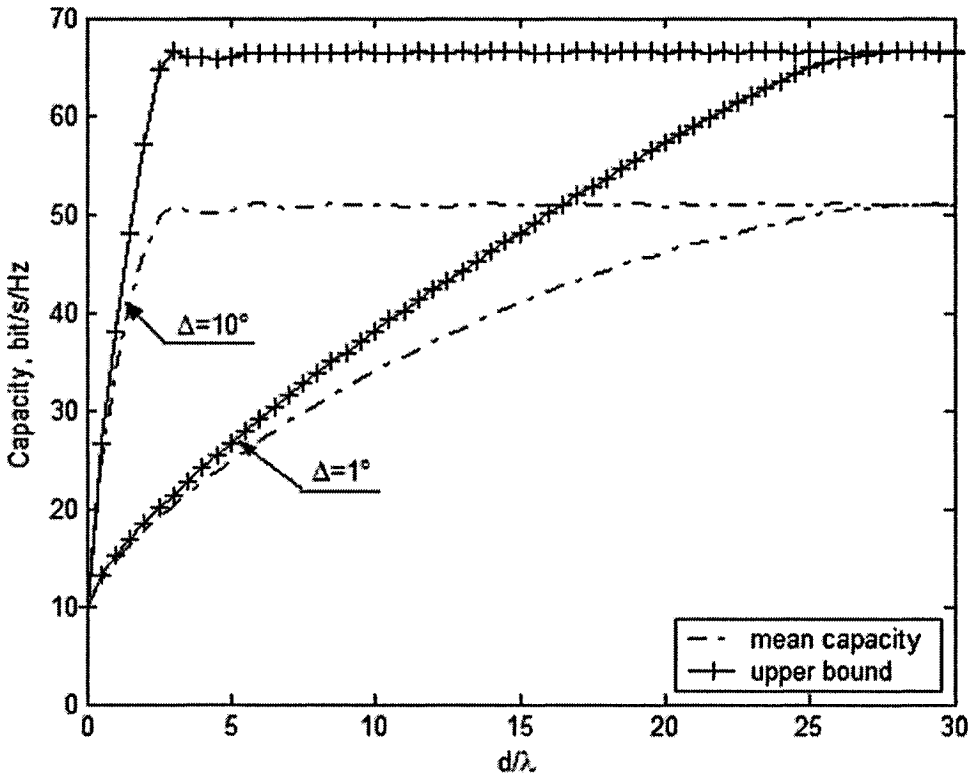

Figure 4-4. MIMO capacity of the "average" channel (the upper bound) and the mean (ergodic) capacity versus d for different $\Delta, N=20, n=10$, and $\rho = 30dB$

4.3.2 Capacity of UCA

4.3.2.1 Simulation Results

For comparison purpose, we use the same channel as in section 4.3.1, and deploy UCA which has the same aperture as ULA (see

Figure 4-5). The aperture of UCA/ULA is $L=(n-1)d=2r$, where the number of receiver elements in UCA /ULA is $n=10$, d is the antenna spacing in ULA, r is the radius of UCA. Set $d=5\lambda$ which is larger than $d_{\min}=2.86\lambda$. As mentioned in section 4.3.1, ULA achieves its saturation capacity $\langle C\rangle \approx 51$bit/s/Hz (see Figure 4-4)

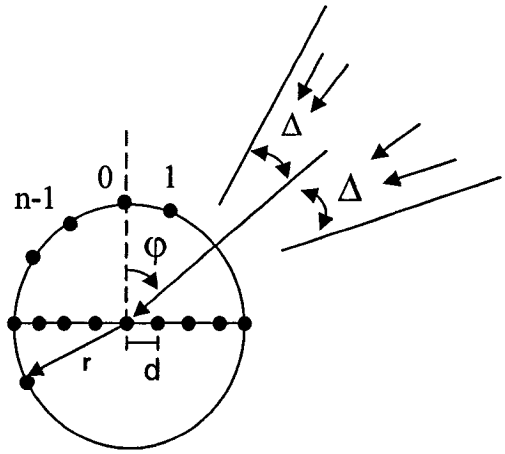

Figure 4-5. Incoming multipath signals arrive UCA/ULA , $L=(n-1)d=2r$

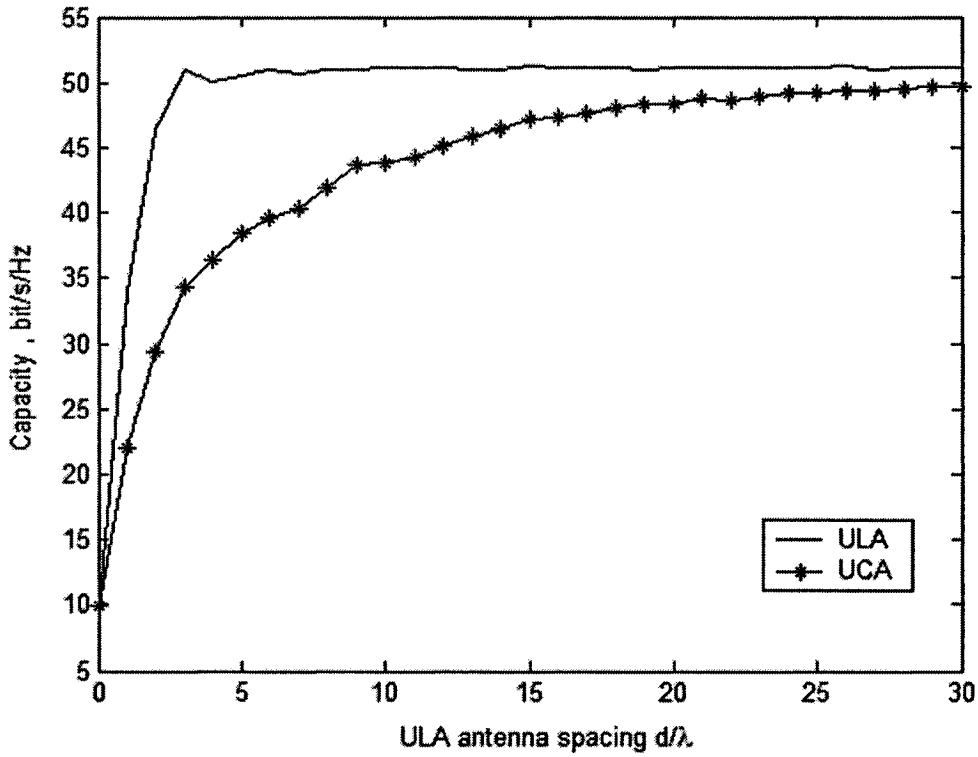

Figure 4-6. UCA/ULA with same aperture, the mean capacity versus d for $\Delta=10°, N=20, n=10$ and $\rho=30dB$

From Figure 4-6, we can find that: (1) For large d (respectively large r), the capacity of UCA saturates and doesn't change significantly, which is the same as that of ULA. (2) The capacity of UCA does not increase linearly with radius r before it saturates,

which is different from that of ULA. (3) Before the capacity achieves saturation, the capacity of UCA is smaller than that of ULA.

As mentioned in chapter 3, the adjacent element correlations change periodically around the circle. Some elements of UCA are "lost" because of their high correlation, and this results in the capacity loss. On the contrary, the adjacent element correlations do not change along the line in ULA. To achieve the same capacity as that of ULA, we have to add more receiver elements in UCA.

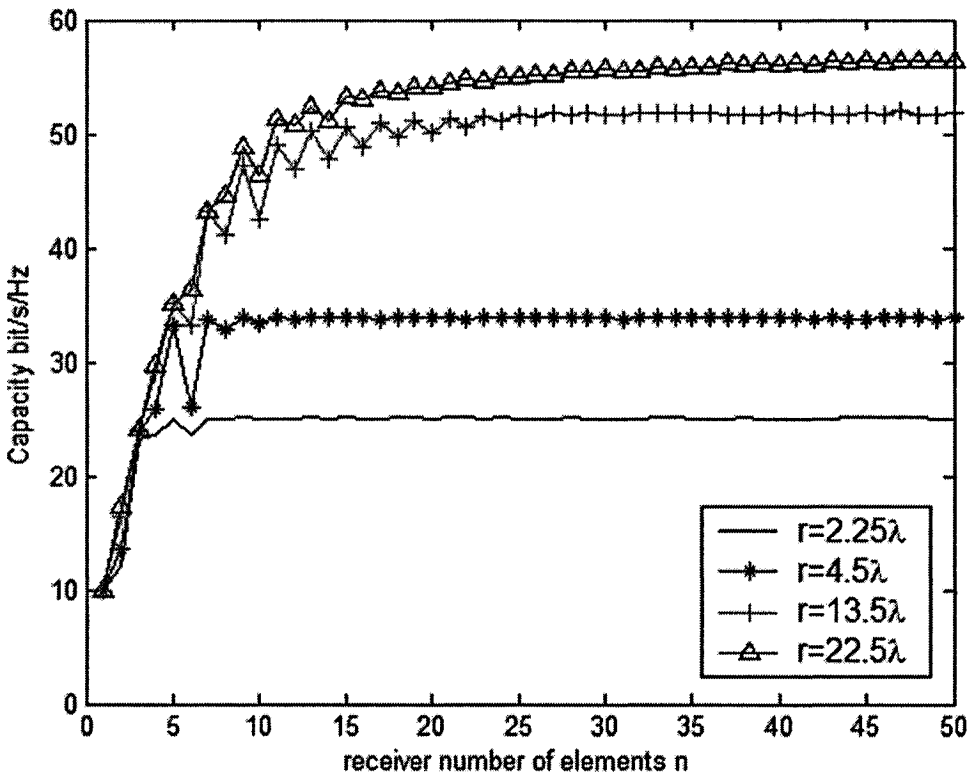

Figure 4-7 mean capacity of UCA versus receiver elements n_r for different aperture $L = 2r$, $\Delta = 10°, N = 20$ and $\rho = 30dB$, incoming signal from broadside

Put $n = 11$ receiver elements in UCA with the same aperture as before, then change the radius of the circular array, compute the mean capacity of the channel with the radius of UCA increasing (see Figure 4-8).

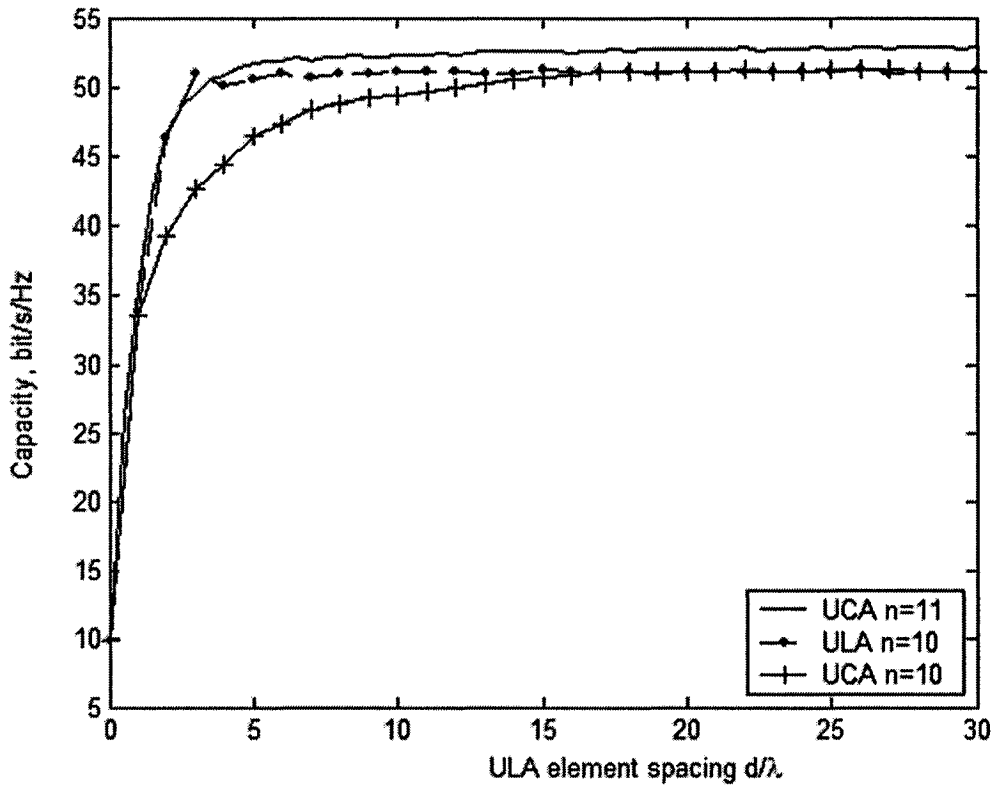

Figure 4-8. Mean capacity of UCA versus element spacing d for UCA/ULA $L = 2r = 9d$, $\Delta = 10°, N = 20,$ and $\rho = 30dB$, incoming signal from broadside

From Figure 4-7 and Figure 4-8, we find that: (1) UCA achieve the same saturation capacity with ULA at approximately $n = 11$. (2) The Capacity of UCA does not increase linearly with number of receive elements increasing.

4.3.2.2 Validation

The single cluster uniform PAS model becomes as the famous Clark model when the angular spread of the cluster is set as 2π, which was used in [40]. Note in [40] , assuming independent transmit array, which results in the transmitter covariance matrix $\mathbf{R}_s = \mathbf{I}_s$, for large numbers of transmit antennas ($S \to \infty$), the ergotic capacity converges to the deterministic quantity,

$$\lim_{S\to\infty} \langle C \rangle = C = \log_2 \det\left(\mathbf{I}_n + \frac{\rho}{n} \mathbf{R} \right) \tag{4.13}$$

where n is the number of receive elements, $\mathbf{R}$ is the channel correlation matrix. In fact, their assumption is impractical. However, we know that equation (4.13) is actually an upper bound of the MIMO channel capacity (see equation(4.11)). In this special case, the components of $\mathbf{R}$ are Bessel functions. As shown in Figure 4-9, Monte-Carlo simulation results agree with equation (4.13).

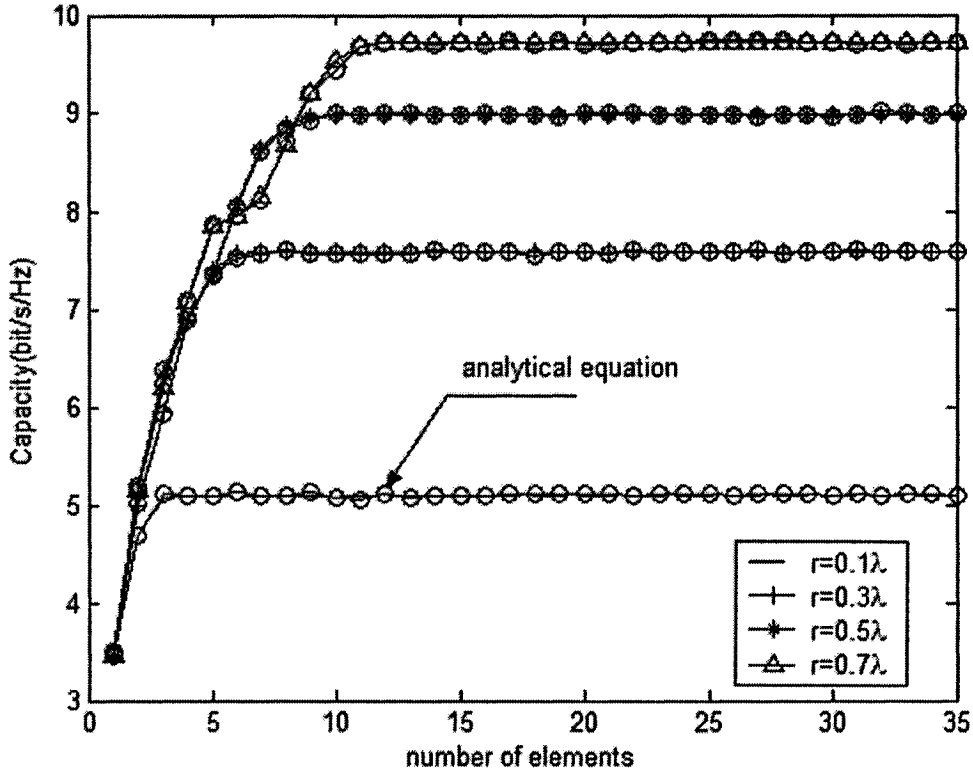

Figure 4-9. Isotropic cluster channel capacity upper bound versus number of elements for different circular array radius

For this isotropic case, we find both the mean capacity of UCA and its upper bound has the same behavior as those of ULA. When we increase the circular radius (antenna spacing), the capacity of UCA saturates at the first null of the adjacent element correlation R_{01}, hence $r_{sat}/\lambda = \dfrac{\xi_1}{2\pi \cdot 2 \cdot \sin\dfrac{\pi}{n}}$, where ξ_1=2.405 is first root of $J_0(x)=0$.

For an example, $n=5$, the correlation between the 0-th element and l-th element is

$R_{0l} = J_0(kd_l)$ $(l = 0,1,\cdots,n_r - 1)$ where $d_l = 2r\sin\frac{\pi l}{n}$. The Capacity of UCA saturates at $r_{sat} = \frac{2.405}{2\pi \cdot 2 \cdot \sin\frac{\pi}{5}}$ =0.6. This agrees with Figure 4-10.

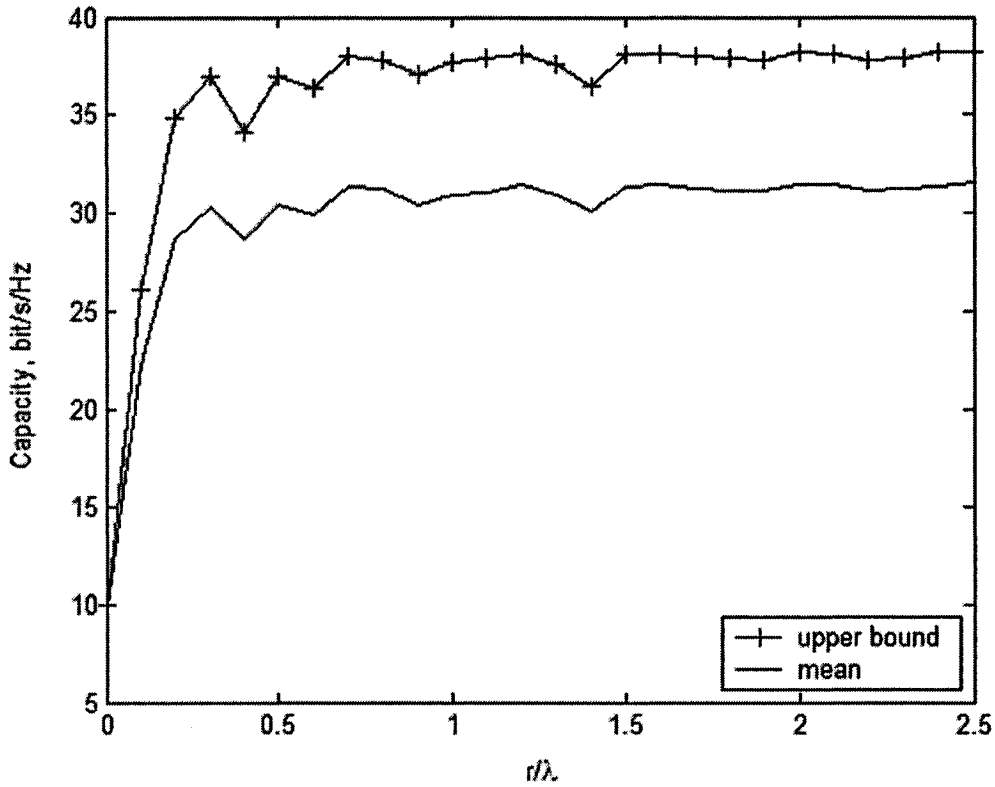

Figure 4-10. The capacity of UCA versus array radius r, isotropic cluster, $N = 20$ and $n = 5$

4.4 Effect of the 2nd cluster on MIMO Channel Capacity

4.4.1 Validation

As mentioned in section chapter 3, when two clusters merge to one bigger cluster, the channel correlation using two-cluster channel model is consistent with that using single cluster channel model. For the same reason, the performance matrix of MIMO system, such as channel capacity and combining gain and so on, which use two-cluster channel model, should logically agree with that using single cluster model.

Set mean AOA $\varphi_1 = -5°, \varphi_2 = 5°$,angular spread $\Delta_1 = \Delta_2 = 10°$, multipath $N = 20$, and $n = 10$. Compute the capacity and its upper bound. Then using the single cluster model ($[\varphi - \Delta, \varphi + \Delta]$, $\varphi = 0°, \Delta = 10°$) to compute those capacities. See Figure 4-11, the capacities using different channel models achieve the same values.

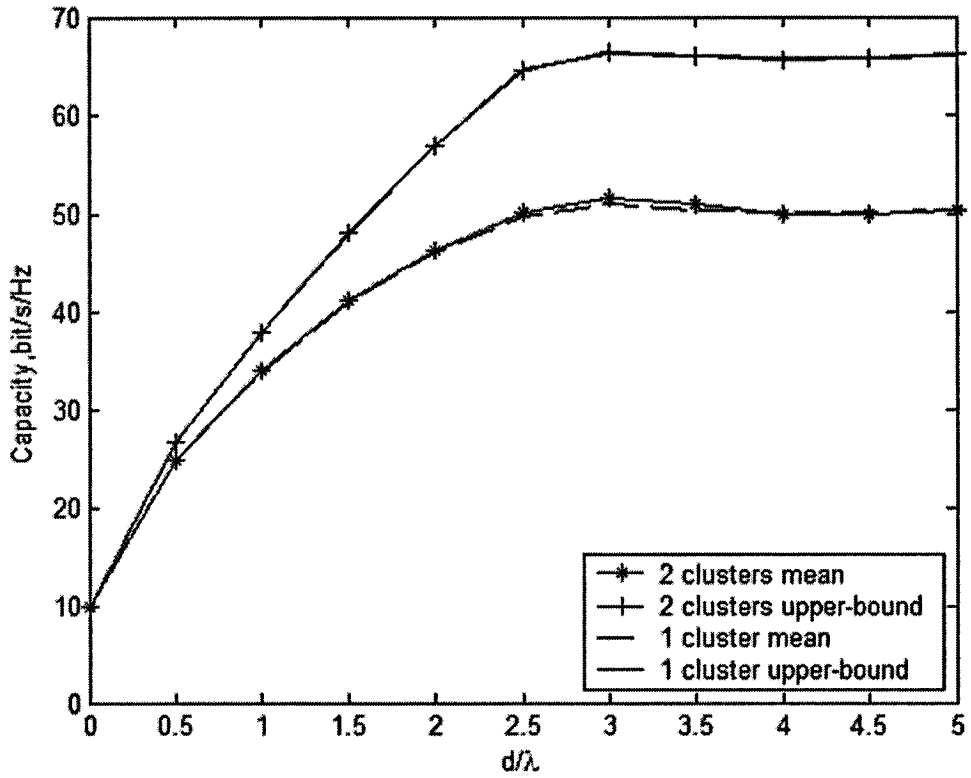

Figure 4-11 two clusters merger to one bigger cluster , the capacity and its upper bound of ULA versus d , number of elements $n = 10$, multipath N=20, and $\rho = 30dB$

4.4.2 Effect of Cluster Locations

We consider the effect of the 2nd cluster location on the channel capacity of ULA.

4.4.2.1 Case 1: Two Symmetric Clusters

Two clusters with same angular spread are located symmetrically with the broadside direction and incoming signal multipath is uniformly distributed in two clusters. We compute the mean and upper bound capacity of ULA using the two-symmetric- cluster model whose correlation was discussed in section 3.3.2. The mean

channel capacity and its upper bound vary with element spacing d, as shown in Figure 4-12 and Figure 4-13

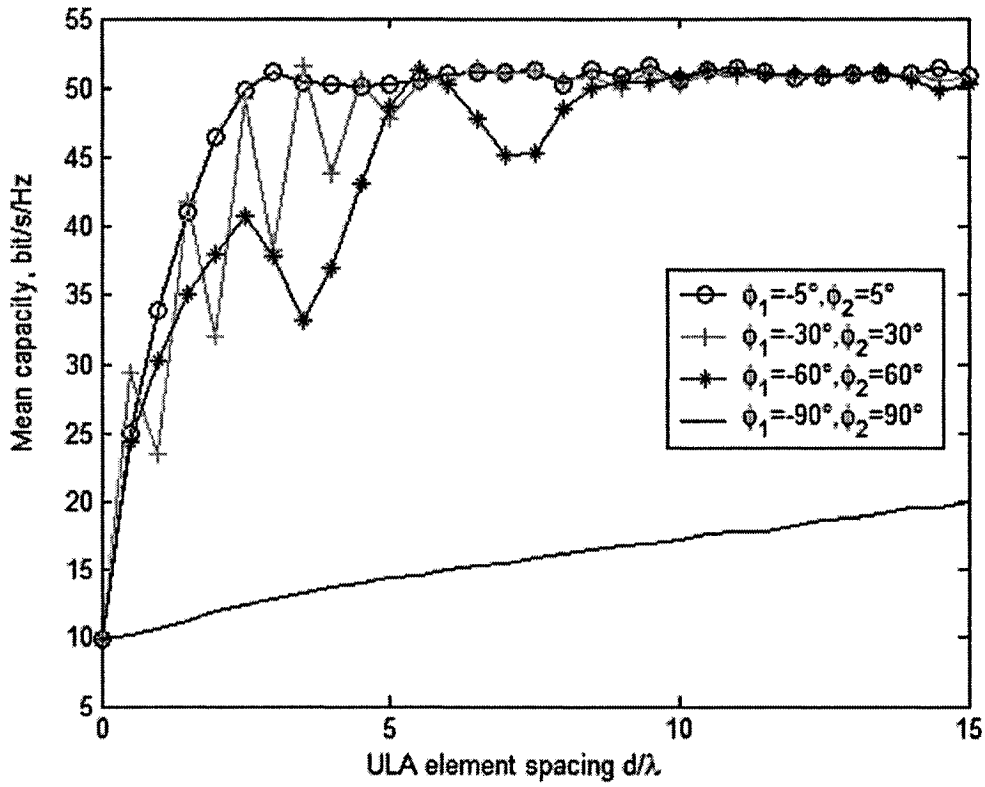

Figure 4-12. Mean channel capacity of two-symmetric-cluster channel versus d for different mean AOA, multipath $N_1 = N_2 = 10, n = 10, \Delta_1 = \Delta_2 = 10°$, and $\rho = 30dB$

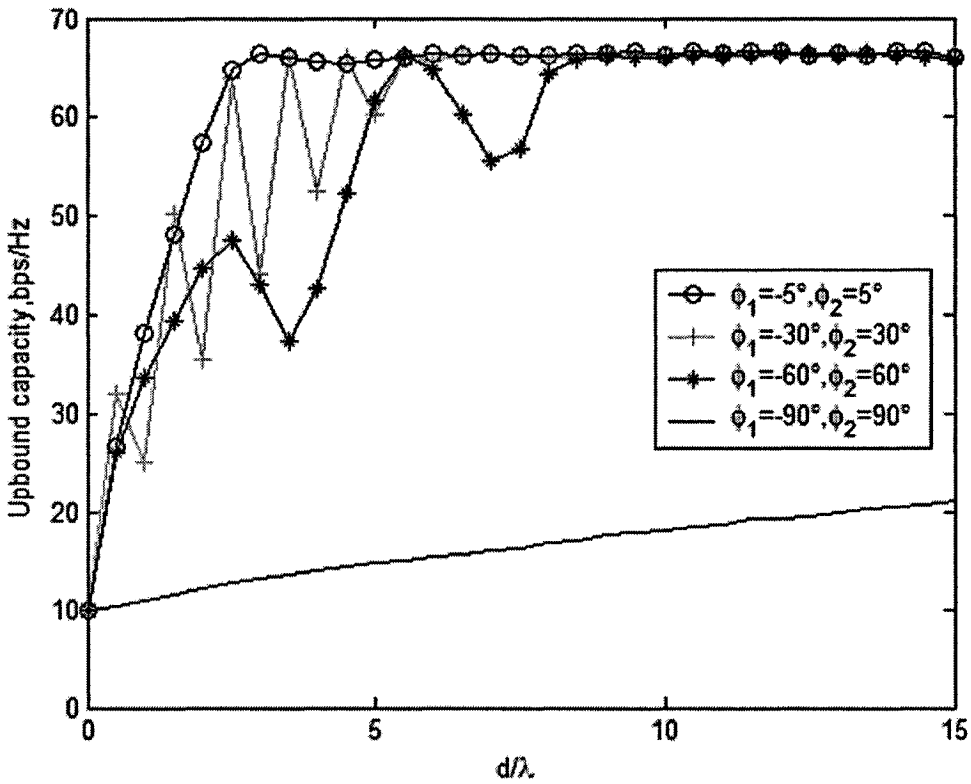

Figure 4-13. Channel capacity upper bound of two-symmetric-cluster channel versus d for different mean AOA, multipath $N_1 = N_2 = 10, n = 10, \Delta_1 = \Delta_2 = 10°$, and $\rho = 30dB$

We have the following conclusions: (1) for small d, the channel capacity of two-cluster channel oscillates with element spacing d, which never occurs in single cluster channel model. (2) For large d, the capacity of two-cluster channel doesn't change significantly with d, and its value is the same as that of using the one bigger cluster channel. (3) The closer to "endfire" the two clusters are located, the higher the loss of the channel capacity and the larger antenna spacing d is required to achieve the full capacity. The limiting case is that both clusters are located at "endfire", the capacity loss is significant even for large d.

4.4.2.2 Case 2: Asymmetric Clusters

The 1st cluster with $\Delta = 10°$ is located in broadside direction, and the 2nd one is at $\Delta = 10°$ at mean AOA $\varphi_2 = 30°, 60°, 90°$, the receiver has $n = 10$ elements and $\rho = 30dB$.

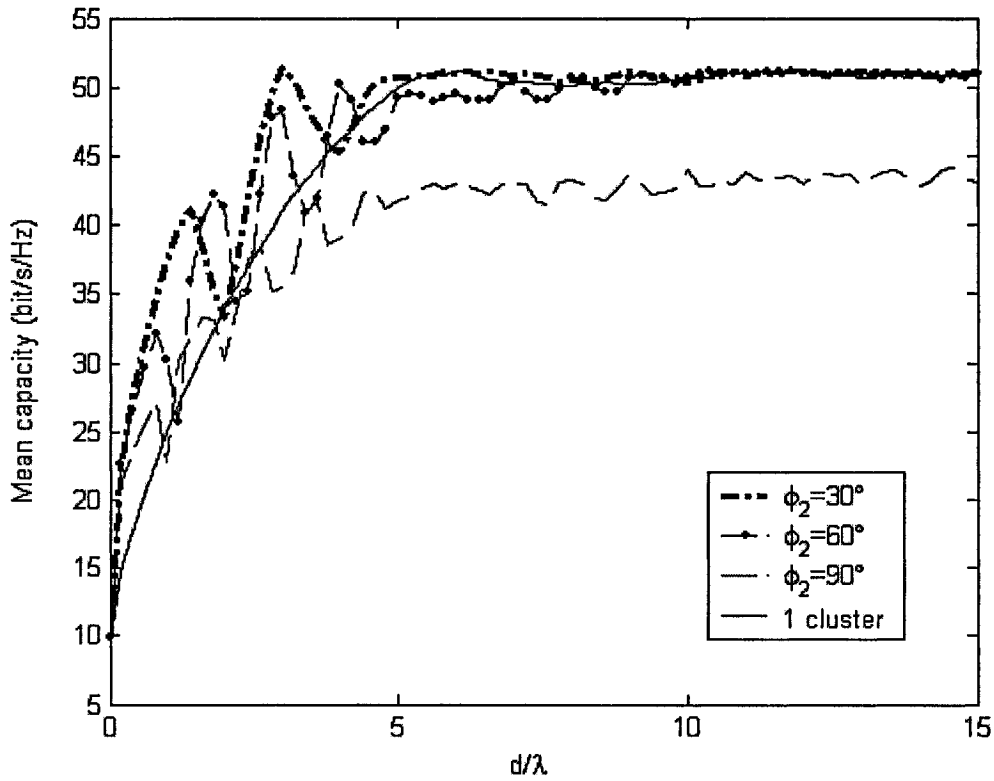

Figure 4-14. The mean capacity versus d when the 1st cluster at broadside, adding the 2nd one with different mean AOA φ_2, $N_1 = N_2 = 10, n = 10, \Delta_1 = \Delta_2 = 10°$ and $\rho = 30dB$

From Figure 4-14, clearly, moving the 2nd cluster to the endfire direction results in lower capacity and lower capacity growth for small spacing. Hence, larger spacing is required to achieve the full capacity. This is in full agreement with the correlation behaviors studied in chapter 3. The channel capacity also oscillates for small d. The 2nd cluster contributes to the channel capacity less when it is located nearer to the inline direction. However the mean capacity for the case for $\varphi_2 = 90^0$ is smaller even for large d because of small contribution of the second cluster.

4.4.2.3 Case 3: Optimum Location

In our two-cluster channel model, what location of the Rx array can maximize the channel capacity? To find this optimum structure, we fix the locations of both clusters, and compute the channel capacity while rotating the receiver array.

The 1st cluster is located in broadside with $\Delta = 10°$, the 2nd cluster is located at mean AOA $\varphi_2 = 90°$ with $\Delta = 10°$. The number of receiver elements is $n_r = 10$. Then we rotate the antenna array clockwise at $\alpha = 15°, 30°, 45°$, where α is the angle between the array line and its original location. This scenario is shown in Figure 4-15.

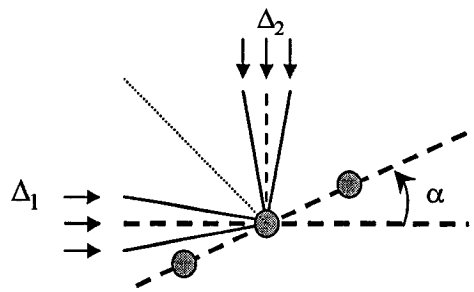

Figure 4-15. Rotate receiver elements in 2-cluster AOA model

Figure 4-16 shows the mean capacity of 2 clusters of multipath channel, in which the angular spread is $\Delta_1 = \Delta_2 = 10°$, multipath $N_1 = N_2 = 10$. Clearly, the maximum capacity is achieved for most d when the array is oriented symmetrically with respect to the clusters, $\alpha = 45^0$ (i.e., the broadside direction coincides with the cluster symmetry line). Any deviation results in capacity decrease for most d. It is especially pronounced when the array endfire is located along one of the clusters, $\alpha = 0^0$, which basically eliminates the contribution of that cluster and results in lower capacity. Due to the geometry symmetry, the capacity behavior for $\alpha \in [45^0, 90^0]$ is the same.

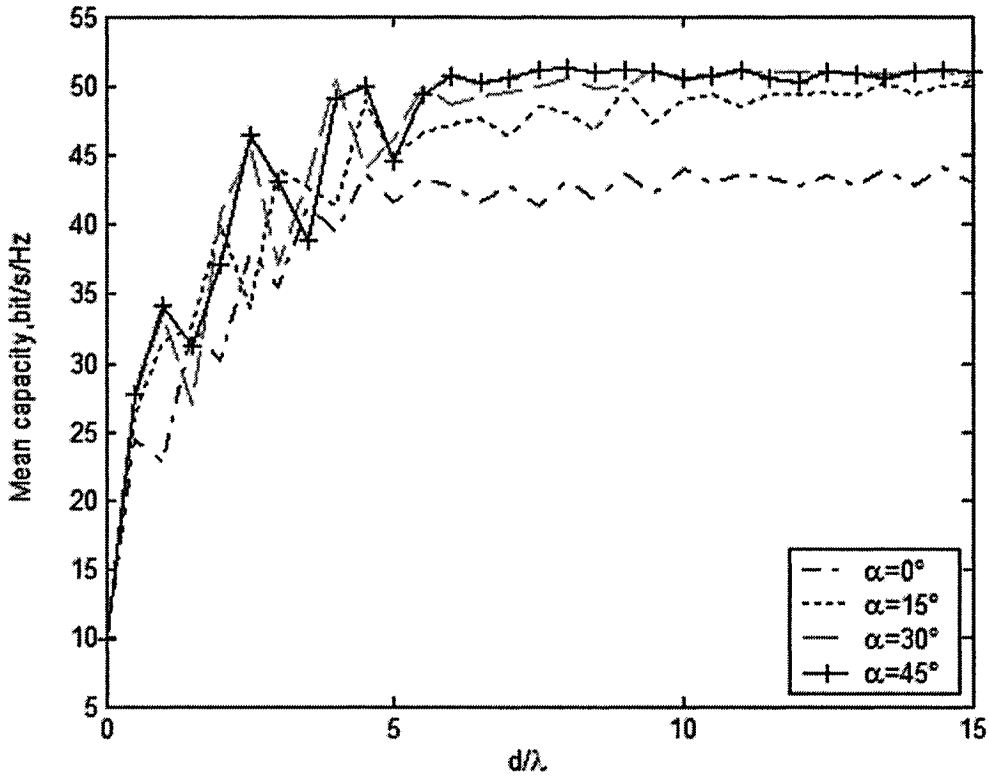

Figure 4-16. Rotate receive arrays with 2 orthogonal cluster channel for different α
$N_1 = N_2 = 10, n = 10, \Delta_1 = \Delta_2 = 10°$ and $\rho = 30dB$

4.4.3 Capacity of UCA

In this section, we study the capacity of UCA using the two-cluster channel model. We use the same validation method as in ULA. As indicated in Figure 4-17, simulation shows that the capacity of UCA using two-cluster channel agrees that using the one bigger cluster channel, as it should be.

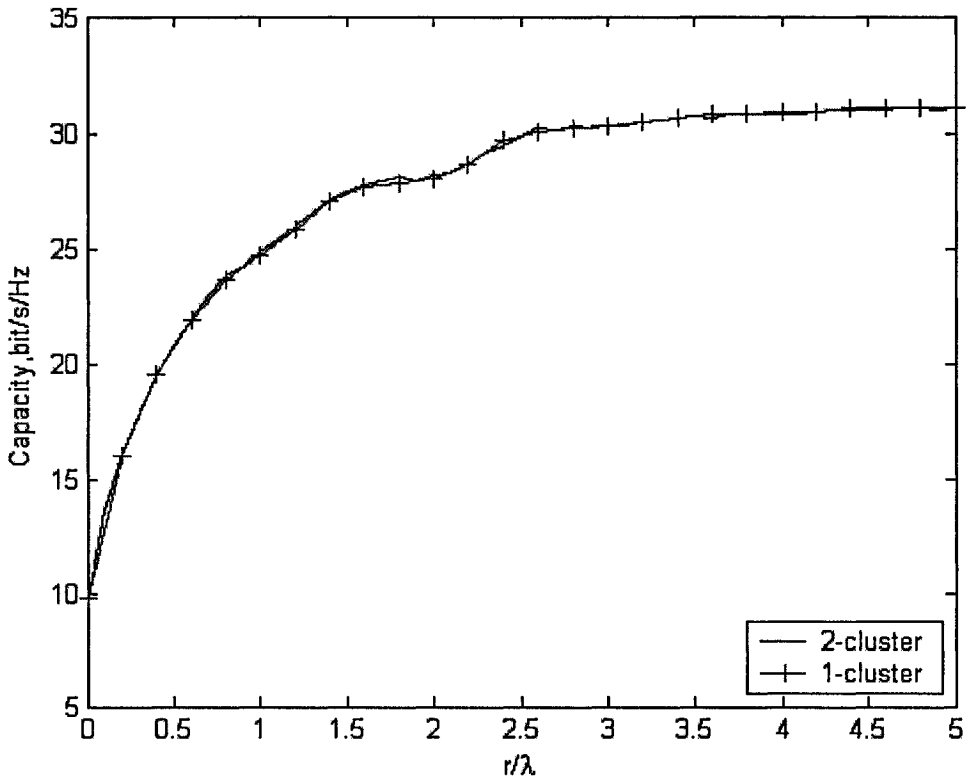

Figure 4-17. Two clusters merge to one bigger cluster, the mean capacity of UCA versus circular radius r, $n=10, \varphi_1=-15°, \varphi_2=15°$, $\Delta_1=\Delta_2=30°$, $N=20$

We study the capacity of UCA using two-symmetric-cluster channel. As shown in Figure 4-18, comparing with Figure 4-12, we can see: (1) Similar to ULA, the capacity of UCA also oscillates with circular radius, but the oscillation is weaker than that of ULA. The oscillating is the most strongest at $\varphi=90°$. (2) Obviously, the effects of the cluster locations on the capacity of UCA are small because the circular array is circular symmetric, as it should be.

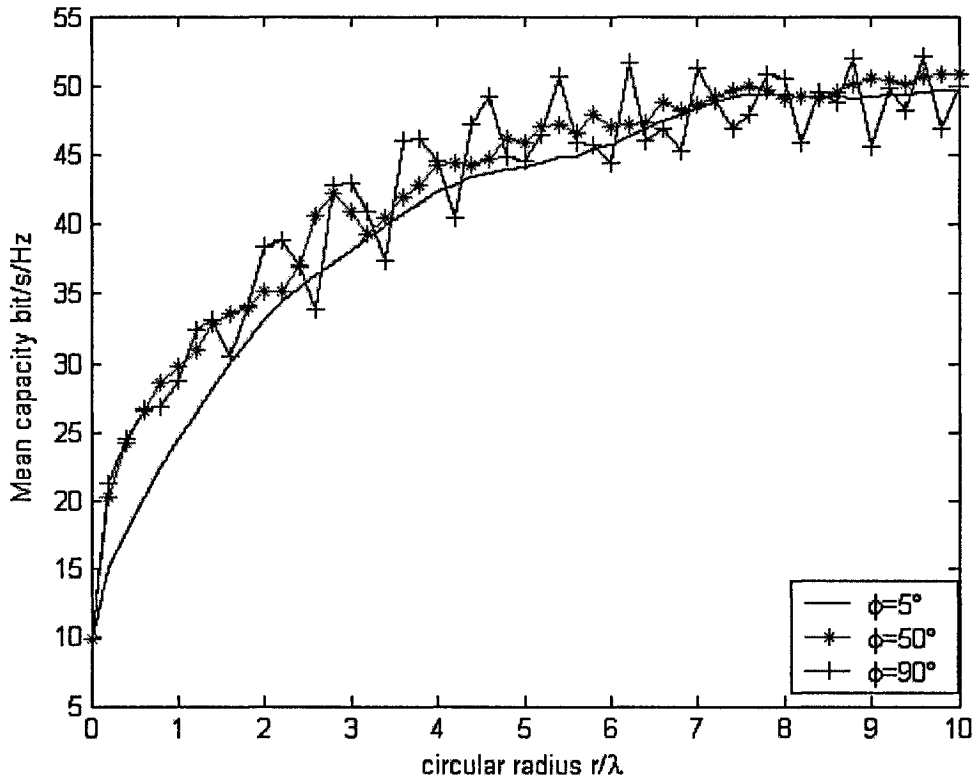

Figure 4-18. The mean capacity of UCA versus circular radius r using two-symmetric-cluster channel for different mean AOA $\varphi_1 = \varphi_2 = \varphi$, number of elements $n = 10$, $\Delta_1 = \Delta_2 = \Delta = 10°$ and $\rho = 30dB$

4.5 Summary

In this chapter, we presented an overview of the information-theoretic channel capacity for the MIMO wireless communications. The contributions in this chapter include:

- We proved that the channel capacity with UCA is lower than ULA with the same aperture because some elements in UCA are "lost" due to correlation. The behavior of channel capacity is in full agreement with the correlation behavior studied in chapter 3.
- We evaluated the channel capacity of a MIMO channel with both ULA and UCA using the two-cluster multipath channel model.

- To have an insight on the effects of the 2nd cluster on the channel capacity, we studied the capacity of a two-cluster channel for various cluster locations and array geometries
- We demonstrated that the maximum capacity is achieved provided that the minimum element spacing is respected. When two cluster are widely separated (i.e., the angular separation is larger than the cluster widths), it is possible to orient the antenna array in such a way that the correlation is minimized and the capacity are maximized
- We also described the Monte-Carlo simulations that validate our calculations

Chapter 5 Combining Diversity

5.1 Introduction

As mentioned in chapter 4, employing MIMO can improve channel capacity. Another advantage of MIMO is that multiple antennas can provide array gain. There are two types of array gain when combining signals. One is "array gain", which is defined as the average power of the combined signal relative to the individual average powers from elements to element. Another is the diversity gain , which is related to a certain outage probability level, say 1%. The diversity gain highly depends on the spatial correlation coefficients between the antenna elements [41].

Diversity is a common technique to compensate for fading channel impairments and always implemented by using two or more antennas. Spatial diversity techniques are the most popular, which have been used to combat multipath fading and mitigate co-channel interference in mobile wireless communication systems. The key idea of spatial diversity is while one antenna addresses a serious fading, another antenna may see a signal peak, and receiver is able to combine these signals at any time. The most common combining methods are selection combining (SC), maximal ratio combining (MRC) and equal gain combining (EGC) [2].

Although spatial diversity is a powerful communication receiver technique, it is reduced by the correlation of the fading signals between the antenna branches. The limited physical space for base station antennas ensures the receiver signals at least partially correlated, Moreover the use of a compact space diversity receiver in mobile phones and portable terminals enhanced this problem. Therefore, it is important to understand how the correlation between received signals affects the diversity gain. Practically, it is of great interest to find out the minimum antenna separation to get maximum diversity gain [45].

In this chapter, we present the theoretical results of the diversity gain in correlated Rayleigh fading channel. Using the two-cluster channel model developed in chapter 2, we compute the diversity gain versus the antenna spacing using Maximum Ratio Combining (MRC). Finally give the effects of the 2nd cluster on diversity gain.

5.2 Theoretical Results

5.2.1 MRC Combing

As shown in Figure 5-1 , the principle of MRC is to choose weighting factor α_i and to use linear coherent combining of branch signals so that the output SNR is maximized.

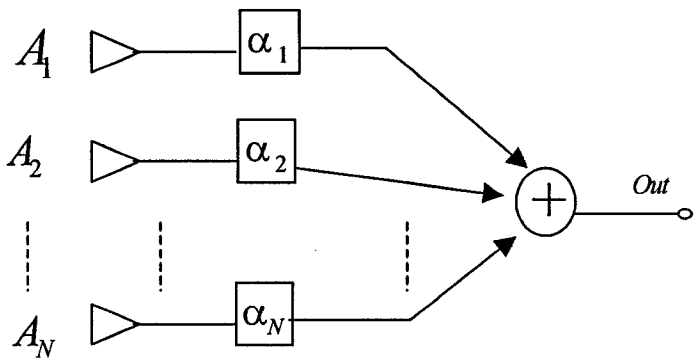

Figure 5- 1. Maximum Ratio Combining (MRC)

Assume incoming signals are plane waves, the individual branch input signals are

$$x_n = g_n A e^{j\omega t} + \xi_n \tag{5.1}$$

Where A is the complex envelope, g_n is the channel gain (complex Gaussian random variable). ξ_n is additive noise. In our discussion, we drop the time factor $e^{j\omega t}$ since it appears everywhere and we are interested in amplitudes only. Then the output signal of the combiner is

$$x_{out} = \sum_{n=1}^{N} \alpha_n x_n = \sum_n \alpha_n g_n A + \sum_n \alpha_n \xi_n \tag{5.2}$$

The signal and noise components are given by the first and the second term correspondingly. The signal power at the output of the combiner is:

$$P_s = \left\langle \left| \sum_n \alpha_n g_n A \right|^2 \right\rangle = \frac{1}{2} |A|^2 \left| \sum_n \alpha_n g_n \right|^2 \tag{5.3}$$

Respectively the noise power at the output of the combiner is

$$P_{\xi} = \left\langle \left| \sum_n \alpha_n \xi_n \right|^2 \right\rangle = \sum_n |\alpha_n|^2 \sigma_n^2 \tag{5.4}$$

where σ_n^2 is the n-th branch noise power. The average output SNR of the MRC is

$$SNR_{out} = \frac{P_s}{P_{\xi}} = \frac{1}{2}|A|^2 \frac{\left| \sum_n \alpha_n g_n \right|^2}{\sum_n |\alpha_n|^2 \sigma_n^2} \tag{5.5}$$

We can maximize (5.5) by using Schwarz inequality [42], and the equality achieved when $\alpha_n = \frac{g_n^*}{\sigma_n^2}$, and the maximum SNR is

$$\gamma_{\max} = \sum_n \gamma_n \tag{5.6}$$

where $\gamma_n = \frac{A^2}{2\sigma_n^2}$ is the n-th branch SNR.

5.2.2 Diversity Gain

Diversity order which is defined as number of independent branches is one of diversity performance metrics. Another is the average SNR diversity gain, which is defined as the reduction in the average SNR of a diversity system that maintains the same BER at the receiver as a system without diversity. In general, the diversity gain obtained by going form one branch (no diversity) to two branches is dominant[43].

Assuming uncorrelated branches in a Rayleigh fading channel, the distribution of SNR_{out} is a chi-square distribution of 2N (N braches), and the outage probability can be expressed as

$$p_{out} \triangleq \Pr\{SNR_{out} \le \gamma\} = 1 - e^{-\frac{\gamma}{\gamma_0}} \sum_{k=1}^{N} \frac{(\gamma/\gamma_0)^{k-1}}{(k-1)!} \tag{5.7}$$

where γ_0 is the average SNR for each branch.

For small $\gamma/\gamma_0 \ll 1$, also p_{out} is small, (5.7) can be simplified as

$$p_{out} \approx \frac{(\gamma/\gamma_0)^N}{N!} \tag{5.8}$$

In this case diversity order is N, and the diversity gain (dB) of a two-branch system is

$$G_d(dB) \triangleq (\gamma_2 - \gamma_1 | P_{out}) = (3 - 10\log P_{out})/2 \tag{5.9}$$

If the signals at the receiver are correlated, the diversity gain will always be reduced, and the effect of correlation can be approximately modeled by introducing equivalent average SNR [44]

$$\gamma_0' = \gamma_0 \left(1 - |R|^2\right) \tag{5.10}$$

where R is the normalized branch correlation, and the approximation requires R is not too close to 1. Respectively the diversity gain of a two-branch system in correlated channel is

$$G_d \triangleq (\gamma_2 - \gamma_1 | P_{out}) = (3 - P_{out}(dB))/2 + 10\log\left(1 - |R|^2\right) \tag{5.11}$$

For small antenna spacing ($d < 0.5\lambda$), the correlation coefficient is close to 1, the approximation (5.11) is not valid any more. In this case, the mutual coupling (MC) effect is significant [45]. When considering the performance of multiple arrays, it should be taken into. Our goal is to study the effect of the 2nd cluster in propagation channel, assuming d is not very small (array is located in the base station), and we will not address MC effect.

5.3 Numerical Results

In chapter 3, we studied the channel correlation based on the two-cluster model. Now, we study the diversity gain using this proposed model. We use the two-symmetric-cluster model whose channel correlation is discussed in detail in section 3.3.2. The scenario is that two clusters with same angular spread $\Delta = 10°$ are located symmetrically at the broadside direction for different mean AOA φ_1. Outage probability is $P_{out} = 1\%$. The results are shown in Figure 5- 2.

Note that when $\varphi_1 = 5°$, two clusters merge to one bigger cluster with mean AOA $\varphi = 0°$ and angular spread $\Delta = 20°$. When the two branches are located at same point ($d = 0$), the gain is 3 dB because the input signal power is doubled with respect to one branch and the noises in these branches are assumed to be independent.

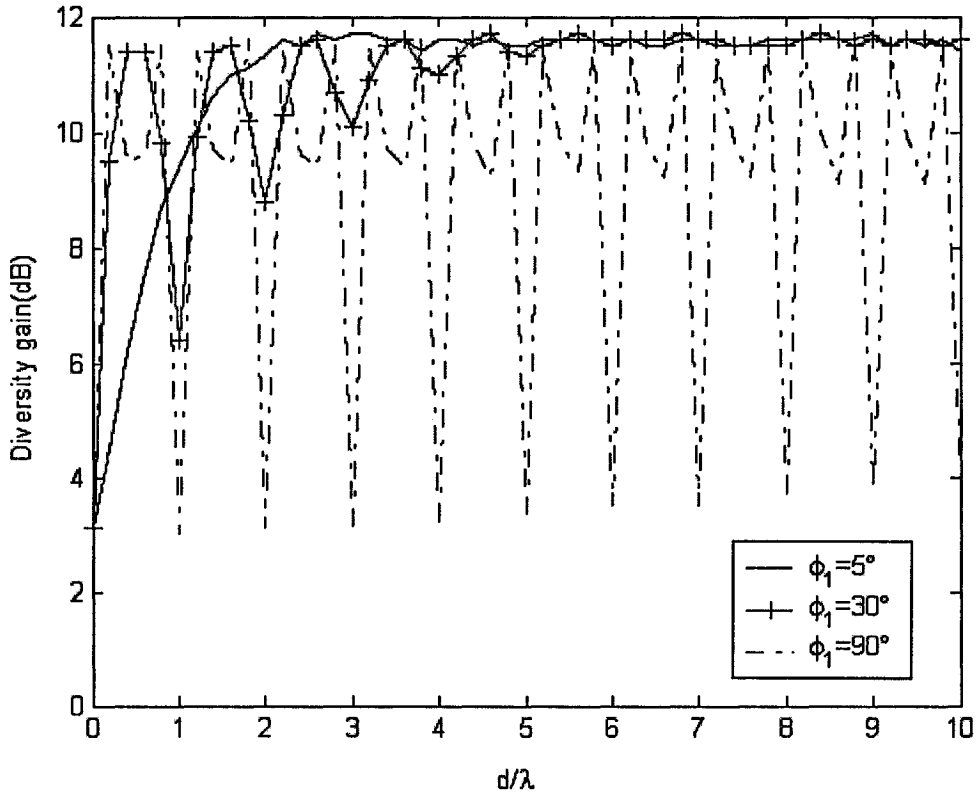

Figure 5- 2. Diversity gain versus antenna spacing for different φ_1 using two-symmetric-cluster model, $\Delta_1 = \Delta_2 = 10°$ outage probability is $p_{out} = 1\%$

To verify this numerical result, Figure 5- 3 shows equation (5.11). As mentioned before, when R is close to 1, the equation (5.11) is not valid. However the oscillation behavior is very similar to those in Figure 5- 2 .

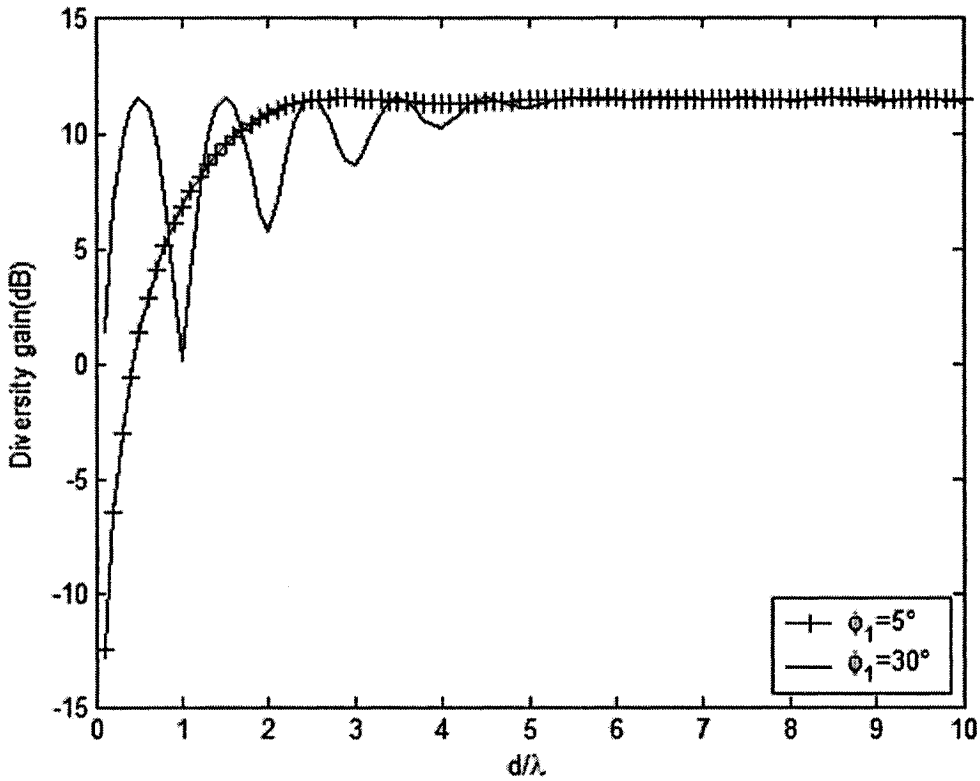

Figure 5- 3. Analytical approximation of diversity gain versus antenna spacing in two-symmetric-cluster channel, $\Delta_1 = \Delta_2 = 10°$, $p_{out} = 1\%$

From Figure 5- 2, we can find the following: (1). After the antenna spacing d increases large enough ($d \geq 5\lambda$), both kinds of channel are uncorrelated, the diversity gain using different channel model achieve the same value $G_d = 11.5dB$, which agrees with equation (5.9). (2) Using single cluster channel model ($\varphi_1 = 5°$), the two branches are required to be separated about 2λ to achieve full diversity gain while using two-cluster model ($\varphi_1 = 30°$), the two branches need to be separated larger ($\geq 5\lambda$). (3) For small d, the diversity gain oscillates with antenna spacing for two-cluster model while it increases almost linearly for single cluster model. Recalling the behavior of the channel capacity versus antenna spacing in chapter 4, we conclude that oscillation in channel correlation results in oscillation in both channel capacity and diversity gain. (4) The oscillations in diversity gain are more pronounced for larger φ_1. Asymptotically, $\varphi_1 = 90°$, the channel is almost totally correlated ($R = 1$) for some d and almost totally

uncorrelated ($R = 0$)for other d , diversity gain never reach the stable whatever the antennas spacing is. (5) These oscillations are much larger than those of the channel capacity. Intuitively, this can be explained by an integral nature of the capacity (when all the local perturbations are averaged out). On the contrary, diversity gain is local in nature since it depends on rare evens (outage) and, hence, it is more sensitive to details of the angular PDF [46].

5.4 Summary

In this chapter, we studied the diversity gain with antennas spacing using two-cluster multipath channel model. We found that:

- Similar to the channel capacity behavior, the 2nd cluster also caused oscillation in diversity gain with the antenna spacing
- The oscillations of diversity gain is much stronger than that of the channel capacity.

Chapter 6 General Conclusions and Future Work

This thesis extends single cluster multipath model to multi-cluster one. Multipath components arriving in different clusters are assumed to be uncorrelated and uniformly angular-distributed within the corresponding clusters. Based on the multi-cluster channel model, the system performance of MIMO antenna systems for wireless communication system such as channel capacity and diversity gain are examined. The results presented agree well with those published in the literature earlier and extend them to the case of multi-cluster channels. Overall, this thesis presents a new insight on correlation properties of multipath clustered channels and on the multi-antenna system performance over such channels.

6.1 Summary

In chapter 1, the motivation for using multiple transmit and multiple receive antenna arrays for wireless communications was first discussed, and then outlined our channel modeling efforts in this research .

In chapter 2, we reviewed the characteristics of wireless propagation channel, such as signal attenuation, time dispersion, and frequency dispersion for conventional single-input single-output (SISO) system, and the angle of arrival (AOA) signal dispersion for MIMO systems. Vector channel model using both uniform linear array (ULA) and uniform circular array (UCA) for SIMO channel were derived. The review of various power azimuth spectrum (PAS) and multi-cluster models were given. We extended single cluster model to multi-cluster one.

In chapter 3, the channel correlation of two-cluster channel is studied in details, including both symmetrical and asymmetrical location of the clusters, and equal/unequal angular spreads and power distributions. It is shown that the correlation coefficient has an oscillatory behavior with respect to the antenna spacing. As a cluster moves away from the array broadside direction, its contribution to the total correlation decreases (inverse cosine law). In the case of identical symmetrically-located clusters, the envelope of

correlation is determined by a single cluster angular spread while the oscillations within the envelope are determined by the inter-cluster angular spread (for both clusters). If the clusters are identical and located asymmetrically (i.e., broadside-endfire), the impact of the endfire cluster is, in many cases, much smaller and can be neglected for proportional power allocation). Hence, one-cluster model can be used, which simplifies the analysis substantially.

In chapter 4, we presented an overview of the information-theoretic channel capacity for the MIMO wireless communications. Using the two-cluster multipath channel model, we evaluate the channel capacity of a MIMO channel with both ULA and UCA. It is shown that the channel capacity with UCA is lower than ULA with the same aperture because some elements in UCA are "lost" due to correlation. The behavior of channel capacity is in full agreement with the correlation behavior studied in chapter 3. To have an insight on the effects of the 2nd cluster on the channel capacity, we study the capacity of a two-cluster channel for various cluster locations and array geometries. We demonstrate that the maximum capacity is achieved provided that the minimum element spacing is respected. When two cluster are widely separated (i.e., the angular separation is larger than the cluster widths), it is possible to orient the antenna array in such a way that the correlation is minimized and, hence, the capacity are maximized. Monte-Carlo simulations which validate our calculations are also described.

In chapter 5, we studied the diversity gain for two-cluster multipath channel model. We found that, similar to the channel capacity behavior, the 2nd cluster also caused oscillation in diversity gain and the oscillation is much stronger than that of the channel capacity.

6.2 Future Work

In the area of channel modeling, we have extended single cluster channel model to multi-cluster one, assuming the PAS within each cluster are uniformly distributed. Actually, measurements have shown that PAS in single cluster channel is Laplacian distributed rather than uniformly distributed, as mentioned in chapter 2. More accurate PAS in multi-cluster channel model need to be considered in the future research. Time dispersion and AOA dispersion effects need to be considered together in later research.

References

[1] T. S. Rappaport, A. Annamalai, R.M. Buehrer and W.H. Tranter, "Wireless Communications: Past Events and a Future Perspective," *IEEE Communications Magazine*, Vol. 40, No. 5, May 2002, pp. 148 -161

[2] T. S. Rappaport, *Wireless Communications Principle and Practice*, New York: Prentice Hall, 1996

[3] B. Sklar, "Rayleigh Fading Channels in Mobile Digital Communication Systems, Part I: Characterization," *IEEE communications magazine*, Sep. 1997, pp. 136-146

[4] B. Sklar, "Rayleigh Fading Channels in Mobile Digital Communication Systems, Part II: Mitigation," *IEEE communications magazine*, Sep. 1997, pp. 148-155

[5] F. Adachi, M.T. Feeney, A.G. Williamson and J.D. Parsons, "Crosscorrelation between the Envelopes of 900 MHz Signals Received at a Mobile Radio Base Station Site," *IEE Proc.*, 1986,133, (6), pp. 506-512

[6] P.C.F. Eggers, "Angular Dispersive Mobile Radio Environments Sensed by Highly Directive Base Station Antennas," *Proceedings of 6th international symposium on Personal, indoor and mobile radio communications*, PIMRC'95, Toronto, Canada, September 1995, pp. 522-526

[7] P.C.F. Eggers, "Angular-temporal Domain Analogies of the Short-term Mobile Radio Propagation Channel at the Base Station", *Proceedings of 7th international symposium on Personal, indoor and mobile radio communications*, PIMRC'96, Taipeh, October 1996, pp. 742-746

[8] J. Fuhl , A. F. Molisch and E. Bonek, "Unified Channel Model for Mobile Radio Systems with Smart Antennas", *IEE Proc-Radar, Sonar Navig.*, Vol. 145, No. 1, Feb. 1998, pp. 32-41

[9] C. P. Mathews and M. D. Zoltowski, "Eigenstructure Techniques for 2-D Angle Estimation with Uniform Circular Arrays," *IEEE Trans. On signal processing*, Vol. 42, No. 9, Sep. 1994, pp. 2395-2407

[10] A. Papoulis, *Probability, Random Variables, and Stochastic Processes*. McGraw Hill, 3rd ed., 1991

[11] K. I. Pedersen, J. B. Andersen, J. P. Kermoal and P. Mogensen, "A Stochastic Multiple-Input-Multiple-Output Radio Channel Model for Evaluation of Space-

Time Coding Algorithms", *IEEE VTS-Fall VTC 2000.* 52nd, Vol. 2, 2000, pp. 893 - 897

[12] R. B. Ertel, P. Cardieri, K. W. Sowerby, T. S. Rappaport, and J. H. Reed, " Overview of Spatial Channel Models for Antenna Array Communication Systems, " *IEEE Personal communications,* Feb. 1998. pp. 10-22

[13] W. C. Y. Lee, *Mobile Communications Engineering*, New York: McGrew Hill, 1982

[14] J. Salz and J. H. Winters, "Effect of Fading Correlation on Adaptive Arrays in Digital Mobile Radio," *IEEE Tran. Veh. Technol.*, Vol. 43, No. 4, Nov. 1994, pp. 1049-1057

[15] W.R. Braun and U. Dersch, " A Physical Mobile Radio Channel Model", *IEEE Tran. Veh. Technol.*, 1991, 40, pp. 472-482

[16] K. I. Pedersen, P. E. Mogensen and B. H. Fleury, "Power Azimuth Spectrum in Outdoor Environments", *Electronics Letters* 28th Vol. 33, No. 18, Aug. 1997, pp.1583-1584

[17] K. I. Pedersen, P. E. Mogensen and B. H. Fleury, " Spatial Channel Characteristics in Outdoor Environments and their Impact on BS Antenna System Performance" *IEEE VTC 98*, pp.719-723

[18] A. Abdi and M. Kaveh, " A Versatile Spatio-temporal Correlation Function for Mobile Fading Channels with Non-isotropic Scattering," in *Proc. IEEE Workshop Statistical Signal Array Processing*, Pocono Manor, PA, 2000, pp. 58-62

[19] M. Lu, T. Lo, and J. Litva, " A Physical Spatio-temporal Model of Multipath Propagation channel," *Proc. IEEE VTC*, 1997, pp. 810-814

[20] A. A. Saleh and R. A. Valenzuela, " A Statistical Model for Indoor Multipath Propagation," *IEEE J. Select. Areas Commun.* , Vol. SAC-5, Feb. 1987, pp.128-137

[21] Q. Spencer, M. Rice, B. Jeffs, and M. Jensen, " A Statistical Model for Angle of Arrival in Indoor Multipath Propagation," in *Proc. 1997 IEEE Veh. Technol. Conf.*, Vol. 3, Phoenix, AZ, May 4-7, 1997, pp. 1415-1419

[22] J.G. Proakis and M. Salehi, *Communications Systems Engineering*, 2nd ed., Prentice Hall, Upper Saddle River, 2002.

[23] P. Zetterberg and P. L. Espensen, "A Downlink Beam Steering Technique for GSM/DCS1800/PCS1900," *IEEE Seventh International Symposium on Personal, Indoor and Mobile Radio Communications,* Oct. , 1996, Vol. 2 , pp. 535 -539

[24] P. Zetterberg and B. Ottersten, " The Spectrum Efficiency of a Base Station Antenna Array System for Spatially Selective Transmission," *IEEE Transactions on Vehicular Technology,* vol. 44, No. 3,pp. 651-660, August 1995

[25] B. Ottersten, "Spatial Division Multiple Access (SDMA) in Wireless Communications," *Proc. Nordic Radio Symp.*, Apr., 1995

[26] K. I. Pedersen, P. E. Mogensen and B. H. Fleury, "A Stochastic Model of the Temporal and Azimuthal Dispersion Seen at the Base Station in Outdoor Propagation Environments," *IEEE Trans. Veh. Technol.*, Vol. 49, No.2, Mar. 2000, pp.437-447

[27] P. D. Teal, T. D. Abhayapala and R. A. Kennedy, " Spatial Correlation for General Distributions of Scatters," *IEEE signal processing letters*, Vol. 9, No. 10, Oct., 2002, pp. 305-308

[28] S. Loyka and G. Tsoulos, " Estimating MIMO System Performance Using the Correlation Matrix Approach," *IEEE Commun. Lett.*, Vol. 6, No. 1, Jan. 2002, pp.19-21

[29] L. Schumacher, K. I. Pedersen and P. E. Mogensen, "From Antenna Spacing to Theoretical Capacities - Guidelines for Simulating MIMO Systems", *Proceedings of 13th IEEE International Symposium on Personal Indoor Mobile and Radio Communications*, September, 2002

[30] G. J. Foschini, "Layered Space-time Architecture for Wireless Communication in Fading Environments when Using Multi-element Antennas," *Bell Labs Tech. J.*, pp. 41–59, Autumn 1996

[31] I. E. Telatar, "Capacity of Multi-antenna Gaussian Channels," *Bell labs Technical Memorandum*, 1995

[32] L.J. Greenstein, J.B. Andersen, H.L. Bertoni, S. Kozono, D.G. Michelson, and W.H. Tranter, "Channel and Propagation Models for Wireless System Design i and ii," *IEEE Journal on Selected Areas in Communications*, Vol. 20, No. 3, April 2002, pp. 493 -495

[33] D. Chizhik, J. Ling, P.W. Wolniansky, R.A. Valenzuela, N. Costa and K. Huber, "Multiple-input-multiple-output Measurements and Modeling in Manhattan", *IEEE Journal on Selected Areas in Communications.* Vol. 21, No. 3, Apr. 2003, pp.321-331

[34] N. Al-Dhahir, "Overview and Comparison of Equalization Schemes for Space-time-coded Signals with Application to EDGE," *IEEE Trans. Sign. Proc.*, Vol. 50, No. 10, pp. 2477–2488, Oct 2002.

[35] D. Chizhik, J. Ling, P. Wolniansky, R. Valenzuela, N. Costa, and K. Huber, "Multiple-input-multiple-output Measurements and Modeling in Manhattan," in *Proceedings of IEEE Vehicular Tech.* Conf., 2002.

[36] A. Goldsmith, S. A. Jafar, N. Jindal, and S. Vishwanath, "Capacity Limits of MIMO Channels", *IEEE Journal on Selected Areas in Communications*, Vol. 21, No. 5, June 2003, pp. 684 -702

[37] G.J. Foschini and M.J. Gans, "On Limits of Wireless Communications in a Fading Environment when Using Multiple Antennas," *Wireless Personal Communications*, Vol. 6, No. 3, pp. 311-335, Mar. 1998

[38] S. Loyka, A. Kouki, "Correlation and MIMO Communication Architecture (Invited)", *8th International Symposium on Microwave and Optical Technology*, Montreal, Canada, June 19-23, 2001.

[39] D. S. Shiu, G.J. Foschini , M. J. Gans, and J. M. Kahn, " Fading Correlation and its Effect on the Capacity of Multi-element Antenna Systems," *IEEE Tran. Commun.* , Vol. 48, No. 3, pp. 502-513, Mar. 2000

[40] Pollock, T.S., Abhayapala, T.D. and Kennedy, R.A., "Antenna Saturation Effects on Dense Array MIMO Capacity ", *Proc. International Conference on Acoustics, Speech, and Signal Processing*, ICASSP'2003, Hong Kong, April 6-10, 2003

[41] J. Bach Andersen, "Array Gain and Capacity for Known Random Channels with Multiple Element Arrays at Both Ends", *IEEE Journal on Selected Areas in Communications-Wireless Communication Series*, November, 2000, Vol. 18, No. 11, pp. 2172-2178

[42] W. C. Jakes, Ed., *Microwave Mobile Communications*. New York: Wiley, 1974

[43] J. G. Proakis, *Digital communications*, third edition, New York: McGraw-Hill, 1995

[44] M. Schwartz, W. R. Bennett, and S. Stein, *Communication Systems and Techniques*. New York: McGraw-Hill, 1966

[45] J. Luo, J.R Zeidler, and S. McLaughlin, "Performance Analysis of Compact Antenna Arrays with MRC in Correlated Nakagami Fading Channels," *IEEE Transactions on Vehicular Technology*, Vol. 50, No. 1, Jan. 2001, pp. 267 –277

[46] S. Loyka and G. Zhao, "Extending Salz-Winters Model to Multiple-Cluster Wireless Channels", submitted

Appendix Simulation Programs

File list

Single cluster channel with ULA
Rray.m – instantanous correaltion matrix
Aver_ray.m – Monto carlo average
Work_ray_cor – channel correlation coefficient/envelope correlation
Work_ray_cap –channel capacity

Sigle cluster channel with UCA
Rray_UCA.m - instantaneous correlation matrix
Aver_ray_UCA.m – averge values using Monte-Carlo
Work_ray_UCA_cor.m – correlation of UCA
Work_ray_UCA_ULA.m – capacity of ULA/UCA comparison
Work_ray_UCA_fixr.m –capacity of UCA versus number of elements
Work_iso_UCA.m —capacity of UCA using isotropic cluster channel
Work_iso_UCA_valid.m – capacity of UCA validation

Two –clsuter channel with ULA
Cray – instantaneous correlation matrix of single cluster
Rcluster – instantaneous correlation matrix of two-cluster channel
Aver_cluster -- average value using Monte-Carlo using Rcluster
Work_cluster_cap – channel capacity
Work_cluster_sym – symetric clusters
Work_clsuter_rotate – rotate ULA
Work_cluster_assym_fixp –fixed power allocation case
Work_clsuter_assym_prop – proportional power allocation case

Crcluster – contributions from clusters comparison
Aver_clsuter- average contributions using Crcluster
Work_cluster_com –work file for contributions from clusters comparison

Prcluster— power unequal distribued in two clusters
Aver_cluster_cor – average value using Prcluster
Work_cluster_pun – work file for power unblanced cluster channel

Rcluster_diversity – sample diversity
Work_cluster_diversity – work file for diversity gain

Two –clsuter channnel with UCA
Cray_UCA –channel matrix
Rxluster_UCA – instantaneous correlation matrix
Aver_cluster_UCA – mean value using Monte-Carlo
Work_cluster_fixn – capacity of UCA versus radius
Work_cluster_fixr - capacity of UCA versus Rx antennas

	Single cluster	Two-cluster			
ULA					
One-cluster	Rray	Cray			
clusters		Rcluster	CRcluster	Prcluster	Rcluster_diversity
average	Aver_ray	Aver_cluster	Aver_Ccluster	Aver_Pcluster	
workfile	Work_ray_cor	Work_cluster_sym	Work_clsuter_com	Work_Pcluster	Work_cluster_diversity
	Work_ray_cap	Work_cluster_cap			
		Work_cluster_rotate			
		Work_cluster_assym_fixp			
		Work_cluster_assym_prop			
			Contributions comparison	*Power fix allocation*	*Diversity gain*
UCA					
One-cluster	Rray_UCA	Cray_UCA			
cluster		Rcluster_UCA			
average	Aver_ray_UCA	Aver_cluster_UCA			
workfile	Work_ray_UCA_cor	Work_cluster_fixn			
	Work_ray_UCA_ULA	Work_cluster_fixr			
	Work_ray_UCA_fixr				
	Work_iso_UCA				
	Work_iso_UCA_valid				

One cluster model

1.ULA

Rray.m – instantanous correaltion matrix
Aver_ray.m – Monto carlo average
Work_ray_cor – channel correlation coefficient/envelope correlation
Work_ray_cap –channel capacity

Rray.m

```
function  R = Rray(N,n,d,dfi,fi0)
%
% This is a file for computing correlation matrix of a multipath matrix
% channel N rays exist for every Tx (the same AOA set for every Tx)
with (i)independent
% phases and the same magnitude or (ii) independent complex Gausian
gains,
% uncorrelated from Tx to Tx.
%
% fi - angle-of-arrival (AOA)
% dfi - angular spread
% fi0 - mean angle of arrival
% ksi - phase shift between two adjacent elements
% n - the number of antennas
% N - the number of rays
% psi - their phases
% a - Tx complex gains
%

fi = rand(N,1)*2*dfi-dfi+fi0;                    % uniform in[fi0-dfi,
fi0+dfi]

ksi = 2*pi*d*sin(fi);                            % N rays phase

for j = 1:n                                      % number of Tx
   a = 1/sqrt(2)*(randn(N,1) + 1i*randn(N,1));   % Rayleigh fading
   for i = 1:n                                   % number of Rx
       h(i,j) = trace(diag(a.*exp(-1i*i*ksi)));  % channel
   end                                           % end for Rx
end                                              % end for Tx
Rr = 1/(n*N)*h*h';                               % normalized
correlation matrix
R = {Rr};                                        % output data
```

Aver_ray.m

```
function A = Aver_ray(M,N,n,d,dfi,fi0,ro)
%
% This is a file for computing the average correlation matrix and the
mean
% (ergodic) capacity of a multipath matrix channel.Instantaneous
correlation
% matrix R is computed by Rray.
%
% N - the number of rays
% R and Rt - instantaneous Rx and Tx brach correlations
% ctr - mean capacity (by averaging M trials)
% Rtr- mean Rx correlations (over M trials)
% M - the number of trials
% d - element spacing of Rx array
% dfi - angular spread
% fi0 - average AOA
% ro - average SNR (ro/n - average SNR per Rx branch)
% cor - mean adjacent correlation coefficient
% cor_enve --mean adjacent envelope correlation

ctr=0;                                          % initialize
Rtr(n,n)=0;
A = zeros(n,n,2);
cor1=0;cor2=0;cor3=0;
cor = 0;
for m=1:M                                       % loop for trials
   Rout = Rray(N,n,d,dfi,fi0);                  % instantaneous R
   R = Rout{1};                                 % R --2*2  correlation
matrix
   cor1=cor1+R(1,1)*real(R(2,1));               % x1*x2 --see Lee's
book
   cor2=cor2+R(1,1)*imag(R(2,1));               % x1*y2
   cor3=cor3+ R(1,1).^2;                        % x1*x1
   cor=cor+R(2,1);                              % correlation
coefficient
   ctr = log2(det(eye(n)+ro/n*R))+ctr;          % intantaneous capacity
   Rtr = R+Rtr;                                 % sum correlation
matrix
end                                             % end loop for trials
cor = cor/M;                                    % mean correlation
coefficient
cor1=cor1/M;                                    % average x1*x2
cor2=cor2/M;                                    % average x1*y2
cor3=cor3/M;                                    % average x1*x1
cor_enve=(cor1.^2+cor2.^2)/cor3.^2;             % envelope correlation
Rtr=Rtr/M;                                      % average correlation
matrix
cavtr = log2(det(eye(n)+ro/n*Rtr));             % upperbound capacity

A = {Rtr ctr/M cavtr abs(cor) cor_enve};        % output data
```

Work_ray_cap.m

```
% This is a working file for envelope correlation estimation  using one
% cluster model. Instantaneous correlation matrix is computed by Rray
and
% the averaging by Aver_ray.
%
% M - the number of trials
% n - the number of antennas
% d - element spacing (in wavelength)
% dfi - the angular spread of incoming signals
% fi0 - the average angle
% ro - average SNR (ro/n - average SNR per Rx branch)
% S_fi- power azimuth spread

close all;                                          %initialize
clear all;
M = 10000; N=10; n = 2; ro = 10^3;
tic;                                                %time initialize
format short;                                       %data format
format compact;

sig_fi=[3 5 10 20 45.5 180];                        % in paper "unified
model..."
for fi_0=0:30:90                                    % loop for fi0 (degree)
   fi0=fi_0*pi/180;                                 % mean AOA (arc)
   for  s_index=1:length(sig_fi)                    % loop for angular
spread
      S_fi=sig_fi(s_index);                         % angular spread
      dfi = sqrt(3)*S_fi*pi/180;                    % uniform PAS

      InDat = [M N n S_fi fi0*180/pi ro];           % input data
                                                    % data file name
      s = ['cor_ray' int2str(M) '_' int2str(N) '_' int2str(n) '_'
int2str(fi0*180/pi) '_' int2str(S_fi) '.dat'];
      fid = fopen(s,'w');                           % open file
                                                    % write to file
      fprintf(fid,'M=%g\t N=%g\t n=%g\t  S_fi=%g\t fi0=%g\t
ro=%g\n\n',InDat);
                                                    % list on screen
      fprintf('\n\n  M=%g\t N=%g\t n=%g\t S_fi=%g\t fi0=%g\t
ro=%g\n\n',InDat);
                                                    % write to file
      fprintf(fid,'\t   d\t\t   cor\t\t   cor_enve\t\t time\n\n');
                                                    % list on screen
      fprintf('    d\t       cor\t   cor_enve     time\n\n');
      for i = 0:0.05:5                              % loop for antenna
spacing d
         d = i;                                     % set d/wavelength
change
         Out = Aver_ray(M,N,n,d,dfi,fi0,ro);        % average  by Aver_ray
         cor = Out{4};                              % Rx correlaton
coefficient
         cor_enve=Out{5};                           % Rx envelope
correlation
         Out_data = [d cor cor_enve toc];           % output data
```

```
                                                    % write output data to
file
         fprintf(fid,'%8.3f\t %8.2f\t %8.2f\t %8.2f\n',Out_data);
                                                    % list on screen
         fprintf('%8.3f  %8.2f %8.2f %8.2f\n',Out_data);
      end                                           % end loop for d
      status = fclose(fid);                         % close file
   end                                              % end loop for dfi
end                                                 % end loop for fi0
```

Work_ray_cor.m

```
% This is a working file for correlation and capacity estimation of
% matrix multipath (ray) channel using Slaz-Winters model.
% Vectorization of loops is employed. Instantaneous correlation matrix
% is computed by Rray and the averaging by Aver_ray.
%
% M - the number of trials
% n - the number of antennas
% d - element spacing (in wavelength)
% dfi - the angular spread of incoming signals
% fi0 - the average angle
% ro - average SNR (ro/n - average SNR per Rx branch)

clear all;                                              % initialize
M = 1000; N=20; n = 10; fi0 = 0*pi/180; ro = 10^3;
tic;                                                    % time initialize
format short;                                           % data format
format compact;
for k = 1:1                                             % void loop
   for df = 10:10                                       % loop for dfi
      dfi = df*pi/180;
      InDat = [M N n dfi*180/pi fi0*180/pi ro];         % input data
                                                        % file name
      s = ['one-cluster-' int2str(M) '_' int2str(N) '_' int2str(n) '_'
int2str(dfi*180/pi) '_' int2str(fi0*180/pi) '.dat'];
      fid = fopen(s,'w');                               % write to file
      fprintf(fid,'M=%g\t N=%g\t n=%g\t   dfi=%g\t fi0=%g\t
ro=%g\n\n',InDat);
                                                        % list on screen
      fprintf('\n\n  M=%g\t   N=%g\t n=%g\t  dfi=%g\t  fi0=%g\t
ro=%g\n\n',InDat);
                                                        % write to file
head
      fprintf(fid,'\t   d\t\t   ctr\t\t  cavtr\t\t  time\n\n');
                                                        % list on screen
      fprintf('    d\t       ctr\t cavtr       time\n\n');
      for i =0:0.5:30                                   % loop for d
         d = i ;
         Out = Aver_ray(M,N,n,d,dfi,fi0,ro);            % average value
         Rtr = Out{1};                          % correlation matrix
         ctr = Out{2};                                  % mean capcity
         cavtr = Out{3};                                % upper bound
         cor = Out{4};                          % correlation coefficient
         cor_enve = Out{5};                     % envelope correlation
         Out_data = [d ctr cavtr toc];                  % output data
                                                        % write to file
         fprintf(fid,'%8.3f\t %8.2f\t %8.2f\t %8.2f\n',Out_data);
                                                        % list on screen
         fprintf('%8.3f   %8.2f   %8.2f   %8.2f\n',Out_data);
      end                                               % end loop for d
      status = fclose(fid);                             % file close
   end                                                  % end loop for dfi
end                                                     % end loop for k
```

2.UCA

Rray_UCA.m - instantaneous correlation matrix
Aver_ray_UCA.m – averge values using Monte-Carlo
Work_ray_UCA_cor.m – correlation of UCA
Work_ray_UCA_ULA.m – capacity of ULA/UCA comparison
Work_ray_UCA_fixr.m –capacity of UCA versus number of elements
Work_iso_UCA.m —capacity of UCA using isotropic cluster channel
Work_iso_UCA_valid.m – capacity of UCA validation

Rray_UCA.m

```
function  R = Rray_UCA(N,nt,nr,r,dfi,fi0)
%
% This is a file for computing correlation matrix of a multipath matrix
channel
% N rays exist for every Tx (the same AOA set for every Tx) with
% (i) independent phases and the same magnitude or
% (ii) independent complex Gausian gains, uncorrelated from Tx to Tx.
% (iii) for uniform circular array
%
% fi - angle-of-arrival (AOA)
% dfi - angular spread
% fi0 - mean angle of arrival
% ksi - phase shift between 1 element and its i-th neighbour
% nt - the number of TX antennas
% nr - the number of Rx antennas
% N - the number of rays
% psi - their phases
% a - Tx complex gains


fi = rand(N,1)*2*dfi-dfi+fi0;            %uniform in [fi0-dfi,fi0+dfi]

for j = 1:nt                                          %loop for Tx
      a = 1/sqrt(2)*(randn(N,1) + 1i*randn(N,1)); %Rayleigh fading
   for i = 1:nr                                       %loop for Rx
      ksi = 2*pi*r*cos(fi-i*2*pi/nr);                 %array vector
      h(i,j) = trace(diag(a.*exp(-1i*ksi)));          %channnel matrix
   end
end

Rr = 1/(nr*N)*h*h';                                   %Rx normalized
correlation
R = {Rr};                                             %output data
```

Aver_ray_UCA.m

```
function A = Aver_ray_UCA(M,N,nt,nr,r,dfi,fi0,ro)
```

```
%
% This is a file for computing the average correlation matrix and the
mean
% (ergodic) capacity of a multipath matrix channel. Instantaneous
correlation
% matrix R is computed by Rray_UCA.
%
% N - the number of rays
% R and Rt - instantaneous Rx and Tx brach correlations
% Rtr - mean Rx correlation matrix (over M trials)
% M - the number of trials
% d - element spacing of Rx array
% dfi - angular spread
% fi0 - average AOA
% ro - average SNR (ro/n - average SNR per Rx branch)
% nr - number of Rx
% nt - number of Tx
% ctr and cavtr -- mean /upper bound of capacity
% cor(nr)- adjacent correlation

ctr=0;
Rtr(nr,nr)=0;
cor(nr)=0;
n=max(nr,nt);
A = zeros(n,n,2);

for m=1:M                                          % loop for trails
   Rout = Rray_UCA(N,nt,nr,r,dfi,fi0);             % instantaneous  matrix
   R = Rout{1};                                    % instantaneous R
   ctr = log2(det(eye(nr)+ro/nt*R))+ctr;           % instanteous capacity
   Rtr = R+Rtr;                                    % sum correlation
matrix
end                                                % end loop for trails

Rtr=Rtr/M;                                         % average correlation
matrix
cavtr = log2(det(eye(nr)+ro/nt*Rtr));              % upper bound capacity

cor(1) = Rtr(nr,1);                                %correlation for nth
                                                   %and 1th
for i=2:nr                                         % loop for Rx
    cor(i)= Rtr(i,i-1);                            % adjacent correlatin
end                                                % end loop for i

A = {Rtr ctr/M cavtr abs(cor) };                   % output data
```

Work_ray_UCA_cor.m

```
% This is a working file for capacity and correlation estimation of
matrix
% multipath (ray) channel using Slaz-Winters model. Instantaneous
correlation
```

```
% matrix is  computed by Rray and the averaging by Aver_cor_UCA.
%
% M - the number of trials
% nr - the number Rx of antennas
% nr - the number Tx of antennas
% d - element spacing (in wavelength)
% dfi - the angular spread of incoming signals
% fi0 - the average angle
% ro - average SNR (ro/n - average SNR per Rx branch)
% r -- radius of UCA
% N - number of multipath
clear all;                                                  %initialize
close all;
M = 100; fi0 = 0*pi/180; ro = 1000; nt=10; N=60;
tic;
format short;
format compact;
for d = 5:5                                                  %ULA element
spacing
    r=22.5;                                                  %(nr-1)*d/2
   for df = 10:10                                            %loop for dfi
      dfi = df*pi/180;
      InDat = [M r dfi*180/pi fi0*180/pi ro];                %input data
                                                             %file name
      s = ['ray_cluster_' int2str(M) '_' num2str(r) '_'
int2str(dfi*180/pi) '_' int2str(fi0*180/pi) '.dat'];
      fid = fopen(s,'w');                                    %write to file
      fprintf(fid,'M=%g\t r=%g\t dfi=%g\t fi0=%g\t ro=%g\n\n',InDat);
      fprintf('\n\n  M=%g\t   r=%g\t dfi=%g\t  fi0=%g\t
ro=%g\n\n',InDat);
      fprintf(fid,'\t   nr\t\t   ctr\t\t  cavtr\t\t  cor\t\t
time\n\n');
      fprintf('    nr\t       ctr\t  cavtr   cor    time\n\n');
      for i = 10:10                                          %loop for nr
         nr=i;
         Out = Aver_ray_UCA(M,N,nt,nr,r,dfi,fi0,ro);     % average data
         Rtr = Out{1};                                       % correlation
matrix
         ctr = Out{2};                                       % mean capacity
         cavtr = Out{3};                                     % upperbound
capacity
         cor=Out{4};                                         % adjacent
correlation
         cor_max = max(cor);                               % max adjacent
correlation

         Out_data = [nr ctr cavtr cor_max toc];              %output data
         fprintf(fid,'%8.3f\t %8.2f\t %8.2f\t %8.2f\t
%8.2f\n',Out_data);
         fprintf('%8.3f   %8.2f   %8.2f   %8.2f    %8.2f\n',Out_data);
      end                                                    %end loop nr
      status = fclose(fid);                                  % close file
   end                                                       % end loop dfi
end                                                          % end loop d
```

Work_ray_UCA_ULA.m

```
% This is a working file for capacity estimation of matrix multipath
(ray)
% channel using one clusters model. Instantaneous correlation matrix is
% computed by Rray and the averaging by Aver_ray_UCA.
% UCA has same apterture as ULA
% M - the number of trials
% nt - the number of Tx antennas
% nr - the number of Rx antennas
% d - element spacing (in wavelength)
% r --UCA radius(in wavelength)
% dfi - the angular spread of incoming signals
% fi0 - the average angle
% ro - average SNR (ro/n - average SNR per Rx branch)

clear all;                                                    %initialize
close all;
M = 1000; fi0 = 0*pi/180; ro = 10^3; N=20; nt=10;nr=10;
tic;
format short;
format compact;
for rr = 1:1                                                  %void loop
    for df = 10:10                                            %loop for dfi
      dfi = df*pi/180;
      InDat = [M N nr dfi*180/pi fi0*180/pi ro];          %input data
                                                              %file name
      s = ['UCA_ray_' int2str(M) '_' num2str(N) '_' num2str(nr) '_'
int2str(dfi*180/pi) '_' int2str(fi0*180/pi) '.dat'];
      fid = fopen(s,'w');                                     %write to file
      fprintf(fid,'M=%g\t N=%g\t  n=%g\t dfi=%g\t fi0=%g\t
ro=%g\n\n',InDat);
                                                              %list on screen
      fprintf('\n\n  M=%g\t   N=%g\t  n=%g\t dfi=%g\t  fi0=%g\t
ro=%g\n\n',InDat);
      fprintf(fid,'\t   d\t\t   ctr\t\t  cavtr\t\t  time\n\n');
      fprintf('    d\t       ctr\t cavtr       time\n\n');
      for d = 0:0.2:5                                         %loop for d
(ULA)
         r = (nr-1)/2*d;                                      %ULA same
aperture
         Out = Aver_ray_UCA(M,N,nt,nr,r,dfi,fi0,ro);          %average value
         Rtr = Out{1};                                        %correlation
matrix
         ctr = Out{2};                                        %mean capacity
         cavtr = Out{3};                                      %upperbound
capacity
         cor = Out{4};                                        %adjacent
correlation
         Out_data = [d ctr cavtr toc];                        %output data
                                                              %write to file
         fprintf(fid,'%8.3f\t %8.2f\t %8.2f\t %8.2f\n',Out_data);
         fprintf('%8.3f   %8.2f   %8.2f   %8.2f\n',Out_data);
      end                                                     %end loop for d
      status = fclose(fid);                                   %close file
   end                                                        %end loop for
dfi
```

```
end                                                    %end loop for rr
```

Work_ray_UCA_fixr.m

```
% This is a working file for capacity estimation of matrix multipath
(ray)
% channel using one clusters model. Instantaneous correlation matrix is
% computed by Rray and the averaging by Aver_ray_UCA.
% UCA has same apterture as ULA
% M - the number of trials
% nt - the number of Tx antennas
% nr - the number of Rx antennas
% d - element spacing (in wavelength)
% r --UCA radius(in wavelength)
% dfi - the angular spread of incoming signals
% fi0 - the average angle
% ro - average SNR (ro/n - average SNR per Rx branch)

clear all;                                             %initialize
close all;
M = 1000; fi0 = 0*pi/180; ro = 10^3; N=50; nt=10;
tic;
format short;
format compact;
for d = 5:5                                            %ULA full
capacity
    r=(nt-1)/2*d;                                      %same size with
ULA
    for df = 10:10                                     %loop for dfi
      dfi = df*pi/180;
      InDat = [M N nt dfi*180/pi fi0*180/pi ro];       %input data
                                                       %file name
      s = ['UCA_ray_' int2str(M) '_' num2str(N) '_' num2str(nt) '_'
int2str(dfi*180/pi) '_' int2str(fi0*180/pi) '.dat'];
      fid = fopen(s,'w');                              %write to file
      fprintf(fid,'M=%g\t N=%g\t  nt=%g\t dfi=%g\t fi0=%g\t
ro=%g\n\n',InDat);
                                                       %list on screen
      fprintf('\n\n  M=%g\t   N=%g\t  nt=%g\t dfi=%g\t  fi0=%g\t
ro=%g\n\n',InDat);
      fprintf(fid,'\t   nr\t\t   ctr\t\t  cavtr\t\t  time\n\n');
      fprintf('    nr\t       ctr\t cavtr       time\n\n');
      for i = 2:50                                     %loop for nr
         nr = i;
         Out = Aver_ray_UCA(M,N,nt,nr,r,dfi,fi0,ro);   %average value
         Rtr = Out{1};                                 %correlation matrix
         ctr = Out{2};                                 %mean capacity
         cavtr = Out{3};                               %upperbound capacity
         cor = Out{4};                                 %adjacent correlation
         Out_data = [nr ctr cavtr toc];                 %output data
                                                       %write to file
         fprintf(fid,'%8.3f\t %8.2f\t %8.2f\t %8.2f\n',Out_data);
         fprintf('%8.3f   %8.2f   %8.2f   %8.2f\n',Out_data);
      end                                              %end loop for nr
```

```
      status = fclose(fid);                                    %close file
   end                                                       %end loop for dfi
end                                                          %end loop for d
```

Work_iso_UCA.m

```
% This is a working file for capacity estimation of matrix multipath
(ray)
% channel using one clusters model. Instantaneous correlation matrix is
% computed by Rray and the averaging by Aver_ray_UCA.
% UCA has same apterture as ULA
% M - the number of trials
% nt - the number of Tx antennas
% nr - the number of Rx antennas
% d - element spacing (in wavelength)
% r --UCA radius(in wavelength)
% dfi - the angular spread of incoming signals
% fi0 - the average angle
% ro - average SNR (ro/n - average SNR per Rx branch)

clear all;                                                   %initialize
close all;
M = 1000; fi0 = 0*pi/180; ro = 10^3; N=20; nt=5;nr=5;
tic;
format short;
format compact;
for rr = 1:1                                                 %void loop
    for df = 180:180                                         %isotropic case
      dfi = df*pi/180;
      InDat = [M N nr dfi*180/pi fi0*180/pi ro];             %input data
                                                             %file name
      s = ['UCA_iso_' int2str(M) '_' num2str(N) '_' num2str(nr) '_'
int2str(dfi*180/pi) '_' int2str(fi0*180/pi) '.dat'];
      fid = fopen(s,'w');                                    %write to file
      fprintf(fid,'M=%g\t N=%g\t  n=%g\t dfi=%g\t fi0=%g\t
ro=%g\n\n',InDat);
                                                             %list on screen
      fprintf('\n\n  M=%g\t   N=%g\t  n=%g\t dfi=%g\t  fi0=%g\t
ro=%g\n\n',InDat);
      fprintf(fid,'\t   d\t\t   ctr\t\t  cavtr\t\t  time\n\n');
      fprintf('    d\t       ctr\t cavtr       time\n\n');
      for i = 0:0.1:5                                        %loop for radius
         r = i;
         Out = Aver_ray_UCA(M,N,nt,nr,r,dfi,fi0,ro);   %average value
         Rtr = Out{1};                                  %correlation matrix
         ctr = Out{2};                                  %mean capacity
         cavtr = Out{3};                                %upperbound capacity
         cor = Out{4};                                  %adjacent correlation
         Out_data = [r ctr cavtr toc];                       %output data
                                                             %write to file
         fprintf(fid,'%8.3f\t %8.2f\t %8.2f\t %8.2f\n',Out_data);
```

```
        fprintf('%8.3f   %8.2f   %8.2f   %8.2f\n',Out_data);
      end                                                    %end loop for d
      status = fclose(fid);                                  %close file
   end                                                    %end loop for dfi
end                                                       %end loop for rr
```

Work_iso_UCA_valid.m

```
% This is a working file for capacity estimation of matrix multipath
(ray)
% channel using one clusters model. Instantaneous correlation matrix is
% computed by Rray and the averaging by Aver_ray_UCA.
% UCA has same apterture as ULA
% M - the number of trials
% nt - the number of Tx antennas
% nr - the number of Rx antennas
% d - element spacing (in wavelength)
% r --UCA radius(in wavelength)
% dfi - the angular spread of incoming signals
% fi0 - the average angle
% ro - average SNR (ro/n - average SNR per Rx branch)

clear all;                                                %initialize
close all;
M = 1000; fi0 = 0*pi/180; ro = 10;
tic;
format short;
format compact;
for rr =3:2:7                                             %void loop
    r=rr/10;
    for df = 180:180                                      %isotropic case
      dfi = df*pi/180;
      InDat = [M r dfi*180/pi fi0*180/pi ro];             %input data
                                                          %file name
      s = ['UCA_iso_valid_' int2str(M) '_' num2str(r) '_'
int2str(dfi*180/pi) '_' int2str(fi0*180/pi) '.dat'];
      fid = fopen(s,'w');                                 %write to file
      fprintf(fid,'M=%g\t r=%g\t dfi=%g\t fi0=%g\t ro=%g\n\n',InDat);
                                                          %list on screen
      fprintf('\n\n  M=%g\t   r=%g\t dfi=%g\t  fi0=%g\t
ro=%g\n\n',InDat);
      fprintf(fid,'\t   n\t\t   ctr\t\t  cavtr\t\t  time\n\n');
      fprintf('    n\t       ctr\t cavtr       time\n\n');
      for i = 1:35
         n = i;
         N=2*n;
         Out = Aver_ray_UCA(M,N,n,n,r,dfi,fi0,ro);    %average value
         Rtr = Out{1};                                %correlation matrix
         ctr = Out{2};                                 %mean capacity
         cavtr = Out{3};                              %upperbound capacity
         cor = Out{4};                               %adjacent correlation
         Out_data = [n ctr cavtr toc];                    %output data
                                                         %write to file
```

```
        fprintf(fid,'%8.3f\t %8.2f\t %8.2f\t %8.2f\n',Out_data);
        fprintf('%8.3f   %8.2f   %8.2f   %8.2f\n',Out_data);
      end                                                    %end loop for d
      status = fclose(fid);                                  %close file
   end                                                       %end loop for dfi
end                                                          %end loop for rr
```

Two-cluster channel model

1.ULA

Cray – instantaneous correlation matrix of single cluster
Rcluster – instantaneous correlation matrix of two-cluster channel
Aver_cluster -- average value using Monte-Carlo using Rcluster
Work_cluster_cap – channel capacity
Work_cluster_sym – symetric clusters
Work_clsuter_rotate – rotate ULA

Crcluster – contributions from clusters comparison
Aver_clsuter- average contributions using Crcluster
Work_cluster_com –work file for contributions from clusters comparison

Prcluster— power unequal distribued in two clusters
Aver_cluster_cor – average value using Prcluster
Work_cluster_pun – work file for power unblanced cluster channel

Rcluster_diversity – sample diversity
Work_cluster_diversity – work file for diversity gain

Cray.m

```
function  hc = Cray(N,nt,nr,d,dfi,fi0)
%
% This is a file for computing channel matrix of a cluster. N rays
exist for
% every Tx (the same AOA set for every Tx) with (i) independent phases
and
% the same  magnitude or (ii) independent complex Gausian gains,
% uncorrelated from Tx to Tx.
%
% fi - angle-of-arrival (AOA)
% dfi - angular spread,assme equal for each cluster
% fi0 - mean angle of arrival with this cluster
% ksi - phase shift between two adjacent elements
% nt - the number of Rx antennas
% nr - the number of Rx antennas
% N - the number of rays
% psi - their phases
```

```
% a - Tx complex gains
% pdf of fi is 1/dfi in [fi0-dfi/2,fi0+dfi/2]

fi = (rand(N,1)-1/2)*dfi+fi0;                    % uniform in [fi0-
dfi/2,fi0+dfi/2]

ksi = 2*pi*d*sin(fi);                            % N rays phase

for j = 1:nt                                     % number of Tx
   a = 1/sqrt(2)*(randn(N,1) + 1i*randn(N,1));   % Rayleigh fading
   for i = 1:nr                                  % number of Rx
       h(i,j) = trace(diag(a.*exp(-1i*i*ksi)));  % channel matrix
   end                                           % end for Rx
end                                              % end for Tx

hc={h};                                          % output data
```

Rcluster.m

```
function R=Rcluster(L,N1,N2,nt,nr,d,dfi_c1,dfi_c2,fi0,dfi0)
%%This file is to computing correlation matrix of a multipath channel
%with clusters ,(i)assume scattering among clusters independent
%(ii)each cluster has channel matrix which is computed by Cray

%L--number of clusters
%n--number of antenne
%N1--number of rays in cluster 1
%N2--number of rays in cluster 2
%d--element spacing of Rx arrays
%dfi--angular spread, all clusters have same
%fi0--average AOA of 1st cluster
%dfi0--average AOA spacing of clusters


% this version   for power propotional
% fi  1/2 in [fi0-dfi,fi0+dfi] and 1/2  in [fi0-dfi+dfi0,fi0+dfi+dfi0]

Cout=Cray(N1,nt,nr,d,dfi_c1,fi0) ;       % cluster1 channel
hc1=Cout{1};

fi1=fi0+dfi0;                          % cluster2 mean AOA
Cout1=Cray(N2,nt,nr,d,dfi_c2,fi1);      % cluster2 channel
hc2=Cout1{1};

h=hc1+hc2;                             % total channel matrix
N=N1+N2;                               % total rays

Rr = 1/(nr*N)*h*h';                     % Rx normalize correlation matrix

R = {Rr};                              % output data
```

Aver_clsuter.m

```
function A = Aver_cluster(M,L,N1,N2,nt,nr,d,dfi_c1,dfi_c2,fi0,dfi0,ro)
%
% This is a file for computing the average correlation matrix and the
mean (ergodic)
% capacity of ULA using two-cluster channel.
% Instantaneous correlation matrix R is computed by Rcluster.
%
% L - number of clusters
% N - the number of rays in each cluster
% R - instantaneous Rx brach correlations
% ctr - mean capacity (by averaging M trials)
% cavtr --upper bound of capacity
% Rtr - mean Rx correlation matrix (over M trials)
% cor - mean adjacent correlation coefficient
% cor_enve --mean adjacent envelope correlation
% M - the number of trials
% d - element spacing of Rx array
% dfi - angular spread
% fi0 - average AOA
% dfi0 - cluster angular spacing
% ro - average SNR (ro/n - average SNR per Rx branch)
%
ctr=0;                                          % initialize
Rtr(nr,nr)=0;
n=max(nr,nt);
A = zeros(n,n,2);
cor1=0;cor2=0;cor3=0;
cor = 0;
for m=1:M                                       % loop for trials
   Rout = Rcluster(L,N1,N2,nt,nr,d,dfi_c1,dfi_c2,fi0,dfi0);  %
instantaneous R
   R = Rout{1};                                 % R --2*2  correlation
matrix
   cor1=cor1+R(1,1)*real(R(2,1));               % x1*x2 --see Lee's
book
   cor2=cor2+R(1,1)*imag(R(2,1));               % x1*y2
   cor3=cor3+ R(1,1).^2;                        % x1*x1
   cor=cor+R(2,1);                              % correlation
coefficient
   ctr = log2(det(eye(nr)+ro/nt*R))+ctr;          % intantaneous
capacity
   Rtr = R+Rtr;                                 % sum correlation
matrix
end                                             % end loop for trials
cor = cor/M;                                    % mean correlation
coefficient
cor1=cor1/M;                                    % average x1*x2
cor2=cor2/M;                                    % average x1*y2
cor3=cor3/M;                                    % average x1*x1
cor_enve=(cor1.^2+cor2.^2)/cor3.^2;             % envelope correlation
Rtr=Rtr/M;                                      % average correlation
matrix
cavtr = log2(det(eye(nr)+ro/nt*Rtr));             % upperbound capacity
```

```
A = {Rtr ctr/M cavtr abs(cor) cor_enve};          % output data
```

Work_cluster_cap.m

```
% This is a working file for capacity estimation of matrix multipath
% (cluster of rays) channel using Slaz-Winters model
% Vectorization of loops is employed. Instantaneous correlation matrix
% is computed by cluster and the averaging by Aver_cluster.
%
% M - the number of trials
% n - the number of antennas
% d - element spacing (in wavelength)
% L - number of clusters
% dfi - the angular spread of incoming signals,assume all cluster has
same dfi
% fi0 - the average angle of 1st cluster
% dfi0 - the cluster spacing angle
% ro - average SNR (ro/n - average SNR per Rx branch)
% N-number of rays in each cluster

clear all;
close all;
M =1000; L=2; N1=10; N2=10; n = 10; ro = 10^3;fi0=0*pi/180;
dfi_c1 = 10*pi/180;
tic;
format short;
format compact;
for k = 30:30:90                                %loop for dfi0
   dfi0=k*pi/180;
   for i0 = 1:1                                 %loop for dfi_c2/dfi_c1

      dfi_c2=i0*dfi_c1;
                                                % input data
      InDat = [M L N1 N2 n dfi_c1*180/pi dfi_c2*180/pi fi0*180/pi
dfi0*180/pi ro];
                                                % file name
      s = ['two_cluster_' int2str(M) '_' int2str(L) '_' int2str(N1) '_'
int2str(N2) '_' int2str(n) '_' num2str(dfi_c1*180/pi) '_'
num2str(dfi_c2*180/pi) '_' int2str(fi0*180/pi) '_' int2str(dfi0*180/pi)
'.dat'];

      fid = fopen(s,'w');                       % write to file
      fprintf(fid,'M=%g\t L=%g\t N1=%g\t N2=%g\t n=%g\t   dfi_c1=%g\t
dfi_c2=%g\t fi0=%g\t dfi0=%g\t ro=%g\n\n',InDat);
                                                % list on screen
      fprintf('\n\n  M=%g\t  L=%g\t N1=%g\t N2=%g\t n=%g\t  dfi_c1=%g\t
dfi_c2=%g\t fi0=%g\t dfi0=%g\t ro=%g\n\n',InDat);
                                                % write to file
```

```
      fprintf(fid,'\t   d\t\t   ctr\t\t  cavtr\t\t  cor\t\t  cor_enve
\t\t  time\n\n');
                                          % list on screen
      fprintf('    d\t       ctr\t cavtr\t  cor\t cor_enve
time\n\n');
      for i = 0:0.2:10                    %loop for d

         d = i;                           % average value
         Out = Aver_cluster(M,L,N1,N2,n,n,d,dfi_c1,dfi_c2,fi0,dfi0,ro);
         Rtr = Out{1};                    % correlation matrix
         ctr = Out{2};                    % mean capacity
         cavtr = Out{3};                  % upper bound
         cor= Out{4};                % adjacent correlation coefficient
         cor_enve = Out{5};           % adjacent envelope correlation
         Out_data = [d ctr cavtr cor cor_enve toc];     %output data
                                          % write to file
         fprintf(fid,'%8.3f\t %8.2f\t %8.2f\t %8.2f\t %8.2f\t
%8.2f\n',Out_data);
                                          % list on screen
         fprintf('%8.3f   %8.2f   %8.2f  %8.2f %8.2f
%8.2f\n',Out_data);
      end                                 % end for d
      status = fclose(fid);               % close file
   end                                    % end for dfi_c2/dfi_c1
end                                       % end for dfi0
```

work_cluster_sym.m

```
% This is a working file for correlation estimation of 2-cluster model
% Vectorization of loops is employed. Instantaneous correlation matrix
is
% computed by cluster and the averaging by% Aver_cluster.
%
% M - the number of trials
% n - the number of antennas , only with 2 elements
% d - element spacing (in wavelength)
% L - number of clusters,only with 2 clusters
% dfi - the angular spread of incoming signals,assume all cluster has
same dfi
% fi0 - the average angle of 1st cluster
% dfi0 - the cluster spacing angle
% ro - average SNR (ro/n - average SNR per Rx branch)
% N1- number of rays in cluster1
% N2 - number of rays in cluister2

clear all;                                          % initialize
close all;
M = 1000; L=2; N1=20;N2=20; n = 2;  ro = 10^3;
tic;                                               % time initilize
format short;                                       % data format
format compact;
for k = 30:30                                       % loop for fi0
   fi0 = -k*pi/180;                              % cluster 1 mean AOA
   dfi0=2*k*pi/180;                              % cluster 2 symmetric
```

```
   for df = 10:10                                          % small dfi
      dfi = df*pi/180;
                                                           % input data
      InDat = [M L N1 N2 n dfi*180/pi fi0*180/pi dfi0*180/pi ro];
                                                           % file name
      s = ['sym_cor_' int2str(M) '_' int2str(L) '_' int2str(N1) '_'
int2str(N2) '_' int2str(n) '_' int2str(dfi*180/pi) '_'
int2str(fi0*180/pi) '_' int2str(dfi0*180/pi) '.dat'];
      fid = fopen(s,'w');                                  % open file
                                                % write parameters to file
      fprintf(fid,'M=%g\t L=%g\t N1=%g\t N2=%g\t n=%g\t   dfi=%g\t
fi0=%g\t dfi0=%g\t ro=%g\n\n',InDat);
                                                          % list on screen
      fprintf('\n\n  M=%g\t  L=%g\t N1=%g\t N2=%g\t n=%g\t  dfi=%g\t
fi0=%g\t dfi0=%g\t ro=%g\n\n',InDat);
      fprintf(fid,'\t   d\t\t   cor_r\t\t  time\n\n');  % write to file
      fprintf('    d\t      cor_r     time\n\n');       % list on screen
      for i = 0:0.1:10                                 % loop for d
         d = i;
                                                       % average of M trials
         Out = Aver_cluster(M,L,N1,N2,n,n,d,dfi,dfi,fi0,dfi0,ro);
         cor_r=Out{4};                          % correlation  coefficient
         Out_data = [d  cor_r toc];             % output data
         fprintf(fid,'%8.3f\t %8.2f\t %8.2f\n',Out_data);%wrtie to file
         fprintf('%8.3f  %8.2f %8.2f\n',Out_data);     % list on screen
      end                                               % end loop for d
      status = fclose(fid);                              % close file
   end                                                 % end loop for dfi
end                                                    % end loop for fi0
```

Work_cluster_assym_fixp.m

```
%This file is to observe clusters angular spread impact on correlation
%coefficient of ULA using two-cluster channel. Correlation coeffcient
is
%computed by two ways: 1)analytical approxiamation equation. 2)closed
form
%expression-bessell expansion
%
%fi0-cluster 1 mean AOA
%fi1-cluster 2 mean AOA
%delta1-anular spread of 1st cluster,
%delta2-anular spread of 2nd cluster,
%d - antenna spacing
%fi-(proportional powerallocation)
%-delta1/(delta1+delta1) in [fi0-delta1/2, fi0+delta1/2] and
%-delta2/(delta1+delta1)[fi1-delta2/2, fi0+delta2/2]



close all;clear all;                                   %initialize
del=10; delta1=del*pi/180;
d0=0.1;  d=0:d0:10;                                    %d0 -step of d
```

```
fi0 = 0;                                                %cluster 1 mean AOA
fi1=30*pi/180;                                          %cluster 2 mean AOA

z=2*pi*d; z=z';
t(1,:)='-+r';                                           %line style
t(2,:)='-*g';
t(3,:)='-ob';
t(4,:)='-xc';
t(5,:)='-sm';
t(6,:)='-dy';

for g=1:3                                               %loop for g
    rio=(g-1)*0.5;                                      %rio=delta2/delta1
    delta2=(g-1)*0.5*delta1;
%delta2=(0,0.5,1)*delta1

    %correlation approxiamation
    x1=delta1/2*z;
    R1=1/(1+rio)*sinc(x1/pi);                           %contribution from
cluster 1

    x2=delta2/2*z*cos(fi1);
    R2=rio/(1+rio)*exp(1j*z*sin(fi1)).*sinc(x2/pi);%contribution from
cluster 2

    Ra=R1+R2;                                           %correlation
coefficient
    Ra=abs(Ra);                                         %magnitude

    Rxx=0;                                              %Bessel expansion
    Rxy=0;
    Rxx0=besselj(0,z);
    for m=1:100

Rxx=Rxx+2*besselj(2*m,z)*(sin(m*delta1)+cos(2*m*fi1)*sin(m*delta2))/(m*
(delta1+delta2));
        Rxy=Rxy+2*besselj(2*m-1,z)*sin((2*m-1)*delta2/2)/((2*m-
1)*(delta1+delta2)/2)*sin((2*m-1)*fi1);
    end

    Rxx=Rxx+Rxx0;
    R=sqrt(Rxx.^2+Rxy.^2);                              %correaltion
coefficent

    plot(d,R,t(g,:));                                   %compare the resluts
    hold on;
    plot(d,Ra,t(g+1,:));
end                                                     %end loop for g

xlabel('d/\lambda');
ylabel('correlation coefficient');
legend('\Delta_2=0\circ','\Delta_2=5\circ','\Delta_2=10\circ');
```

Work_cluster_assym_prop.m

```
%This file is to observe clusters power allocation impact on
correlation
%coefficient using fix power allocation scheme.Correlation
approxiamation
%is deployed

%fi0-cluster 1 mean AOA
%fi1-cluster 2 mean AOA
%delta1-anular spread of 1st cluster,
%delta2-anular spread of 2nd cluster,
%d - antenna spacing
%fi 1/2 in [fi0-delta1/2, fi0+delta1/2] and 1/2 in [fi1-
delta2/2,fi0+delta2/2]
%(equal power)

close all;clear all;                                    %initialize
del=10; delta1=del*pi/180;
d0=0.1;  d=0:d0:10;                                     %d0 -step of d
fi0 = 0;                                                %cluster 1 mean AOA
fi1=30*pi/180;                                          %cluster 2 mean AOA

z=2*pi*d; z=z';

t(1,:)='-+r';                                           %line style
t(2,:)='-*g';
t(3,:)='-ob';

for g=1:3                                               %loop for g
    delta2=(g-1)*0.5*delta1;
%delta2=(0,0.5,1)*delta1

    %correlation approxiamation
    x1=delta1/2*z;
    R1=1/2*sinc(x1/pi);                                 %contribution from
cluster 1

    x2=delta2/2*z*cos(fi1);
    R2=1/2*exp(1j*z*sin(fi1)).*sinc(x2/pi);             %contribution from
cluster 2

    Ra=R1+R2;                                           %correlation
coefficient
    Ra=abs(Ra);                                         %magnitude

    plot(d,Ra,t(g,:));
    hold on;
end

xlabel('d/\lambda');
ylabel('correlation coefficient');
legend('\Delta_2=0\circ','\Delta_2=5\circ','\Delta_2=10\circ');
```

Work_cluster_rotate.m

```
 % This is a working file for capacity estimation of matrix multipath
% (cluster of rays) channel using two-cluster model
% Vectorization of loops is employed. Instantaneous correlation matrix
% is computed by cluster and the averaging by Aver_cluster.
% Rotate ULA elements
% M - the number of trials
% n - the number of antennas
% d - element spacing (in wavelength)
% L - number of clusters
% dfi - the angular spread of incoming signals,assume all cluster has
same dfi
% fi0 - the average angle of 1st cluster
% dfi0 - the cluster spacing angle
% ro - average SNR (ro/n - average SNR per Rx branch)
% N-number of rays in each cluster

clear all;                                    %initialize
close all;
M = 1000; L=2; N1=10; N2=10;n = 10;  ro = 10^3;

tic;
format short;
format compact;
for k = 0:15:90                               %loop for dfi0
    fi0 =(0-k)*pi/180;                         %1st cluster initial at 0
    dfi0=pi/2;                                 %2nd cluster initial at 90,
                                               %fix  dfi0=fi1-fi0=90
                                              % rotate elements unclockwise
 for df = 10:10                                %loop for cluster 1 dfi
      dfi_c1 = df*pi/180;
      for dfr=1:1                              %loop for cluster 2 dfi
        dfi_c2 =dfi_c1*dfr;
                                               % input data
        InDat = [M L N1 N2 n dfi_c1*180/pi dfi_c2*180/pi fi0*180/pi
dfi0*180/pi k];
                                               % file name
        s = ['two_cluster_rotate_' int2str(M) '_' int2str(L) '_'
int2str(N1) '_' int2str(N2) '_' int2str(n) '_' num2str(dfi_c1*180/pi)
'_' num2str(dfi_c2*180/pi) '_' int2str(fi0*180/pi) '_'
int2str(dfi0*180/pi) '_' int2str(k) '.dat'];

        fid = fopen(s,'w');                    % write to file
        fprintf(fid,'M=%g\t L=%g\t N1=%g\t N2=%g\t n=%g\t   dfi_c1=%g\t
dfi_c2=%g\t fi0=%g\t dfi0=%g\t k=%g\n\n',InDat);
                                               % list on screen
        fprintf('\n\n  M=%g\t  L=%g\t N1=%g\t N2=%g\t n=%g\t
dfi_c1=%g\t  dfi_c2=%g\t fi0=%g\t dfi0=%g\t ro=%g\n\n',InDat);
                                               % write to file
        fprintf(fid,'\t   d\t\t   ctr\t\t  cavtr\t\t  time\n\n');
                                               % list on screen
        fprintf('\n\n    d\t       ctr\t cavtr       time\n\n');
        for i = 0:0.2:10                       %loop for d
            d = i;                             % average value
```

```
            Out =
Aver_cluster(M,L,N1,N2,n,n,d,dfi_c1,dfi_c2,fi0,dfi0,ro);
            Rtr = Out{1};                    % correlation matrix
            ctr = Out{2};                    % mean capacity
            cavtr = Out{3};          % upper bound
            cor= Out{4};             % adjacent correlation coefficient
            cor_enve = Out{5};       % adjacent envelope correlation
            Out_data = [d ctr cavtr toc];    %output data
                                             % write to file
            fprintf(fid,'%8.3f\t %8.2f\t %8.2f\t %8.2f\n',Out_data);
                                             % list on screen
            fprintf('%8.3f   %8.2f   %8.2f   %8.2f\n',Out_data);
        end                                  % end for d
      status = fclose(fid);                  % close file
   end                                       % end for dfi_c2/dfi_c1
  end                                        % end for dfi_c1
end                                          % end for k
```

Crcluster.m

```
function R=CRcluster(L,N1,N2,nt,nr,d,dfi_c1,dfi_c2,fi0,dfi0)
%%This file is to computing correlation matrix of a multipath channel
%with clusters ,(i)assume scattering among clusters independent
%(ii)each cluster has channel matrix which is computed by Cray

%L--number of clusters
%n--number of antenne
%N1--number of rays in cluster 1
%N2--number of rays in cluster 2
%d--element spacing of Rx arrays
%dfi--angular spread, all clusters have same
%fi0--average AOA of 1st cluster
%dfi0--average AOA spacing of clusters


Cout=Cray(N1,nt,nr,d,dfi_c1,fi0) ;       % cluster1 channel

hc1=Cout{1};

fi1=fi0+dfi0;                          % cluster2 mean AOA
Cout1=Cray(N2,nt,nr,d,dfi_c2,fi1);       % cluster2 channel
hc2=Cout1{1};

h=hc1+hc2;                             % total channel matrix
N=N1+N2;                               % total rays

Rr1=1/(nr*N)*hc1*hc1';                  %contribution from cluster 1
Rr2=1/(nr*N)*hc2*hc2';                  %contribution from cluster 2

Rr = 1/(nr*N)*h*h';                    % Rx normalize correlation matrix
```

```
R = {Rr1 Rr2 Rr};                    % output data
```

Aver_Ccluster.m

```
function A = Aver_Ccluster(M,L,N1,N2,nt,nr,d,dfi_c1,dfi_c2,fi0,dfi0,ro)

%
% This is a file for computing the average correlation matrix and the
mean (ergodic)
% capacity using two-cluster channel. Instantaneous correlation matrix
R is computed
% by CRcluster.
%
% L - number of clusters
% N - the number of rays in each cluster
% R and Rt - instantaneous Rx and Tx brach correlations
% ctr - mean capacity (by averaging M trials)
% cavtr --upper bound of capacity
% Rtr and RtrT - mean Rx and Tx correlations (over M trials)
% M - the number of trials
% d - element spacing of Rx array
% dfi - angular spread
% fi0 - average AOA
% dfi0 - cluster angular spacing
% ro - average SNR (ro/n - average SNR per Rx branch)
%

cor=0;cor1=0;cor2=0;                                    %initialize
for m=1:M                                               %loop for trials
   Rout = CRcluster(L,N1,N2,nt,nr,d,dfi_c1,dfi_c2,fi0,dfi0);

   R1 = Rout{1};
%contribuion-cluster 1
   R2 = Rout{2};
%contribuion-cluster 2
   R =Rout{3};                                    %channel contribution

   cor1=cor1+R1(2,1);                              %sum over all trials
   cor2=cor2+R2(2,1);
   cor=cor+R(2,1);
end                                                     %end loop trials

cor1=cor1/M;                                            %average over
trials
cor2=cor2/M;
cor=cor/M;
cor1=abs(cor1);                                         %magnitude
cor2=abs(cor2);
cor=abs(cor);

A = {cor1 cor2 cor};                                    %output data
```

Work_cluster_com.m

```
% This is a working file for correlation estimation of 2-cluster model
,R1
% and R2 comparable, we set d=2.38, the first null point of Bessel
function
% Vectorization of loops is employed.spline function is deployed
%Instantaneous correlation matrix is computed by cluster and the
averaging by
% Aver_cluster.
%
% M - the number of trials
% n - the number of antennas , only with 2 elements
% d - element spacing (in wavelength)
% L - number of clusters,only with 2 clusters
% dfi - the angular spread of incoming signals,assume all cluster has
same dfi
% fi0 - the average angle of 1st cluster
% dfi0 - the cluster spacing angle
% ro - average SNR (ro/n - average SNR per Rx branch)
% N- number of rays in each cluster
% cor_1-contribution from cluster 1
% cor_2 - contribution from cluster 2
% ratio - ratio of cor_2 to cor_1

clear all;close all;                                        %initialize
M = 1000; L=2; N1=10;N2=10; nt = 2; nr=2;
ro = 10^3; fi0 =0*pi/180;delta2=0;
tic;
format short;
format compact;
d = 2.38;
cor_1 = 1/2;

for df = 10:10                                               % loop for dfi_c1
    dfi_c1 = df*pi/180;
    for rio=5:5                                              % loop for  ratio
        ratio=rio/10;

        InDat = [M L N1 nr dfi_c1*180/pi fi0*180/pi d ro ratio];
                                                             % input data

        s = ['R1_R2_phi_' int2str(M) '_' int2str(L) '_' int2str(N1) '_'
int2str(nr) '_' num2str(dfi_c1*180/pi) '_' int2str(fi0*180/pi) '_'
num2str(d) '_' num2str(ratio) '.dat'];
                                                             % file name
        fid = fopen(s,'w');                                  % write to file

        fprintf(fid,'M=%g\t L=%g\t N=%g\t n=%g\t   dfi_c1=%g\t fi0=%g\t
d=%g\t ro=%g ratio=%g\n\n',InDat);
        fprintf('\n\n  M=%g\t  L=%g\t N=%g\t n=%g\t  dfi_c1=%g\t
fi0=%g\t d=%g\t ro=%g ratio=%g\n\n',InDat);
        fprintf(fid,'\t   fi2\t\t  cos(fi2)\t\t  delta2\t\t
cos(fi2)*delta2\t\t time\n\n');
        fprintf('    fi2\t cos(fi2)    delta2  cos(fi2)*delta2
time\n\n');
```

```
        k=0; k0=3;                                          %k0 -step
        while k  <50                                        %loop for dfi0
            dfi0=k*pi/180;
            fi1=fi0+dfi0;                                %mean AOA of cluter 2
            for i0=1:21                                  %loop for dfi_c2
                dfi_c2 =dfi_c1*(5-0.2*(i0-1));
                Out =
Aver_Ccluster(M,L,N1,N2,nt,nr,d,dfi_c1,dfi_c2,fi0,dfi0,ro);
                cor_2(i0,:)=Out{2};
%contribution of cluster 2
            end                                          %end loop for dfi_c2
            %use spline fuction to solve equation
            dfr=5:-0.2:1;                                %dfi_c2/dfi_c1
            ddfr=5:-0.002:1;                             %use for scale
            ccor_2=spline(dfr,cor_2,ddfr);               %ccor_2--1*201 matrix

            for i=1:size(ccor_2,2)                       %search in ccor
                if ccor_2(i)>ratio*cor_1                 %find require value
                    break;                               %if find break
                end
                i0=i-1;                              %backward one is required
            end                                          %end search
             delta2=ddfr(i0)*dfi_c1*180/pi;              %required dfi_c2
             k1=cos(fi1);
             k2=delta2*k1;
             Out_data = [fi1*180/pi  k1  delta2 k2 toc];   %output data
             fprintf(fid,'%8.2f\t %8.2f\t %8.2f\t %8.2f\t
%8.2f\n',Out_data);
                                                         %write to file
file
             fprintf('%8.2f  %8.2f %8.2f %8.2f %8.2f\n',Out_data);
                                                         % list on screen
             k=k+k0;                                     %next dfi0
        end                                              %end loop for dfi0
         status = fclose(fid);                           %close file
    end                                                  %end loop for ratio
end                                                      %end loop for dfi_c1
```

Prcluster.m

```
function R=PRcluster(L,N1,N2,nt,nr,d,dfi,fi0,dfi0)
%This file is to computing correlation matrix of a multipath channel
%with clusters ,(i)assume scattering among clusters independent
%(ii)each cluster has channel matrix which is computed by Cray,

%L--number of clusters
%n--number of antenne
%N1--number of rays, in 1st cluster rays
%N2--number of rays, in 2nd cluster rays
```

```
%d--element spacing of Rx arrays
%dfi--angular spread, all clusters have same
%fi0--average AOA of 1st cluster
%dfi0--average AOA spacing of clusters


% this version   for power unblanced
% fi  1/2 in [fi0-dfi,fi0+dfi] and 1/2  in [fi0-dfi+dfi0,fi0+dfi+dfi0]
% power in 2nd cluster = half power in 1st cluster

Cout=Cray(N1,nt,nr,d,dfi,fi0) ;          % cluster1 channel
hc1=Cout{1};

fi1=fi0+dfi0;                          % cluster2 mean AOA
Cout1=Cray(N2,nt,nr,d,dfi,fi1);          % cluster2 channel

hc2=Cout1{1};
%amplitude of 2nd cluster=1/sqrt(2) amlitude of 1st cluster
h=hc1+hc2/sqrt(2);                     % total channel matrix
N=N1+N2;                               % total multipath

Rr = 1/(nr*N)*h*h';                     % Rx normalize correlation matrix

R = {Rr};                              % output data
```

Aver_Pcluster_cor.m

```
function A = Aver_Pcluster_cor(M,L,N1,N2,nt,nr,d,dfi,fi0,dfi0,ro)
%
% This is a file for computing the average correlation matrix and the
mean (ergodic)
% capacity of a multipath matrix channel. Instantaneous correlation
matrix R is computed
% by Rcluster/PRcluster.
%
% L - number of clusters
% n - number of antennas
% N1 - the number of rays in cluster 1
% N2 - the number of rays in cluster 2
% M - the number of trials
% d - element spacing of Rx array
% dfi - angular spread
% fi0 - average AOA
% dfi0 - clusters angular spacing
% ro- average SNR (ro/n - average SNR per Rx branch)


cor1=0;cor2=0;cor3=0;                              % initialize
cor = 0;
for m=1:M                                          % loop for trials
   Rout = PRcluster(L,N1,N2,nt,nr,d,dfi,fi0,dfi0);  % instantaneous R
```

```
   R = Rout{1};                                    % R --2*2  correlation
matrix
   cor1=cor1+R(1,1)*real(R(2,1));                  % x1*x2 --see Lee's
book
   cor2=cor2+R(1,1)*imag(R(2,1));                  % x1*y2
   cor3=cor3+ R(1,1).^2;                           % x1*x1
   cor=cor+R(2,1);                                 % correlation
coefficient
end                                                % end loop for trials
cor = cor/M;                                       % mean correlation
coefficient
cor1=cor1/M;                                       % average x1*x2
cor2=cor2/M;                                       % average x1*y2
cor3=cor3/M;                                       % average x1*x1
cor_enve=(cor1.^2+cor2.^2)/cor3.^2;                % envelope correlation

A = {abs(cor) cor_enve};                           % output data
```

Work_Pcluster_pun.m

```
% This is a working file for correlation estimation of 2-cluster model
,
% unbalnce power between 2-clusters refer to Laurent Schumacher paper
% Vectorization of loops is employed. Instantaneous correlation matrix
is
% computed by cluster and the averaging by Aver_cluster.
%
% M - the number of trials
% n - the number of antennas , only with 2 elements
% d - element spacing (in wavelength)
% L - number of clusters,only with 2 clusters
% dfi - the angular spread of incoming signals,assume all cluster has
same dfi
% fi0 - the average angle of 1st cluster
% dfi0 - the cluster spacing angle
% ro - average SNR (ro/n - average SNR per Rx branch)
% N1- number of rays in 1st cluster
% N2- number of rays in 2nd cluster

clear all;                                                %initialize
close all;
M = 5000; L=2; N1=20;N2=10; n = 2;  ro = 10^3;
tic;                                                      % time
initialize
format short;                                             % data format
format compact;
for k = 90:90                                             %  loop for fi0
   fi0 = -k*pi/180;                                       % -90 cluster
   dfi0=2*k*pi/180;                                       % 90 cluster

   for df = 104:104                          % consistant with the paper
```

```
      dfi = df*pi/180;
                                                          % input data
      InDat = [M L N1 N2 n dfi*180/pi fi0*180/pi dfi0*180/pi ro];
                                                          % file name
      s = ['power_unequal_' int2str(M) '_' int2str(L) '_' int2str(N1)
'_' int2str(N2) '_' int2str(n) '_' int2str(dfi*180/pi) '_'
int2str(fi0*180/pi) '_' int2str(dfi0*180/pi) '.dat'];
      fid = fopen(s,'w');                                 % open file
                                                          % write
parameters to file
      fprintf(fid,'M=%g\t L=%g\t N1=%g\t N2=%g\t n=%g\t   dfi=%g\t
fi0=%g\t dfi0=%g\t ro=%g\n\n',InDat);
                                                          % list on
screen
      fprintf('\n\n  M=%g\t  L=%g\t N1=%g\t N2=%g\t n=%g\t  dfi=%g\t
fi0=%g\t dfi0=%g\t ro=%g\n\n',InDat);
      fprintf(fid,'\t   d\t\t   cor_r\t\t  time\n\n');  % write to file
      fprintf('    d\t      cor_r     time\n\n');       % list on
screen

      for i = 0:0.02:5                                    % loop for d
         d = i;
                                                         % average trails
         Out = Aver_Pcluster_cor(M,L,N1,N2,n,n,d,dfi,fi0,dfi0,ro);
         cor_r=Out{2};                                % envelope correlation
         Out_data = [d  cor_r toc];                       % output data
         fprintf(fid,'%8.3f\t %8.2f\t %8.2f\n',Out_data); %wrtie to
file
         fprintf('%8.3f  %8.2f %8.2f\n',Out_data);     % list on screen
      end                                                % end loop for d
      status = fclose(fid);                               % close file
   end                                                 % end loop for dfi
end                                                    % end loop for fi0
```

Rcluster_diversity.m

```
function  R=Rcluster_diversity(L,N1,N2,nt,nr,d,dfi_c1,dfi_c2,fi0,dfi0)
%This file is to computing diversity gain of a multipath channel with
clusters,
%(i)assume scattering among clusters independent (ii)each cluster with
N rays
%has channel matrix which is computed by Cray,

%L--number of clusters
%nt--number of transmitt antennas
%nr- number of receive antennas
%N1--number of rays, in 1st cluster rays
%N2--number of rays, in 2nd cluster rays
%d--element spacing of Rx arrays
%dfi_c1-- cluster 1 angular spread
%dfi_c2-- cluster 2 angular spread
%fi0--average AOA of 1st cluster
%dfi0--average AOA spacing of clusters
```

```
%snr-snr at Rx output

Cout=Cray(N1,nt,nr,d,dfi_c1,fi0) ;          % cluster1 channel
hc1=Cout{1};

fi1=fi0+dfi0;                               % cluster2 mean AOA
Cout1=Cray(N2,nt,nr,d,dfi_c2,fi1);          % cluster2 channel
hc2=Cout1{1};

h=hc1+hc2;                                  % total channel matrix
N=N1+N2;                                    % total rays

y = (h'*h)/N;                               % normalize by total power
snr = abs(y);                               % Rx average SNR
R = snr;                                    % output data
```

Work_clsuter_diversity.m

```
% ------------------------------------------------------------------------
---
% This is the working file to calculate the diversity gain vs element
spacing
% ------------------------------------------------------------------------
---
% using two-cluster model
% filename: work_clsuter_diversity.m
%
% variables:
% -----
% N1 - the number of rays in 1st cluster
% N2 - the number of rays in 2nd cluster
% n_tx - the number of transmit antennas
% d - element spacing of rx antenna
% dfi - angular spread
% fi0 - 1st cluster mean angle of arrival
% dfi0 -- angle between 2nd cluster mean AOA and 1st cluster mean AOA
%
%
% ------------------------------------------------------------------------
---
%  History:
% ------------------------------------------------------------------------
---
%  Date         | Author     | Details
% ------------------------------------------------------------------------
---
%  March 1, 2003 | Leo Chan   | Creation
%
%  May 22, 2003  | Guangze zhao | Major modification: add the 2nd
cluster
```

```
% ------------------------------------------------------------------
---

clear all;
M = 10^6;                                          % number of samples
L = 2;                                             % number of clusters
N1 = 10;                                           % number of rays in
cluster 1
N2 = 10;                                           % number of rays in
cluster 2
n_tx = 1;                                          % number of Tx antenna

min_snr = 1;                                       % minimum signal to
noise ratio

df = 10;                                           % angular spread in
degrees
dfi = df/180*pi;                                   % angular spread in
radians

tic;
format short;
format compact;

fi0_array = [-5,-30,-60,-90]*pi/180;               %mean AOA of cluster 1

df_array = [10];                                   %angular spread of
clusters
dfi_array = df_array / 180 * pi;

antenna_spacing_lowerbound = 0;                    %bound of d
antenna_spacing_upperbound = 10;                   %bound of d
antenna_spacing_step = 0.2;                        %step of d

snr_lowerbound = -45;                              %bound of snr(dB)
snr_upperbound = 20;                               %bound of snr
outage_threshold = 10.^(-2);                       %outage probability
snr_step = 0.1;                                    %step of snr
found = 0;

for dfi_index = 1:size(dfi_array,2)                %loop for anglar spread
    dfi = dfi_array(dfi_index);
    for fi0_index = 1:size(fi0_array,2)            %loop for mean AOA of
cluster 1
        fi0 = fi0_array(fi0_index);
        dfi0 = 2*abs(fi0);                         %symmetric case: two
clusters
        fi1 = fi0 + dfi0;                          %symmetric with
broadside
        filename = ['work_cluster_diversity' int2str(L) '_ray1_'
int2str(N1) '_ray2_' int2str(N2) '_angular_spread_' int2str(dfi*180/pi)
'_center1_' int2str(fi0*180/pi) '_center2_' int2str(fi1*180/pi)
'.dat'];
        fprintf('...Processing %s\n', filename);%list on screen
        fid = fopen(filename,'w');                 %write to file

        fprintf(fid,'// ------------------------------\n');
```

```
        fprintf(fid,'// Angular Spread        : %d
degrees\n',dfi*180/pi);
        fprintf(fid,'// mean AOA of cluster 1 : %d
degrees\n',fi0*180/pi);
        fprintf(fid,'// mean AOA of cluster 2 : %d
degrees\n',fi1*180/pi);
        fprintf(fid,'// Outage Threshold      :
%d\n',outage_threshold);
        fprintf(fid,'// ------------------------------\n');
        fprintf(fid,'spacing, snr_for_1_antenna,
snr_for_2_antenna,diversity_gain\n');


        for antenna_spacing_index =
antenna_spacing_lowerbound:antenna_spacing_step:antenna_spacing_upperbo
und
                                                %loop for antenna
spacing d

            % ----------------------
            %  processing 1 element
            % ----------------------
            nb_antenna = 1;                     %only one Rx antenna

            for sample_index = 1:M              %loop for samples

              snr(sample_index)
=Rcluster_diversity(L,N1,N2,n_tx,nb_antenna,antenna_spacing_index,dfi,d
fi,fi0,dfi0);
                                                % instantaneous(sample)
snr
            end                                 % for sample_index = 1:M

            snr_index = snr_lowerbound;
            found = 0;
            while ( (snr_index < snr_upperbound) & (found == 0) )
                                                %loop for snr
               snr_index_scaler = 10.^(snr_index/10);
                                                %snr linear scale
               j=find(snr<snr_index_scaler);    %samples snr<require snr
               prob_outage = size(j,2)/size(snr,2); %outage probability

               if (prob_outage >= outage_threshold) %outage prob is
required?
                  snr_index_1_antenna = snr_index;
                  found = 1;                    %end loop for this snr
                  fprintf('   Found! Spacing: %f, # of Antenna: %d,
SNR: %f\n',antenna_spacing_index,nb_antenna,snr_index);
               end % if (prob_outage == probability_threshold)
               snr_index = snr_index + snr_step;%next snr
            end                                 %end loop for all snr

            % ----------------------
            %  processing 2 element
            % ----------------------
            nb_antenna = 2;                     %two Rx antennas
```

```
            for sample_index = 1:M              %loop for samples

              snr(sample_index) =
Rcluster_diversity(L,N1,N2,n_tx,nb_antenna,antenna_spacing_index,dfi,df
i,fi0,dfi0);
                                                % instantaneous(sample)
snr
            end                                 % for sample_index = 1:M

            snr_index = snr_lowerbound;
            found = 0;
            while ( (snr_index < snr_upperbound) & (found == 0) )
                                                %loop for snr
               snr_index_scaler = 10.^(snr_index/10);
                                                %snr linear scale
               j=find(snr<snr_index_scaler);    %samples snr<require snr
               prob_outage = size(j,2)/size(snr,2);%outage probability

               if (prob_outage >= outage_threshold)
                                                %outage prob is
required?
                  snr_index_2_antenna = snr_index;
                  found = 1;                    %end loop for this snr
                  fprintf('   Found! Spacing: %f, # of Antenna: %d,
SNR: %f\n',antenna_spacing_index,nb_antenna,snr_index);
               end                              % if (prob_outage ==
probability_threshold)
               snr_index = snr_index + snr_step;%next snr
            end                                 %end loop for all snr

            fprintf(fid,'%f, %f, %f, %f\n',antenna_spacing_index,
snr_index_1_antenna, snr_index_2_antenna, (snr_index_2_antenna -
snr_index_1_antenna));
                                                %write to file
         end %for antenna_spacing_index =
1:size(antenna_spacing_array,2)

        status = fclose(fid);                    % close file
      end %for fi0_index = 1:size(fi0_array,2)
end %for dfi_inex = 1:size(dfi_array,2)
```

2.UCA

```
Cray_UCA -channel matrix
Rxluster_UCA - instantaneous correlation matrix
Aver_cluster_UCA - mean value using Monte-Carlo
Work_cluster_fixn - capacity of UCA versus radius
Work_cluster_fixr - capacity of UCA versus Rx antennas
```

Cray_UCA.m

```
function  hc = Cray_UCA(N,nt,nr,r,dfi,fi0)
%
% This is a file for computing correlation and capacity matrix of UCA
```

```
% using two-cluster channel. N rays exist for every Tx (the same AOA
% set for every Tx) with (i) independent phases and the same magnitude
or
% (ii) independent complex Gausian gains, uncorrelated from Tx to Tx.
% (iii) for uniform circular array
%
% fi - angle-of-arrival (AOA)
% dfi - angular spread
% fi0 - mean angle of arrival
% ksi - phase shift between 1 element and its i-th neighbour
% nt - the number of TX antennas
% nr - the number of Rx antennas
% N - the number of rays
% psi - their phases
% a - Tx complex gains


fi = (rand(N,1)-1/2)*dfi+fi0;                          %uniform in [fi0-
dfi,fi0+dfi]

for j = 1:nt                                           %loop for Tx
      a = 1/sqrt(2)*(randn(N,1) + 1i*randn(N,1));      %Rayleigh fading
   for i = 1:nr                                        %loop for Rx
      ksi = 2*pi*r*cos(fi-i*2*pi/nr);                  %array vector
      h(i,j) = trace(diag(a.*exp(-1i*ksi)));           %channnel matrix
   end                                                 %end loop for nr
end                                                    %end loop for nt

hc={h};                                                %output data
```

Rxluster_UCA.m

```
function R=Rcluster_UCA(L,N1,N2,nt,nr,r,dfi_c1,dfi_c2,fi0,dfi0)
%%This file is to computing correlation matrix of a multipath channel
%with clusters ,(i)assume scattering among clusters independent
%(ii)each cluster has channel matrix which is computed by Cray

%L--number of clusters
%n--number of antenne
%N1--number of rays in cluster 1
%N2--number of rays in cluster 2
%r--radius of UCA
%dfi--angular spread, all clusters have same
%fi0--average AOA of 1st cluster
%dfi0--average AOA spacing of clusters


% this version   for power propotional
% fi  1/2 in [fi0-dfi,fi0+dfi] and 1/2  in [fi0-dfi+dfi0,fi0+dfi+dfi0]

Cout=Cray_UCA(N1,nt,nr,r,dfi_c1,fi0); % cluster1 channel
hc1=Cout{1};
```

```
fi1=fi0+dfi0;                          % cluster2 mean AOA
Cout1=Cray_UCA(N2,nt,nr,r,dfi_c2,fi1);% cluster2 channel
hc2=Cout1{1};

h=hc1+hc2;                             % total channel matrix
N=N1+N2;                               % total rays

Rr = 1/(nr*N)*h*h';                     % Rx normalize correlation matrix

R = {Rr};                              % output data
```

Aver_cluster_UCA .m

```
function A =
Aver_cluster_UCA(M,L,N1,N2,nt,nr,r,dfi_c1,dfi_c2,fi0,dfi0,ro)
%% This is a file for computing the average correlation matrix and the
mean
% (ergodic) capacity of two-cluster channel. Instantaneous correlation
% matrix R is computed by Rcluster_UCA.

% L - number of clusters
% N1 - the number of rays in  cluster 1
% N2 - the number of rays in  cluster 2
% R  - instantaneous Rx  brach correlations
% ctr - mean capacity (by averaging M trials)
% cavtr --upper bound of capacity
% Rtr - mean Rx  correlations (over M trials)
% M - the number of trials
% r - circular radius
% dfi_c1, dfi_c2 - angular spread
% fi0 - average AOA
% dfi0 - cluster 2 mean AOA- cluster 1 mean AOA
% ro - average SNR (ro/n - average SNR per Rx branch)


ctr=0;
Rtr(nr,nr)=0;
cor(nr)=0;
n=max(nr,nt);
A = zeros(n,n,2);

for m=1:M                                          % loop for trails
                                                   % instantaneous  matrix
   Rout = Rcluster_UCA(L,N1,N2,nt,nr,r,dfi_c1,dfi_c2,fi0,dfi0);
   R = Rout{1};                                    % instantaneous R
   ctr = log2(det(eye(nr)+ro/nt*R))+ctr;           % instanteous capacity
   Rtr = R+Rtr;                                    % sum correlation
matrix
end                                                % end loop for trails

Rtr=Rtr/M;                                         % average correlation
matrix
```

```
cavtr = log2(det(eye(nr)+ro/nt*Rtr));          % upper bound capacity

cor(1) = Rtr(nr,1);                            % correlation for nth
and 1th
for i=2:nr                                     % loop for Rx
    cor(i)= Rtr(i,i-1);                        % adjacent correlatin
end                                            % end loop for i

A = {Rtr ctr/M cavtr abs(cor) };               % output data
```

Work_cluster_fixn.m

```
% This is a working file for capacity estimation of matrix multipath
(cluster of rays)
% channel using extended two-cluster model for UCA. Instantaneous
correlation matrix
% is computed by cluster and the averaging by Aver_cluster_UCA
%
% M - the number of trials
% nt,nr - the number of Tx,Rx antennas
% r - cicular radius (in wavelength)
% L - number of clusters
% dfi_c1 - 1st cluster the angular spread of incoming signals
% dfi_c2 - 2nd cluster the angular spread of incoming signals
% fi0 - the average angle of 1st cluster
% dfi0 - the cluster spacing angle between 1st cluster and 2nd cluster
% ro - average SNR (ro/n - average SNR per Rx branch)
% N1- number of rays in cluster 1
% N2- number of rays in cluster 2

close all;clear all;                                    %initialize
M =1000; L=2; N1=20; N2=20; ro = 10^3;
dfi_c1 = 10*pi/180; dfi_c2 = 10*pi/180; nt=10;nr=10;
tic;
format short;
format compact;
for k = 10:20:90                                        %loop for fi0
   fi0=-k*pi/180; dfi0=2*k*pi/180;                      %symmetric case
   for i0 = 1:1                                         %void loop
                                                        %input data
      InDat = [M L N1 N2 nt nr dfi_c1*180/pi dfi_c2*180/pi fi0*180/pi
dfi0*180/pi ro];
                                                        %file name
      s = ['UCA-2cluster-fixn' int2str(M) '_' int2str(L) '_'
int2str(N1) '_' int2str(N2) '_' num2str(nt) '_' num2str(nr) '_'
num2str(dfi_c1*180/pi) '_' num2str(dfi_c2*180/pi) '_'
int2str(fi0*180/pi) '_' int2str(dfi0*180/pi) '.dat'];

      fid = fopen(s,'w');                               %write to file
      fprintf(fid,'M=%g\t L=%g\t N1=%g\t N2=%g\t nt=%g\t  nr=%g\t
dfi_c1=%g\t dfi_c2=%g\t fi0=%g\t dfi0=%g\t ro=%g\n\n',InDat);
                                                        %list on screen
```

```
      fprintf('\n\n  M=%g\t  L=%g\t N1=%g\t N2=%g\t nt=%g\t  nr=%g\t
dfi_c1=%g\t  dfi_c2=%g\t fi0=%g\t dfi0=%g\t ro=%g\n\n',InDat);
                                                    %write to file
      fprintf(fid,'\t   r\t\t   ctr\t\t  cavtr\t\t  time\n\n');

      fprintf('    r\t     ctr\t cavtr     time\n\n');%list on screen
      for r = 0:0.2:10                              %loop for radius
                                                    %averge values
         Out =
Aver_cluster_UCA(M,L,N1,N2,nt,nr,r,dfi_c1,dfi_c2,fi0,dfi0,ro);
         Rtr = Out{1};                              %correlation
matrix
         ctr = Out{2};                              %mean capacity
         cavtr = Out{3};                            %capacity upper
bound
         cor = Out{4};                              %adjacent
correlation
         Out_data = [r ctr cavtr toc];              %output data
                                                    %write to file
         fprintf(fid,'%8.3f\t %8.2f\t %8.2f\t %8.2f\n',Out_data);
                                                    %list on screen
         fprintf('%8.3f   %8.2f   %8.2f   %8.2f\n',Out_data);
      end                                           %end loop for r
      status = fclose(fid);                         %close file
   end                                              %end loop for i
end                                                 %end loop for fi0
```

work_cluster_fixr.m

```
% This is a working file for capacity estimation of matrix multipath
(cluster of rays)
% channel using extended two-cluster model for UCA. Instantaneous
correlation matrix
% is computed by cluster and the averaging by Aver_cluster_UCA
%
% M - the number of trials
% nt,nr - the number of Tx,Rx antennas
% r - cicular radius (in wavelength)
% L - number of clusters
% dfi_c1 - 1st cluster the angular spread of incoming signals
% dfi_c2 - 2nd cluster the angular spread of incoming signals
% fi0 - the average angle of 1st cluster
% dfi0 - the cluster spacing angle between 1st cluster and 2nd cluster
% ro - average SNR (ro/n - average SNR per Rx branch)
% N1- number of rays in cluster 1
% N2- number of rays in cluster 2

close all;                                          %initialize
clear all;
M =1000; L=2; N1=10; N2=10; ro = 10^3; fi0=0*pi/180;
dfi0=30*pi/180;dfi_c1 = 10*pi/180; dfi_c2 = 10*pi/180;
nt=10;                                              %fixed Tx
antennas
r=3;                                                %fixed radius
```

```
tic;
format short;
format compact;
for k = 30:30                                                    %void loop
                                                                 %input data
      InDat = [M L N1 N2 r dfi_c1*180/pi dfi_c2*180/pi fi0*180/pi
dfi0*180/pi ro];
                                                                 %file name
      s = ['UCA-2cluster-fixr-' int2str(M) '_' int2str(L) '_'
int2str(N1) '_' int2str(N2) '_' num2str(r) '_'num2str(dfi_c1*180/pi)
'_' num2str(dfi_c2*180/pi) '_' int2str(fi0*180/pi) '_'
int2str(dfi0*180/pi) '.dat'];

      fid = fopen(s,'w');                                        %write to file
      fprintf(fid,'M=%g\t L=%g\t N1=%g\t N2=%g\t r=%g\t   dfi_c1=%g\t
dfi_c2=%g\t fi0=%g\t dfi0=%g\t ro=%g\n\n',InDat);
                                                                 %list on screen
      fprintf('\n\n  M=%g\t  L=%g\t N1=%g\t N2=%g\t r=%g\t  dfi_c1=%g\t
dfi_c2=%g\t fi0=%g\t dfi0=%g\t ro=%g\n\n',InDat);
                                                                 %write to file
      fprintf(fid,'\t   nr\t\t   ctr\t\t  cavtr\t\t  time\n\n');
                                                                 %list on screen
      fprintf('    nr\t       ctr\t cavtr       time\n\n');
      for i = 2:1:20                                             %loop for Rx
antennas
         nr = i;
                                                                 %average values
         Out =
Aver_cluster_UCA(M,L,N1,N2,nt,nr,r,dfi_c1,dfi_c2,fi0,dfi0,ro);
         Rtr = Out{1};                                           %correlation
matrix
         ctr = Out{2};                                           %mean capacity
         cavtr = Out{3};                                         %upper bound
capacity
         cor = Out{4};                                           %adjacent
correlation
         Out_data = [nr ctr cavtr toc];                           %output data
                                                                 %write to file
         fprintf(fid,'%8.3f\t %8.2f\t %8.2f\t %8.2f\n',Out_data);
                                                                 %list on screen
         fprintf('%8.3f   %8.2f   %8.2f   %8.2f\n',Out_data);
      end                                                        %end loop for nr
      status = fclose(fid);                                      %close file
end                                                              %end loop for k
```